

2008

Tumor suppressive effects of the Beta-2 adrenergic receptor and the small GTPase RhoB

Adam E. Carie

University of South Florida

Follow this and additional works at: <http://scholarcommons.usf.edu/etd>



Part of the [American Studies Commons](#)

Scholar Commons Citation

Carie, Adam E., "Tumor suppressive effects of the Beta-2 adrenergic receptor and the small GTPase RhoB" (2008). *Graduate Theses and Dissertations*.

<http://scholarcommons.usf.edu/etd/161>

This Dissertation is brought to you for free and open access by the Graduate School at Scholar Commons. It has been accepted for inclusion in Graduate Theses and Dissertations by an authorized administrator of Scholar Commons. For more information, please contact scholarcommons@usf.edu.

Tumor Suppressive Effects of the Beta-2 Adrenergic Receptor and the Small
GTPase RhoB

by

Adam E. Carie

A dissertation submitted in partial fulfillment
of the requirements for the degree of
Doctor of Philosophy
Department of Cancer Biology
College of Graduate Studies
University of South Florida

Major Professor: Saïd M Sebt, Ph.D.
Srikumar Chellappan, Ph.D.
Hong-Gang Wang, Ph.D.
Noreen Luetkeke, Ph.D.

Date of Approval:
March 24, 2008

Keywords: MAP Kinase, Protein Kinase A, cAMP, Rho, Tumor Suppression

© Copyright 2008, Adam Carie

Dedication

This work is dedicated to the loved ones that supported me during my educational career. To my family: my wife, parents, sister and brothers in law, parents in law and grandparents, your confidence in me and guidance helped me to remain steadfast in the pursuit of my doctorate. I would also like to dedicate this work to memory of my late mother, Chereen Ann Carie, the inspiration for my interests in cancer research.

Acknowledgements

I would like to thank my major professor and mentor Dr. Saïd Sebti for all of the time and effort that was invested in my education and training. You always encouraged me to challenge myself, as well as dogma, and to not take anything for granted. You taught me how to think analytically and to dissect problems in a rational manner. You gave me an opportunity to experience research as an undergraduate student, which planted the seed that flourished over the next seven years. I am forever grateful for instilling in me characteristics that, in part, have made me who I am today.

I would also like to thank my committee members, Dr. Srikumar Chellappan, Dr. Noreen Luetke, and Dr. Hong-Gang Wang for their guidance and excellent suggestions for my projects. I appreciate your efforts and approachability, your doors were always open and you were always willing to help. Special thanks goes to Dr. Adrienne Cox, the outside chair for my dissertation defense. Your comments and suggestions helped to mold this thesis into a more complete work.

There are many people that have helped me tremendously throughout the years in the Sebti lab, and through intrainstitutional collaborations. I would especially like to thank Dr. JiaZhi (George) Sun for taking me in as an

undergraduate student and teaching me techniques and skills I would utilize for the remainder of my graduate career. I would also like to thank my bench buddy Michelle Blaskovich for sharing her technical expertise, as well as the occasional buffer, and always making life interesting in the lab (especially when George was around). Likewise, I would like to thank Dr. Aslamuzzaman Kazi and Dr. DeAn Wang for their hard work on our collaborative projects, it was a pleasure working with you both. Finally, to the rest of the Sebti lab members past and present, thank you for always treating me like family, we were a tight knit group and our friendship will continue long after my graduate career is over.

This thesis work is dedicated to my loving family, and to the memory of my late mother, Chereen Ann Carie, who was my inspiration for getting involved in cancer research. I would never have been able to go the distance and complete the Ph.D. program without the loving support of my family and friends, thank you all.

Note to Reader

The original of this document contains color that is necessary for understanding the data. The original dissertation is on file with the USF library in Tampa, Florida.

Table of Contents

List of Tables	iii
List of Figures	vii
Abstract	ix
Background and Significance	1
Chapter 1: A Chemical Biology Approach Identifies a Beta-2 Adrenergic Receptor Agonist that Causes Human Tumor Suppression by Blocking the C-Raf/Mek1/2/Erk1/2 Pathway	
Abstract	14
Introduction	15
Materials and Methods	26
Cell Lines and Transfection	26
Cytoblot Screening for Small Molecules that Decrease Phospho-Erk1/2	27
Western Blotting	27
<i>In Vitro</i> Kinase Assay	28
<i>In Vivo</i> Kinase Assay	30
MTT Assay	30
Alamar Blue Proliferation Assay	30
Soft Agar Assay	31
Apoptosis Assay	31
Total Cellular cAMP Assay	32
PKA Kinase Assay	33
Tumor Suppression in Nude Mouse Xenograft Models	33
Immunohistochemistry and Slide Quantitation	34
Results	36
Discussion	75

Chapter 2: Validation of ARA-211 Activity Ex-Vivo in Fresh Biopsies from Patient Samples	
Abstract	84
Introduction	85
Materials and Methods	88
Human Tissue Array	88
Immunohistochemistry	89
Treatment of Patient Samples <i>Ex-vivo</i>	90
Results	91
Discussion	124
Chapter 3: RhoB, but not RhoA Overexpression Delays ErbB2-Mediated Mammary Tumor Onset and Reduces Tumor Multiplicity in Transgenic Mice	
Abstract	129
Introduction	131
Materials and Methods	137
cDNAs and Gene Subcloning	137
Southern Blot and Genotyping	156
DNA Preparation and PCR	158
Protein Preparation and Analysis	158
Tumor Onset, Growth Rate, and Multiplicity Calculation	159
Results	161
Discussion	172
Conclusions and Future Directions	176
List of References	186
About the Author	End Page

List of Tables

Table 1.	Chemical structures of the compounds identified as Erk1/2 inhibitors from NCI Diversity Set	39
Table 2.	Structure-activity relationship studies identify the ARA family of inhibitors as analogues of epinephrine, and identifies ARA-211 as pirbuterol	45
Table 3.	ARA-211 sensitive and insensitive cell lines tested from the NCI 60 cell line panel do not correlate with C-Raf and B-Raf expression levels	60
Table 4.	Physiological effects of ARA-211 treatment on sensitive cell lines versus insensitive cell lines	71
Table 5	Summary of tissue array results for β 2 AR and P-Erk1/2	105
Table 6	Summary of fresh human tumor biopsy staining results for β 2 AR and P-Erk1/2	109
Table 7	RhoB, but not RhoA overexpression results in a significant delay in ErbB2-mediated tumor onset and multiplicity, but not tumor growth rate	169

List of Figures

Figure 1.	Cancer cells contain numerous, aberrant signal Transduction circuits	2
Figure 2.	Aberrant signaling through receptor tyrosine kinases (RTKs) and downstream signaling through Ras is well characterized	4
Figure 3.	RhoB, a close family member of RhoA, antagonizes Ras malignant transformation and has been suggested to have tumor suppressive effects	6
Figure 4.	High throughput screening of the NCI Diversity Set by cyto blot analysis reveals 3 inhibitors of Erk1/2 activation	38
Figure 5.	ARA-family of compounds selectively inhibit P-Erk1/2 in MDA-MB-231 breast cancer cells	40
Figure 6.	ARA-211 inhibits the kinase activity of Raf-1, but not B-Raf, by inhibiting upstream activation of Raf	42
Figure 7.	ARA-211 stimulates cAMP selectively through β 2 adrenergic receptor activation	47

Figure 8.	ARA-211 mediated cAMP stimulation through β 2 AR activation results in inhibition of P-Erk1/2	48
Figure 9.	ARA-211 mediated cAMP stimulation through β 2 AR activation results in inhibition of P-Erk1/2 through PKA activation, not EPAC activation of Rap1	51
Figure 10.	siRNA and kinase assays validate that ARA-211 mediated cAMP stimulation results in inhibition of P-Erk1/2 through PKA activation	52
Figure 11.	ARA-211 inhibition of MDA-MB-231 cell proliferation requires β 2 AR and inhibition of P-Erk1/2	54
Figure 12.	Direct activation of adenylyl cyclase by forskolin inhibits the proliferation of MDA-MB-231 cells	55
Figure 13.	ARA-211 mediated inhibition of MDA-MB-231 cell proliferation is dependent on the ability to inhibit Mek1/2 and to decrease P-Erk1/2 levels	57
Figure 14.	Western blot verification of β 2 AR, P-Erk1/2, C-Raf and B-Raf expression levels from the NCI 60 cell line panel	62
Figure 15.	ARA-211 induces cAMP formation in MDA-MB-231, SF-539 and ACHN cells but not in A549, SNB-19 and HCT-116 cells	65

Figure 16.	ARA-211 inhibits anchorage independent growth in MDA-MB-231, SF-539 and ACHN cells but not in A549, SNB-19 and HCT-116 cells	66
Figure 17.	ARA-211 induces apoptosis in MDA-MB-231, SF-539 and ACHN cells but not in A549, SNB-19 and HCT-116 cells	67
Figure 18.	ARA-211 treatment of MDA-MB-231 xenografts results in tumor regression, and treatment of AHCN xenografts completely inhibits tumor growth in nude mice	69
Figure 19.	ARA-211 treatment of mice with A549, HCT-116 and SNB-19 xenografts has no effect on tumor growth	70
Figure 20.	ARA-211 suppresses P-Erk1/2 levels, inhibits tumor cell growth and induces apoptosis in human xenografts in nude mice	73
Figure 21.	ARA-211 stimulates crosstalk between β 2 AR and Raf/MEK/Erk1/2 resulting in inhibition of P-Erk1/2 through PKA, but not EPAC	78
Figure 22.	Tissue array identifies human breast tumor samples that express β 2 AR and P-Erk1/2	93
Figure 23.	Tissue array identifies human liver tumor samples that express β 2 AR and P-Erk1/2	95

Figure 24.	Tissue array identifies human bladder tumor samples that express $\beta 2$ AR and P-Erk1/2	97
Figure 25.	Tissue array identifies human ovarian tumor samples that express $\beta 2$ AR and P-Erk1/2	99
Figure 26.	Tissue array identifies human pancreatic tumor samples that express $\beta 2$ AR and P-Erk1/2	101
Figure 27.	Tissue array identifies human prostate tumor samples that express $\beta 2$ AR and P-Erk1/2	103
Figure 28.	Fresh patient samples from Moffitt Cancer Center express P-Erk1/2 and $\beta 2$ AR	108
Figure 29.	<i>Ex-vivo</i> treatment of fresh human tissue demonstrates variable efficacy of ARA-211 to inhibit P-Erk1/2, inhibit proliferation and induce apoptosis	115
Figure 30.	Patient treatment with ARA-211 requires pre-determination of $\beta 2$ AR and P-Erk1/2 expression, as well as <i>ex-vivo</i> treatment to determine efficacy to inhibit proliferation and induce apoptosis	123
Figure 31.	MMTV-TGF α construct linearized by EcoRI digestion for insertion of human RhoA and RhoB genes	139
Figure 32.	Isolation of MMTV, RhoB and RhoA DNA and confirmation of insertion in the correct orientation of RhoB and RhoA sequences in the MMTV vector	142

Figure 33.	RhoA, but not RhoB DNA insertion is confirmed in MMTV vector after restriction enzyme digestion	146
Figure 34.	pcDNA3 vector is linearized by KpnI and XhoI digestion and MMTV-RhoB is inserted into the plasmid	148
Figure 35.	MMTV-RhoB insertion into the pcDNA3 vector is verified by the presence of the 2.7 kb MMTV-RhoB ligation band	151
Figure 36.	Verification of the integration of the 600 bp MMTV-RhoB insert	153
Figure 37.	Final isolation of MMTV-RhoA and MMTV-RhoB transgenes	154
Figure 38.	Southern blot of DNA from transgenic founder mice confirms integration of RhoA or RhoB into the host genome	157
Figure 39.	Schematic for generation of MMTV-RhoB and MMTV-RhoA constructs for generation of transgenic mice that over express human HA-RhoB and HA-RhoA under the MMTV promoter	163
Figure 40.	RhoB, but not RhoA overexpression results in a significant delay in ErbB2-mediated tumor onset	168

Figure 41. Tumors from EB and EA transgenic mice express RhoB and RhoA as determined by detection of HA by western blot

171

Tumor Suppressive Effects of the Beta-2 Adrenergic Receptor and the Small GTPase RhoB

Adam Carie

ABSTRACT

Receptor tyrosine kinases such as ErbB2 contribute greatly to human malignant transformation, but the role that other receptors such as the β 2 adrenergic receptor play in cancer is ill defined. Furthermore, while some GTPases such as Ras and RhoA promote oncogenesis, RhoB has been suggested to have tumor suppressive activity. In this thesis the tumor suppressive activity of β 2 adrenergic receptors (β 2 AR) through blockade of the Ras/Raf/Mek/Erk pathway is demonstrated. Furthermore, this thesis provides strong evidence in support of a tumor suppressive activity of RhoB, but not RhoA, in delaying ErbB2 mammary oncogenesis in a transgenic mouse model.

Chapter 1 describes a chemical biology approach that identifies a beta 2 adrenergic receptor agonist, ARA-211 (also known as pirbuterol) that suppresses the growth of cultured cells and of human tumors grown in nude mice by a mechanism involving stimulation of the β 2 AR, cAMP production and activation of PKA, which in turn leads to the inactivation of C-Raf, Mek1/2 and Erk1/2. Chapter 2 describes the translation of these findings by ex-vivo treatment of fresh

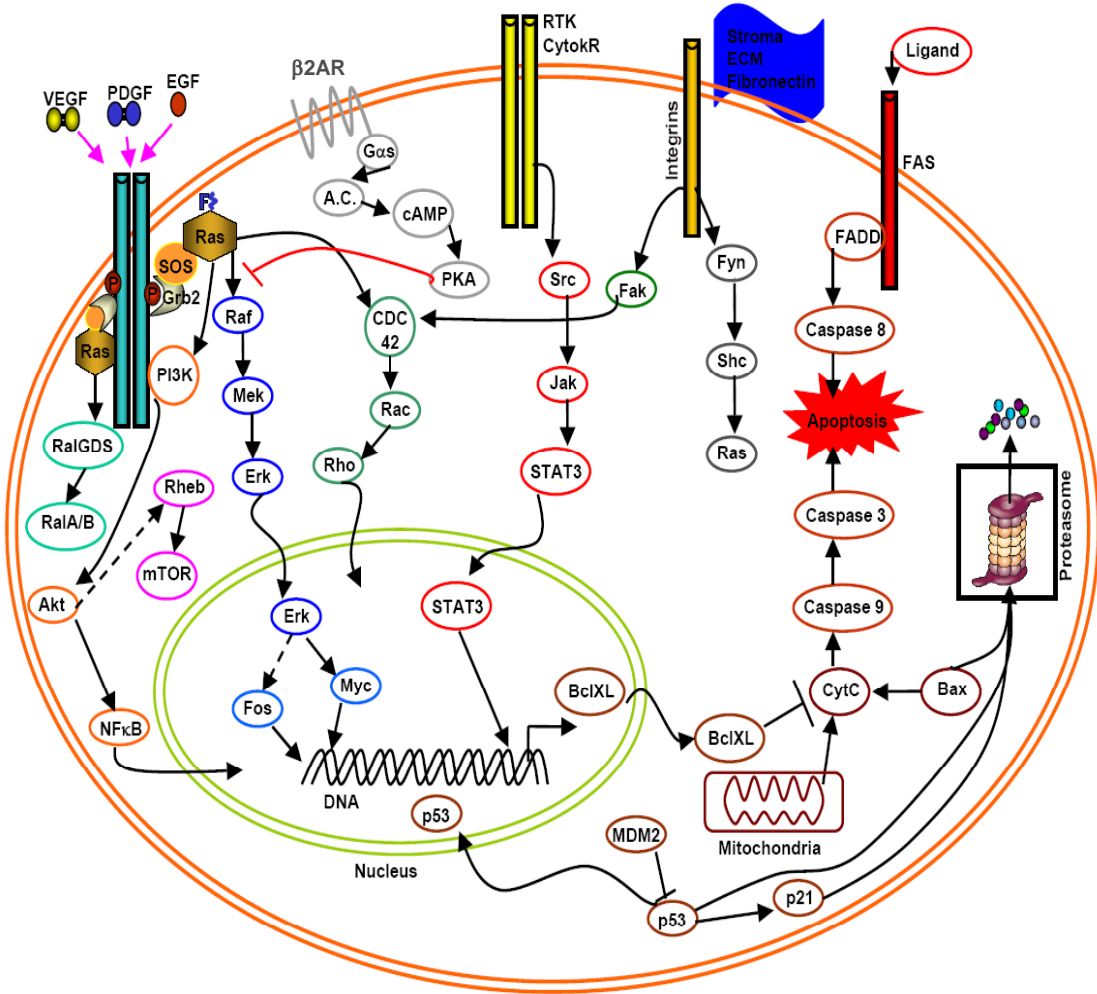
human tumor biopsies, with the ultimate goal of validating this novel therapeutic approach. Chapter 3 describes the generation of transgenic mice that overexpress ErbB2 along with either RhoB or RhoA to determine the effects of these two small GTPases on ErbB2-mediated mammary tumorigenesis. The findings indicate that overexpression of RhoB, but not RhoA, results in decreased multiplicity and delay in the tumor onset mediated by ErbB2 overexpression.

In summary, this thesis work resulted in the discovery of how crosstalk between the β 2 AR/cAMP/PKA circuit with the Raf/Mek/Erk1/2 cascade leads to tumor suppression; and the discovery of the suppression of ErbB2-mediated breast cancer by the GTPase RhoB.

Background and Significance

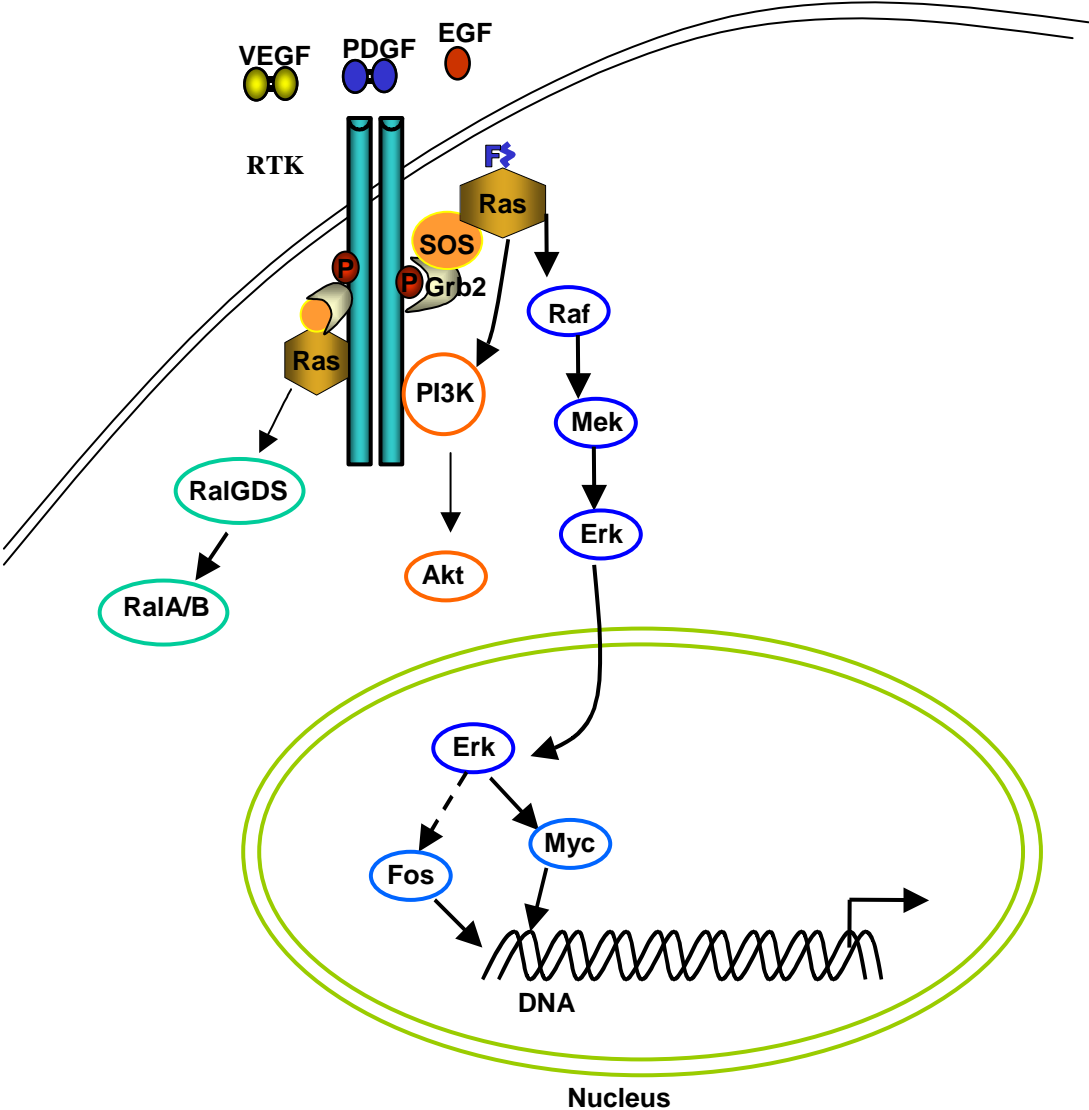
Accumulation of genetic alterations by overexpression or hyperactivation of oncogenes and inactivation or deletion of tumor suppressor genes leads to aberrant signal transduction, which confers the transforming cellular properties that result in hallmarks of cancer. These properties include self-sufficiency in growth signals and resistance to anti-growth signals, evasion of apoptosis, the ability to induce and sustain angiogenesis, the capacity to metastasize and invade foreign tissue, and the potential to replicate limitlessly. Ultimately, the aberrant signal transduction provides a mechanism for the transformation of normal cells to malignant. In general, this aberrant signaling will be the focus of my thesis, however, there are a multitude of irregular signaling pathways found in cancer cells. Figure 1 demonstrates just a few of the many pathways known to be misregulated in cancer.

Figure 1. Cancer cells contain numerous, aberrant signal transduction circuits



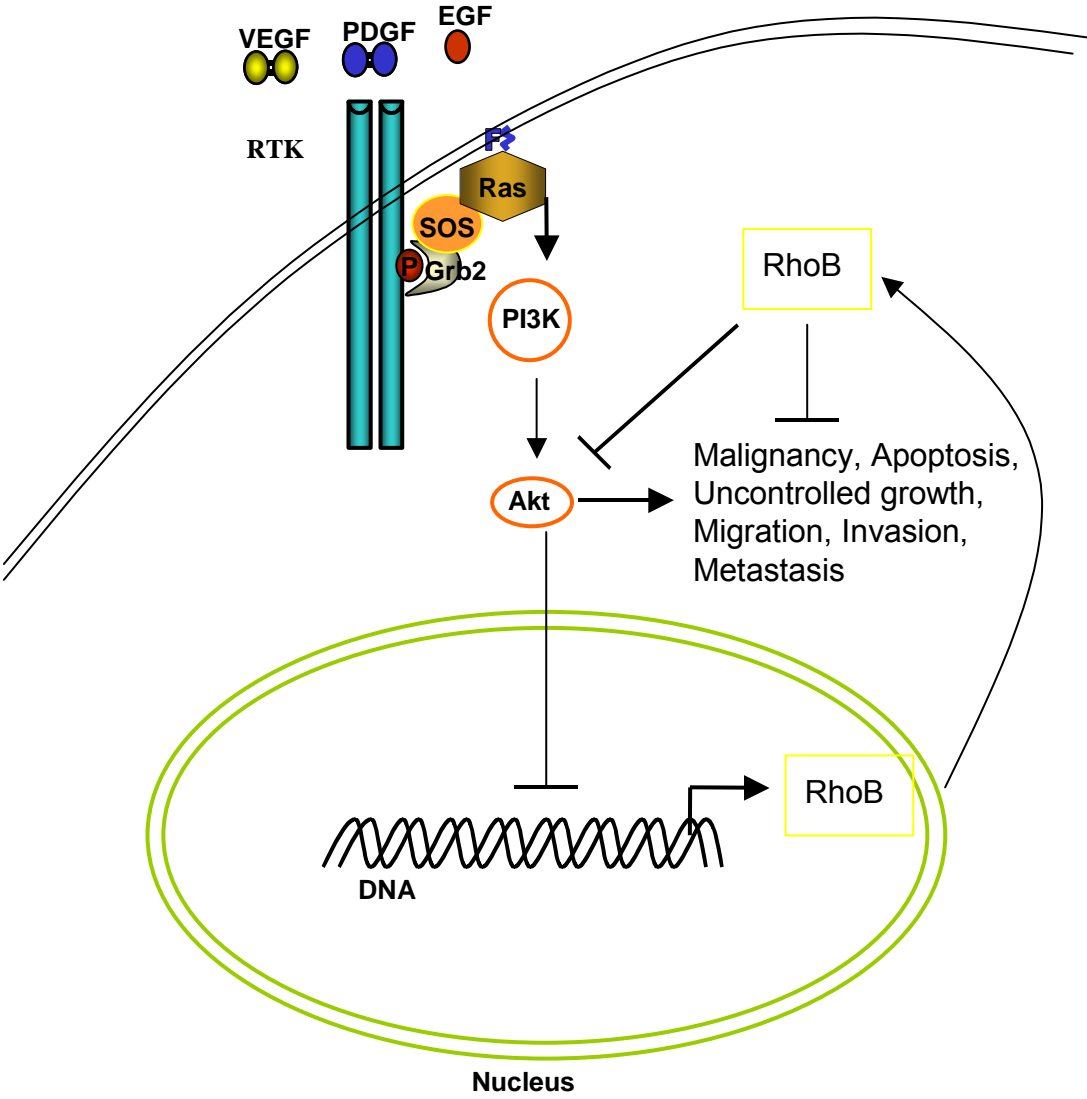
One of the major signal transduction pathways that become aberrant in cancer is that of receptor tyrosine kinases (RTKs). For example, receptor overexpression or mutation of kinase domains leads to persistent activation of downstream signals. The ErbB family of receptor tyrosine kinases is the most intensely studied. There are four members of the ErbB family: ErbB1 (EGFR, Epidermal Growth Factor Receptor), ErbB2, ErbB3 and ErbB4(1). Ligands for these receptors induce homo or heterodimerization leading to activation of intracellular tyrosine kinase domains(2, 3). There is no known ligand for ErbB2, but epidermal growth factor (EGF) can induce heterodimerization of ErbB1 and ErbB2(4, 5). Similarly, neuregulins are known to activate ErbB3 and ErbB4, which can both complex with ErbB2(6). When activated, ErbB2 heterodimers are potent signal transducers, in part, due to their relatively slow rates of receptor internalization and ligand dissociation(4, 7). ErbB2 gene amplification leading to receptor overexpression is common among breast cancer, occurring in approximately 26% of all cases(8). Signal transduction pathways downstream of ErbB2, and many other growth factor receptors, become aberrant in cancer, including persistent activation or mutation of Ras proteins(3). Ras is a central signaling node found mutated in 30 % of all human tumors(9) that confers transforming signals through activation of downstream cascades such as Raf/Mek/Erk, PI3K/Akt and RalGDS/RalA and RalB, as shown in Figure 2. These signals have been shown to result in cell proliferation, survival and metastasis when hyperactive(10).

Figure 2. Aberrant signaling through receptor tyrosine kinases (RTKs) and downstream signaling through Ras is well characterized



In addition to Raf, PI3K and RalGDS mediating Ras cancer-causing activity, other small G-proteins such as RhoA also mediate Ras oncogenesis. The mechanism by which Ras communicates with RhoA is unknown, but there is evidence supporting indirect activation of RhoA by Ras resulting in proliferation and increased cell motility(11, 12). There is evidence supporting regulation of RhoA and Rac1 activity by the Mek/Erk MAPK pathway(13). Rho kinase (RhoK) is an immediate downstream effector of RhoA that stimulates proliferation and migration, possibly through c-MYC as a downstream effector(14). Surprisingly, a close family member of RhoA, RhoB which shares 86% amino acid identity with RhoA, has been suggested to have tumor suppressive activity. Our lab and others have demonstrated *in-vitro* that overexpression of RhoB, but not RhoA, antagonizes the transforming activity of ErbB2, EGFR, H-Ras, PI3K and Akt, but not c-Myc(15, 16). These studies also provide evidence supporting the anti-tumor effects of RhoB through inhibition of phospho-Akt as illustrated in Figure 3.

Figure 3. RhoB, a close family member of RhoA, antagonizes Ras malignant transformation and has been suggested to have tumor suppressive activity



Furthermore, other groups have demonstrated that RhoB is mainly localized to endosomes and can limit cell proliferation, survival and invasion and metastasis(17, 18). RhoB has been suggested to target K-Ras, B-Raf, Cdc6, spindle checkpoint assemblies, and Lipocortin to induce apoptosis regulated by inhibition of farnesyl transferase for cancer therapy(19). RhoB knockout mice studies show that RhoB is not essential to normal development, however the mice showed an increased sensitivity to chemical carcinogenesis by 7,12-dimethylbenz[α]anthracene as well as increased efficiency of intraperitoneal tumor formation(20). Likewise, mouse embryonic fibroblasts lacking RhoB showed increased sensitivity to Ras and E1A transformation-mediated cell adhesion, and increased sensitivity to TGF β signaling(20). Also, targeted ablation of RhoB in transformed cells was shown to protect cells from Taxol-induced apoptosis, but not doxorubicin or UV irradiation, suggesting an apoptotic checkpoint role of RhoB in actin cytoskeleton remodeling(21). Similarly, IHC studies in paraffin-embedded tumor specimens from lung and head and neck cancer patients have demonstrated that RhoB expression is decreased as cancers progress from hyperplastic to deeply invasive carcinoma by immunohistochemistry(22, 23). Finally, oncogenic proteins such as ErbB2, EGFR, Ras, PI3K and Akt all repress the expression of RhoB at the transcriptional level(15). Taken together, these studies suggest that as normal cells acquire initial genetic alterations, RhoB is induced and serves as a gatekeeper to suppress the growth and induce apoptosis of these cells. However, as the cells accumulate more genetic alterations such as ErbB2, EGFR, Ras, PI3K and Akt, these transcriptionally

repress RhoB. Support for this hypothesis was provided by the Sebti lab that showed that forced expression of RhoB reverses malignant transformation by these oncogenes(15). However, *in-vivo* evidence in animal models to support the above hypothesis is lacking. Chapter 3 of this Thesis provides evidence for the role of RhoB, but not its closely related family member RhoA, in suppressing human ErbB2-driven breast cancer in a mouse model where ErbB2 expression is regulated by the mouse mammary tumor virus (MMTV) promoter. This model is highly relevant to human breast cancer where ErbB2 is believed to contribute to at least 26% of the progression of this disease(24). In Chapter 3 the RhoB and RhoA transgenic mice were crossed with the ErbB2 overexpressing mice to study the effects of RhoB and RhoA overexpression on ErbB2-mediated tumor onset, multiplicity and growth rate.

In Chapter 1 and 2 of this thesis the relevance of the crosstalk between the Ras/C-Raf/Mek1/2/Erk1/2 and the beta 2 adrenergic receptor (β 2 AR) signaling circuits to suppression of tumor growth is studied. The β 2 AR is a well-studied and characterized pathway in normal cell physiology. However, we became interested in this signal transduction pathway as we initially searched for novel inhibitors of the Raf/Mek/Erk kinase cascade. Adrenergic receptors belong to a large super-family of membrane spanning proteins known as G-protein coupled receptors. This family contains over 500 members, each containing a membrane-spanning domain of seven α -helices principally made up of 22-28 hydrophobic amino acids each(25-27). When a ligand binds its specific receptor a conformational change takes place that allows for the activation of specific

heterotrimeric G-proteins. Upon activation, the G-proteins active subunit, such as $G_{\alpha s}$, releases GDP and binds GTP, allowing the active subunit to dissociate from the other subunits (such as β & γ) and affect other proteins in its signal transduction pathway. In some cases the $\beta\gamma$ -dimer can also transmit signals that mediate receptor response. It is well documented that adrenergic receptors regulate many facets of the sympathetic nervous system. One of the first second messenger systems discovered was the adrenergic receptor-cAMP- Ca^{++} -pathway. Stimulants such as epinephrine and isoproterenol bind the β -adrenergic receptors resulting in the release of $G_{\alpha s}$ subunits, which stimulate the enzyme adenylyl cyclase(28, 29). Adenylyl cyclase then catalyses the conversion of ATP to cAMP, leading to the activation of cAMP-dependant protein kinases, ultimately resulting in the opening of Ca^{++} channels and a biological response such as increased heart rate(30, 31). On the other hand, inhibitory agonists such as adenosine cause the release of inhibitory $G_{\alpha i}$ subunits that decrease adenylyl cyclase activity. The extensive research in this area of adrenergic receptor function has lead to the discovery of many small molecule drugs that target the different receptors, and lead to physiological responses in heart rate, smooth muscle contraction or dilation and nerve conduction. More recent research has demonstrated that cAMP signaling can modulate normal cell proliferation through crosstalk with signal transduction pathways such as the Raf/Mek/Erk1/2 kinase cascade.

Cell proliferation in complex organisms is controlled by numerous systems involving hundreds of different proteins and signaling mechanisms. One way in

which cAMP is involved in cell proliferation is through the modulation of the mitogen activated protein kinase (MAPK) cascade. The effects of cAMP on the levels of Erk1/2 activation in normal cells are widely variable depending on the type of cells and the intracellular pathways that crosstalk in these cells. One mechanism in which ERKs are activated via cAMP has been shown to involve stimulation of B-Raf, which activates the Mek/Erk1/2 pathway(32, 33). The means through which cAMP activates B-Raf is still unclear, yet probable mechanisms have been proposed involving PKA, Src, and Rap-1(32-35). In cells that express B-Raf it is suggested that Rap-1 activation by Src leads to stimulation of B-Raf and ultimately in the activation of Erk1/2(34). Furthermore, In some leukemia and normal kidney cells studies have shown that cAMP-GEFs, or EPACs (exchange proteins directly activated by cAMP), have an affinity for Rap-1(36-38). This demonstrates yet another mechanism in which cAMP can stimulate Erk1/2 activity, but in a PKA-independent manner. While in many normal cells, such as rat thyroid cells, bone cells, polycystic kidney epithelium, Sertoli cells, cardiac myocytes, granulosa cells, pre-adipocytes, pituitary cells and PC12 cells, cAMP has been shown to stimulate Erk1/2 and proliferation(39-46), only one study in leukemia cells has shown that EPACs activate Erk1/2(47).

There have also been a multitude of mechanisms proposed for the inhibitory consequences of cAMP on the proliferation of normal cells, such as in adipocytes, endothelial cells, NIH 3T3 cells, rat fibroblasts, smooth muscle cells, hepatocytes and pancreatic acinar cells(40, 48-56).. The mechanisms by which this could occur include inhibition of Erk1/2 through a PKA-dependent activation

of Rap-1, up-regulation of Erk phosphatases (MKPs), and inhibition of Raf-1 kinase activity via direct phosphorylation by PKA(49, 57-61). A generally accepted mechanism in which cAMP inhibition of Erk1/2 takes place is through the ability of PKA to block Raf-1 activity. Upon cAMP stimulation the catalytic subunits of PKA are free to phosphorylate downstream targets, including Raf-1. Phosphorylation of Raf-1 by PKA on serine 621 inhibits the Raf-1 kinase domain(50, 52, 62-65). Other inhibitory phosphorylation sites on Raf-1 have been proposed, including serine 259 and 43, but it is not known if PKA subunits phosphorylate these sites *in-vivo*. An alternative mechanism that has been proposed is that of PKA activating c-Src, in turn activating Rap-1, which in the absence of B-Raf, competes with C-Raf for binding sites to Ras(34, 37, 38, 59). While in normal cells extensive studies have investigated the role of cAMP in cell proliferation, only a few studies were carried out in tumor cells. These studies showed that in breast cancer and neuroblastoma cancer cells, cAMP induction results in inhibition of DNA synthesis and induction of apoptosis, respectively(66, 67). However, the effects of cAMP on inhibition of the Ras/Raf/Mek/Erk pathway has not been investigated in tumors. We believe that there is an unmet need to investigate whether stimulation of the adrenergic receptor can be used as a novel approach to cancer chemotherapy. Fundamental questions that need to be addressed include first to determine whether there is crosstalk between the β AR signaling circuit and the Ras/Raf/Mek/Erk circuit. Second, if this crosstalk exists, then to determine whether β AR stimulation results in activation or inactivation of the MAPK pathway, and whether this affects several hallmarks of cancer cells

such as uncontrolled proliferation, anchorage-dependent and -independent growth, apoptosis and tumor growth in animals. Third, the mechanism of the crosstalk should be investigated as well. Therefore, determining how, for example, stimulation of the β AR regulates the Raf/Mek/Erk circuits in cancer is of prime importance. Other important questions that need to be addressed are determining the types of β AR involved (i.e. β 1 or β 2). Finally, the prevalence of the β AR circuits in fresh tumor biopsies, especially those that contain persistently activated Ras/Raf/Mek/Erk signaling needs to be investigated. Chapters 1 and 2 of this Thesis will address the important issues above.

Chapter 1

A Chemical Biology Approach Identifies a Beta-2 Adrenergic Receptor Agonist that Causes Human Tumor Suppression by Blocking the C-Raf/Mek1/2/Erk1/2 Pathway

Data from this Chapter was published by Adam Carie and Said Sebti in the journal *Oncogene*, issue 26, 3777-3788, 2007.

All of the work in this Chapter was performed by Adam Carie except for Figure 1 cyto blot, which was performed by Adrian Kenny

Abstract

A chemical biology approach identifies a beta 2 adrenergic receptor (β 2AR) agonist ARA-211 (pirbuterol), which causes apoptosis and human tumor regression in animal models. β 2AR stimulation of cAMP formation and PKA activation leads to C-Raf (but not B-Raf) kinase inactivation, inhibition of Mek1/2 kinase and decreased phospho-Erk1/2 levels. ARA-211-induced inhibition of the C-Raf/Mek1/2/Erk1/2 pathway is mediated by PKA and not EPAC. ARA-211 is selective and suppresses P-Erk1/2 but not P-JNK, P-p38, P-Akt or P-STAT3 levels. β 2AR stimulation results in inhibition of anchorage-dependent and -independent growth, induction of apoptosis in vitro and tumor regression in vivo. β 2AR antagonists and constitutively active Mek-1 rescue from the effects of ARA-211 demonstrating that β 2AR stimulation and Mek1/2 kinase inhibition are required for ARA-211 antitumor activity. Furthermore, suppression of growth occurs only in human tumors where ARA-211 induces cAMP formation and decreases P-Erk1/2 levels. Thus, β 2AR stimulation results in significant suppression of malignant transformation in cancers where it blocks the C-Raf/Mek1/2/Erk1/2 pathway by a cAMP-dependent activation of PKA, but not EPAC.

Introduction

Malignant transformation of normal cells to cancer cells requires the acquisition of several oncogenic traits such as uncontrolled cell division, resistance to programmed cell death (apoptosis), invasion and angiogenesis(68). These malignant transformation traits are believed to be the consequence of the accumulation of genetic alterations that result in deregulated signal transduction circuits(68). Such genetic alterations can simply be point mutations that result in constitutive activation of key signal transducers such as Ras, a GTP/GDP (guanosine triphosphate/guanosine diphosphate) binding GTPase that contributes to 30% of all human cancers(9). Alternatively, these alterations can involve entire genes such as the receptor tyrosine kinases epidermal growth factor receptor and ErbB2 that are found over expressed in many major human cancers such as breast tumors(69, 70). Often such genetic alterations result in constitutive activation of common downstream signal transduction pathways such as the mitogen activated protein kinase (MAPK) cascades of several serine/threonine kinases including C-Raf, Mek1/2, Erk1/2, p38 and JNK (Jun kinase)(64, 71-73). Other pathways involved in uncontrolled proliferation, apoptosis, invasion and angiogenesis also include those mediated by the signal transducer and activator of transcription 3 (STAT3) and the serine/threonine

kinase Akt(74, 75). Not only have these oncogenic and tumor survival pathways been found constitutively activated in the great majority of human cancers, but also their hyperactivation has been associated with poor prognosis and resistance to chemotherapy in cancer patients(69, 70). This has prompted drug discovery efforts targeting receptor tyrosine kinases, Ras, C-Raf, Mek, Akt and STAT3 to thwart aberrant signal transduction pathways in tumor cells (65, 76-79). For example, inhibitors of receptor tyrosine kinases (RTKs), Ras, C-Raf and Mek1/2 have all been identified and are at various stages of development(63, 80). Some, like the epidermal growth factor receptor (EGFR) kinase inhibitor Tarceva, was approved by the FDA for the treatment of patients with lung cancer(81).

Genetic abnormalities that often predispose or lead to cancer, such as overexpression of growth factors, mutations leading to constitutive activation of cellular receptors, deletion or misregulation of tumor suppressors, or uncontrolled signal transduction pathways often signal directly through the small GTPases Ras. Ras proteins are central nodes in the cellular signaling response from growth factors and receptors. They are localized to the cellular membrane regions by a lipid post-translational modification known as prenylation(9, 82-87). Ras activation occurs through the exchange of guanosine diphosphate nucleotides for guanosine triphosphate nucleotides catalyzed by exchange factors known as GEFs (guanosine nucleotide exchange factors). Activated Ras proteins can interact with more than 20 downstream effectors, the best-characterized being Raf, PI3K (phosphatidylinositol-3'-kinase), and Ral

GTPases. These effectors are responsible for the proliferative, prosurvival, and differentiation effects from Ras signaling(9, 82-87).

RasGTP-mediated prosurvival signaling occurs at least in part through activation of the regulatory subunit of PI3K, which targets it to the membrane to phosphorylate PIP2 (phosphatidylinositol-4,5-bisphosphate), converting it to PIP3 (phosphatidylinositol-3,4,5-triphosphate)(74, 88, 89). PIP3 recruits PDK and Akt through their PH domains, which leads to the phosphorylation of Akt by PDK1 and other kinases(74). Akt is a kinase that has been shown to phosphorylate and inactivate pro-apoptotic proteins including BAD and FKHR (forkhead homologue 1) transcription factors, leading to survival under circumstances that cells would normally undergo apoptosis(74). Furthermore, PI3K has been shown to activate Rac, a Rho family protein that is important for cytoskeletal rearrangement leading to transformation, invasiveness and metastasis(90-93). The PI3K/Akt pathway has been the focus of major drug discovery and development efforts for cancer therapy.

Another important cellular signaling component downstream of Ras is the Ral GDS/Ral pathway. Ral GEFs, such as RalGDS (Ral guanine nucleotide-dissociation stimulator), activate the Ras-like Ral GTPase proteins RalA and RalB. Similar to Ras, the Ral proteins are reliant on prenylation, whereby a 20-carbon lipid geranylgeranyl group is added to the C-terminus, leading to membrane anchorage for downstream signaling to effectors(94-98). The downstream effectors of RalA and RalB have been suggested to be involved in early transforming events due to aberrant Ras signaling. Recently, in cell culture

models, the RalGEF-Ral pathway was shown to be required for Ras mediated transformation(94, 95). Likewise, in a knockout mouse model lacking RalGDS, skin tumors from carcinogen-induced Ras showed impaired growth(99). Although RalA and RalB share 85% sequence identity, it has recently been discovered that these proteins play distinct roles in anchorage-independent growth and cell survival, respectively(94). Furthermore, our lab has demonstrated that Ral proteins are exclusively geranylgeranylated, and that inhibition of the geranylgeranylation of RalB mediates GGTI-induction of apoptosis and inhibition of anchorage-independent growth. In contrast, inhibition of RalA geranylgeranylation mediates GGTI-induced inhibition of anchorage independent growth(94). Currently, GGTI compounds are still in preclinical development; however, clinical candidates are not far off from human trials. Development of GTPase inhibitors is in its infancy compared to the efforts to develop selective kinase inhibitors. One of the first discovered and most targeted kinase pathways is downstream of Ras, and belongs to the mitogen activated protein kinase (MAPK) family.

MAPKs are the effectors in a line of kinases that transduce signals from growth factors and mitogens from the cell surface to the nucleus. With a large number of activators the specific physiological message of the external ligand is translated into cellular responses. Depending on the stimuli, these responses include proliferation, differentiation, and survival. There are four major families of mammalian MAP kinase proteins. They are all known to be activated by growth factors, but only the Raf/Mek/Erk pathway has not been linked to stress

activation. The p38, JNK and Erk5 pathway are activated by cellular stress, as well as by cytokines and growth factors(100). The signaling circuitry provides three steps at which signaling can be positively or negatively regulated. Once activated by upstream signals, the first MAP kinase kinase kinase (MAPKKK) phosphorylates MAP kinase kinase (MAPKK), which in turn, phosphorylates MAPK kinase (MAPK) to target transcription factors to either activate or repress gene expression(100). These kinases are evolutionarily conserved among mammals and are important for development as well as homeostasis.

The Ras/Raf/Mek/Erk kinase cascade has been scrutinized and targeted in the past 20 years. Ras activation of Raf proteins, most notably C-Raf and B-Raf, leads to activation of Mek kinases(87, 101, 102). The pathway bottlenecks at Mek, as Mek1 and Mek2 are the only known activators of Erk1 and Erk2. These terminal serine threonine kinases phosphorylate and regulate over 150 different proteins(103). Most of the activated Erk1/2 goes to the nucleus where it activates transcription factors that control gene expression and functions such as cell proliferation and evasion of apoptosis(104). These effectors play an important role in the oncogenic signaling of Ras.

The Raf serine/threonine kinases (A-Raf, B-Raf and C-Raf or Raf-1) are best known for their activation of downstream Mek kinases. The isoforms are similar in their effectors, but have different expression profiles. C-Raf is ubiquitously expressed, where A-Raf is generally found in the urogenital organs, and B-Raf is primarily neuronal(65). Retroviral Raf protein is a potent oncogene whose constitutive activation results in cellular transformation. The B-Raf

isoform is found mutated in many human tumors, including melanoma, colon, lung and thyroid tumors(105-107). The majority of mutations of B-Raf found in cancer are of the V600E variety(106). The most recent molecularly targeted therapies against mutated B-Raf have poor preclinical profiles or off target effects(108). However, a newly developed inhibitor, PLX4720, demonstrates selective inhibition of mutated B-Raf kinase activity and promising antitumor efficacy for melanoma(109). C-Raf and B-Raf both mediate signals downstream of Ras. Ras activation brings Raf to the membrane where it interacts with many signaling partners. This interaction results in the phosphorylation of Raf. The activation or inhibition of C-Raf kinase activity is dependent on the tyrosine, serine or threonine amino acid site where the phosphorylation events occur(110, 111). Known activators of C-Raf include Src and PKC, which phosphorylate C-Raf on S388, T491, S494 and S499(112). Deactivators include Akt and PKA, which phosphorylate C-Raf on S43, S621 and S259(112). Although many pathways feed into Raf signaling, currently the only validated physiologically relevant downstream targets of C-Raf are the Mek1/2 MAP kinase proteins(111). C-Raf has been widely targeted for cancer therapy. Both small molecule inhibitors as well as anti-sense oligonucleotides (oligo) have been developed to inhibit C-Raf signaling. A lipid-encapsulated C-Raf oligo known as LErafAON finished phase I studies in 2006, and is currently undergoing further clinical development(113). Sorafenib, the most successful small molecule inhibitor of C-Raf kinase, was approved by the FDA for renal cell carcinoma. Upon further clinical and preclinical investigation it was found that Sorafenib not only inhibits

C-Raf and B-Raf kinase activities, but also VEGF, PDGF, Flt3, c-Kit and FGFR signaling(114). Currently Sorafenib is undergoing further clinical investigation for single and combination therapy in hepatocellular carcinoma, non-small cell lung cancer, pancreatic cancer, breast cancer, melanoma, and hematological malignancies(115). The success of Sorafenib as a multi-kinase inhibitor has led to the approval of Sunitinib, an inhibitor that targets Raf along with VEGF-R, PDGF-R and c-Kit signaling. Sunitinib is currently approved for renal cell carcinoma and Imatinib-resistant GIST (gastrointestinal stromal tumors), and is now considered the gold standard of care for these diseases. The success of these compounds in the clinic has led to debate as to whether molecularly targeted therapies for cancer need to be highly specific or broadly specific. Due to the multi-faceted broad spectrum of proteins inhibited by Sorafenib and Sunitinib, it is difficult to determine from this example if blocking Raf kinase activity selectively will be beneficial as a mono-therapy for cancer. However, the number of inhibitors presently clinically available has validated targeting the Raf/Mek/Erk pathway for cancer, whether at the Raf or Mek level.

The MAPK cascades continues downstream of Raf activation with Mek phosphorylation. Mek1 and Mek2 belong to a gene family comprised of 5 Mek proteins altogether. Mek1 and 2 are highly homologous, differing only in the proline-rich region among the kinase sub-domains 9 and 10(116). The proline rich domain is necessary for Raf binding and activation, and this difference may confer substrate specificity for the binding affinity of the different Raf isoforms(117). Mek1 and 2 are also the only known activators of Erk1/2,

representing a classic bottleneck in cell signaling. Several studies have shown that constitutive activation of the Mek pathway is associated with different cancer types, including hepatocellular carcinoma, renal cell carcinoma, breast cancer, squamous cell carcinoma, AML (acute myelogenous leukemia) and CML (chronic myelogenous leukemia) (reviewed in (65)). Therefore, Mek kinase activity has been a sought-after target for cancer therapy. The first inhibitors of Mek activation were developed in the mid-1990's. PD098059 and U-0126 both inhibit the activation of Mek, but did not fit the pharmacological profile necessary for development. The lack of solubility and bioavailability prompted the search for more Mek inhibitors. The first Mek inhibitor to demonstrate antitumor efficacy in mouse models, and subsequently the first to move to clinical trials, was CI-1040. In mouse models CI-1040 inhibited human and mouse colon tumors by as much as 80 percent(77). CI-1040, like PD98059 and U-0126, is noncompetitive with ATP. It binds an allosteric site on Mek, preventing its activation. Phase I and II studies, however, showed that CI-1040 lacked the sufficient antitumor activity, metabolic stability, and bioavailability for further development. Currently there are 2 promising Mek inhibitors undergoing phase II clinical trials. PD-0325901 and AZD6244 are both orally available, selective Mek inhibitors that are noncompetitive with ATP. Both compounds are well tolerated in the clinic, and have been shown to inhibit P-Erk1/2 levels in biopsies of human tumors as well as in peripheral blood mononucleocytes (PBMCs). Dosing with either of the Mek inhibitors alone have yet to show objective response, however stable disease was reported in 12-28 percent of patients. Future efforts for developing these

Mek inhibitors include combination trials to inhibit other known signaling pathways common to cancer progression, such as the PI3K pathway.

The final step in the MAP kinase pathway is the activation of extra-cellular signal-regulated kinase 1 and 2 (Erk1/2), also known as p44 and p42 MAP kinases. There has been a positive correlation with overexpression or constitutive activation of Erk1/2 in both human tumors and tumor cell lines. Likewise, activation is also involved in many physiologically relevant events such as cell motility, proliferation, differentiation, and survival(71, 118, 119). Erk1/2 have been shown to be rapidly phosphorylated downstream of growth factor signaling. Activating phosphorylation events by Mek1 and Mek2 have been described on threonine 183 and tyrosine 185 (116, 120). These activating phosphorylation events allow Erk1/2 to translocate to the nucleus where they target the transcription factors Elk-1, c-Fos, and c-MYC, among others. These targets are thought to be responsible for proliferative effects of Raf/Mek/Erk signaling, as they are tied to increasing transcription of cell cycle regulators and DNA synthesis machinery. Aside from translocation to the nucleus, activated Erk1/2 proteins also activate cytoplasmic signaling modifiers such as microtubule-associated proteins, ribosomal protein S6 kinase, SHP2, EGFR, SOS, C-Raf and Mek(121, 122). The turnover of phosphorylated Erk proteins is mediated by regulatory protein phosphatase that remove the activating phosphate groups from the proteins. Loss of these phosphatases has been described in neoplasia, and is currently targeted for therapeutic intervention. The most characterized phosphatases for Erk1/2 is the mitogen-activated protein phosphatase-1 (MKP-

1). MKP-1 is a dual-specificity, serum-inducible phosphatase selective for Erk1/2 over Mek1(123). Loss of MKP-1 is correlated with increasing grades of prostate, colon, and bladder cancer(124, 125).

In normal cells, the regulation of the MAP kinase pathway is complex. While it is well established that the activation of Erk kinases is regulated by receptor tyrosine kinases such as EGFR and PDGFR via activation of Ras (64, 71-73), more recently, adrenergic receptor (AR) stimulation of cAMP has also been shown to regulate the activation of Erk1/2 in normal cells (reviewed in (34, 36, 126, 127)). For example, in some normal cells such as cardiac myocytes and bone cells cAMP was shown to activate Erk1/2, whereas in others such as adipocytes and endothelial cells it was shown to inhibit Erk1/2 activation(33, 50, 59, 128, 129). The mechanism for the crosstalk between the heterotrimeric G proteins and MAP kinase pathway in normal cells is still relatively unclear, with many signaling mechanisms proposed depending on cell types. Activation of the β_2 AR results in release of the activating subunit $G_{\alpha s}$, which stimulates the enzyme adenylyl cyclase to convert ATP to cAMP. cAMP is a classic second messenger that signals to multiple substrates and controls many physiological events. cAMP activates both protein kinase A (PKA) as well as guanine nucleotide exchange factor EPAC1 and 2 (Exchange Proteins Activated by cAMP), resulting in two different pathways in which communication with C-Raf occurs. In normal cells, PKA is known to phosphorylate C-Raf on multiple serine residues (S43, S259, S233) that inhibit the kinase activity or activation of Raf(112). Likewise, EPAC activation results in GTP-binding and activation of

Rap1, which can compete with C-Raf for binding sites on Ras. Ultimately this competition results in decreased activation of C-Raf and inhibition of downstream MAP kinase signaling. Alternatively, in astrocytes, thyroid cells, kidney cells and megakaryocytic cells it has been shown that cAMP-mediated activation of Rap-1 can result in activation of B-Raf through Src signaling, leading to increased Erk1/2 phosphorylation and cell proliferation(34). In tumor cells, however, little is known about adrenergic receptor regulation of Erk1/2 activation. In this Chapter of the thesis we demonstrate that stimulation of the β 2AR induces significant tumor growth suppression in human cancers where this stimulation results in the inactivation of the C-Raf/Mek1/2/Erk1/2 pathway by a cAMP-dependent activation of PKA, but not the Rap1 guanine nucleotide exchange factor EPAC.

Materials and Methods

Cell Lines and Transfections

All cell lines used were obtained from American Type Tissue Collection (ATCC), (Manassas, VA), or from the DCTD Tumor Repository, (Frederick, MD). Propagation was carried out according to ATCC protocols. Propagation media was obtained from Invitrogen Corporation (Carlsbad, CA). DNA transfections were carried out using TransIT-LT1 transfection reagent (Takara Mirus, Madison, WI) according to the manufacturer's protocol. Briefly, 4×10^5 MDA-MB-231 cells were grown to approximately 70% confluency in medium supplemented with 10% FBS (Atlanta Biologicals, Atlanta, GA) in the absence of antibiotics. For transfection, LT1 was pre-incubated in 200 μ l per transfection in Opti-MEM (Invitrogen) for 20 minutes prior to addition of plasmid. 2 μ g of plasmid DNA (pFC-Mek Stratagene, La Jolla, CA) per transfection was incubated with the Opti-MEM/LT1 mixture for 20 minutes after which the transfection mixture was added to cells and incubated at 37°C for 48 hours. At that time, cells were then treated with either DMSO or ARA-211 (10 μ M) for 48 hours and subsequently assayed for proliferation via Alamar Blue metabolism and harvested for western blot analysis as described below.

Cytoblot Screening for Small Molecules that Decrease Phospho-Erk1/2

MDA-MB-231 cells were plated into sterile, white opaque, 96 well tissue culture plates at a density of 25,000 cells/well, cells were allowed to attach overnight and were treated for 1 hour in the presence of either vehicle control, 20 μ M PD-98059 (EMD Biosciences, San Diego, CA), or 10 μ M of NCI Diversity Set of 2000 compounds (1compound/well) (<http://dtp.nci.nih.gov/>) as described by us (78). Cells were then washed, fixed for one hour at 4°C cold 3.7% formaldehyde and permeabilized for 5-min with ice-cold methanol. Cells were washed, and rocked overnight at 4°C with anti-phospho-p44/42 MAPK (Cell Signaling Technology, Beverly, MA) and Horse Radish Peroxidase conjugated anti-Rabbit IgG secondary antibody (Jackson ImmunoResearch, West Grove, PA). The plates were washed and chemiluminescence reagent added to the wells of the plates, then x-ray film directly placed on top of the plates. Quantification of the results was done using a GS-700 scanning densitometer (Bio-Rad Laboratories, Hercules, CA).

Western Blotting

Treated cell samples were lysed in 30 mM HEPES, 10 mM NaCl, 5 mM MgCl₂, 25 mM NaF, 1 mM EGTA, 1% Triton-X-100, 10% Glycerol, 2 mM Sodium orthovanadate, 10 μ g/mL aprotinin, 10 μ g/mL soybean trypsin inhibitor, 25 μ g/mL leupeptin, 2 mM phenylmethylsulfonylfluoride (PMSF), 6.4 mg/mL p-

nitrophenylphosphate for 30 minutes at 4°C, and proteins run on SDS-PAGE gels then transferred to nitrocellulose membranes. Membranes were blocked in either 5% milk in PBS, pH 7.4, containing 0.1% Tween-20 (PBS-T) or 1% BSA in TBS, pH 7.5, containing 0.1% Tween-20 (TBS-T). Phospho-STAT3 and phospho--AKT antibodies were diluted in 1% BSA in TBS-T while phospho-C-Raf, phospho-Mek, and phospho-p44/p42 MAPK antibodies (Cell Signaling) were diluted in 5% milk in PBS-T for either 1 hour at room temperature or overnight at 4°C. HRP-conjugated secondary antibodies (Jackson ImmunoResearch, West Grove, PA) were diluted in 5% milk in PBS-T or TBS-T at a 1:1000 dilution for one hour at room temperature. Western blots results were visualized using enhanced chemiluminescence. Stripping of the membranes for reblotting was done using stripping buffer (62.5 mM Tris pH 7.6, 2% SDS, 0.7% 2-mercaptoethanol) at 50°C for 30 minutes. Cells treated with ARA-211, 8CPT-2'-O-Me-cAMP, H89 and Forskolin to determine effects on P-Erk 1/2 and other signaling events by Western blot were treated for one hour at varying doses. Pre-treatment with H89 was done for 15 minutes followed by 45 minutes of ARA-211 treatment.

In Vitro Kinase Assays

MDA-MB-231 cells (2×10^6) were lysed for 30 minutes at 4°C in RIPA-150 buffer (10 mM Tris pH 7.5, 150 mM NaCl, 10% glycerol, 5 mM EDTA, 1% Triton X-100, .1% SDS, 100 μ M sodium orthovanadate, 1 μ M aprotinin, 10 μ M leupeptin, 10

μM antipain). Cell debris was pelleted at 13000 rpm for 15 minutes at 4°C and the lysate was rocked overnight with 10 μg of either C-Raf or Mek antibodies (Santa Cruz Biotechnologies, Santa Cruz, CA). 25 μl of protein A/G PLUS agarose (Santa Cruz Biotechnology) was then added and rocked for 4 hours at 4°C . Samples were spun at 2000 rpm for 5 minutes to collect the agarose beads, which were then washed four times with lysis buffer. On the final wash each pellet was divided into 5. Pellets were re-suspended in 30 μl kinase buffer (30 mM HEPES, pH 7.5, 7 mM MnCl_2 , 5 mM MgCl_2 , 1 mM dithiothreitol and 15 μM adenosine triphosphate (ATP) with either 10 μM U-0126 (EMD Biosciences) ARA-211, Raf Kinase Inhibitor (EMD Biosciences), or DMSO vehicle control. Finally, 0.5 μg Mek1 or ERK-2 peptide substrate (Upstate Biotechnologies, Lake Placid, NY) was added, followed by 20 μCi [γ - ^{32}P]-ATP per sample. Samples were then incubated at room temperature for 30 minutes and the reaction terminated by the addition of 30 μl 4x SDS-PAGE sample buffer (33% glycerol, 0.3 M DTT, 6.7% SDS, 15% β -mercaptoethanol, 0.1% bromphenol blue), which was then boiled at 100°C for 5 minutes. Samples were run on a 10% polyacrylamide gel to separate proteins; gels were dried and phosphorylation results visualized via autoradiography.

In Vivo Kinase Assay

Intact MDA-MB-231 cells (2×10^6) were treated either with vehicle control (DMSO), 10 μ M U-0126, 10 μ M Raf Kinase Inhibitor, or 10 μ M ARA-211. Samples were then processed for kinase assays as described above.

MTT Assay

2000 cells per well were plated into 96 well tissue culture plates, and the cells were allowed to attach overnight at 37°C with 10% CO₂. Cells were then treated with increasing concentrations of ARA-211, Forskolin (Sigma-Aldrich, St. Louis, MO) or vehicle (DMSO) and incubated for four days. At that time treatment medium was removed and replaced with 100 μ l of 1mg/ml MTT (Sigma-Aldrich) in media and incubated at 37°C, 10% CO₂ for 3 hours. After 3 hours the MTT media was removed and replaced with 100 μ l/well of DMSO, rocked at room temperature for 5 minutes, then absorbance read at 540 nm on a micro-plate reader.

Alamar Blue Proliferation Assay

For proliferation assays using exogenous constitutively activated Mek or the β 2AR antagonist ICI-118.551, Alamar Blue metabolism assay used to determine cell viability according to the manufacturers protocol (Biosource, Camarillo, CA). Briefly, cells were treated and grown as described above; Alamar Blue was

added to the media at a 1:10 dilution and incubated for 3 hours. Media/Alamar Blue was removed from the cells and aliquoted into 96 well plates (100µl per well) and fluorescence read on a Wallac Victor 2 plate reader at excitation 540nm, and emission 615nm.

Soft Agar Assay

Anchorage independent growth assays were performed as previously described (85). Briefly, agar was diluted to 0.3% in propagation media containing 20,000 cells and either vehicle or ARA-211 and 1ml of cell/agar mixture plated on top of 2ml of a 0.6% layer of agar in medium alone. Cells were grown for three to four weeks at 37°C, 10% CO₂ and were fed weekly with 100µl per well of media/treatment. Quantification of colonies was done using a GS-700 scanning densitometer.

Apoptosis Assay

Apoptosis was analyzed using the Cell Death Detection ELISA (Roche, Indianapolis, IN) measuring cytoplasmic histone-associated mono- and oligonucleosome DNA fragments. Procedures were carried out according to the manufacturer's protocol. Briefly, 1×10^5 cells were plated in 60mm dishes and treated with various doses of ARA-211 or vehicle for 48 hours. Cells were lysed

with the provided lysis buffer and lysate was incubated on the ELISA plate for 1 hour to capture the histone associated DNA indicative of apoptotic cells. Anti-DNA peroxidase conjugated antibody was added to detect the cleaved DNA and the microplate was washed and developed with ABTS substrate which was quantitated by microplate reader at 405nm.

Total cellular cAMP Measurement

The measurement of total cellular cAMP was done using a cAMP Biotrak™ Enzyme immunoassay (EIA) system (Amersham Biosciences, Piscataway, NJ) according to the manufacturer's protocol. Briefly, 2000 cells were plated into each well of a 96 well plate. The next day cells were treated with increasing concentrations of ARA-211 or with vehicle for one hour. Alternatively, MDA-MB-231 cells were pretreated with antagonists to the α 1 (Prazosin, Sigma), α 2 (Yohimbine, Sigma), β 1 (Metoprolol, Sigma), and β 2 (ICI 118.551, Sigma) adrenergic receptors at 100nM for 15 minutes followed by treatment with 10 μ M ARA-211 for 45 minutes. Cells were then lysed directly in the wells using the supplied lysis buffer. The lysate was transferred to a 96-well cAMP ELISA plate, and results were quantified using a Wallac Victor 2 plate reader.

PKA Kinase Assay

PKA kinase assays were performed with the SignaTECT[®] cAMP-Dependent Protein Kinase (PKA) Assay System (Promega, Madison WI) according to the manufacturer's protocol. Briefly, cells were plated (5×10^6) into 100 mm dishes and treated the next day with ARA-211, H-89 (EMD Biosciences), or vehicle for one hour. When pre-treating cells, H89 was dosed for 15 minutes following ARA-211 treatment for 45 minutes. Cells were lysed using a Dounce homogenizer and lysates were incubated in the supplied kinase reaction buffer, with ^{32}P -ATP and biotin labeled PKA peptide substrate for 5 min at 37°C . Once the reactions were quenched they were spotted onto streptavidin membranes and ^{32}P -ATP transfer was measured via scintillation counter.

Antitumor Activity in Nude Mouse Xenograft Models

Female athymic nude (nu/nu) mice, 5-6 weeks old, were purchased from Charles River (Wilmington, MA) and allowed to acclimate in the animal facility for one week. After harvesting, A-549, SNB-19, ACHN, and HCT-116 cells were, resuspended in sterile PBS, and injected s.c. into the right and left flanks (10×10^6 cells per flank) of the mice as previously described (130). For MDA-MB-231, cells were harvested and resuspended in PBS (10×10^6 cells per $50 \mu\text{l}$) and an equal volume of Matrigel (BD Biosciences, San Jose, CA). $100 \mu\text{l}$ of MDA-MB-231 cells in PBS/Matrigel were injected s.c. into the mammary fat pads between

the 2nd and 3rd nipples on each side of the mice. Once the tumors reached approximately 200-300 mm³ the mice were randomized and treated i.p. with 0.1ml vehicle (PBS) or ARA-211. Each treatment group consisted of five mice (2 tumors per mouse, a total of 10 tumors). The tumor volumes were determined by measuring the length (*l*) and width (*w*) and calculating the volume ($V=w^2l/2$). Statistical significance between the control and treated animals was determined using a student's *t* test.

Immunohistochemistry (IHC) and Slide Quantitation

Upon completion of the xenograft study, mice were euthanized and the tumors were removed and fixed in 10% buffered formalin for at least 24 hours. Three tumors per treatment group were then prepared and stained for proliferation marker Ki-67, apoptosis by TUNEL, and phosphor-Erk1/2 as previously described(131). The IHC slides were analyzed at the Analytical Microscopy Core facility of the H. Lee Moffitt Cancer Center & Research Institute. The Ariol SL-50 automated image analysis system (Applied Imaging, Santa Clara, CA) was used for quantitation of each slide as previously described(132). Briefly, high-resolution digital pictures were taken of the entire stained area of each slice of tumor tissue for automatic staining quantitation. Two thresholds were used to signify positive staining, one recognizing background and one recognizing positive brown staining. The percentage of positive staining was calculated by dividing the positive staining by the total staining (positive + negative) divided by

the total area stained, and the intensity of the stain was determined by calculating the integrated optical density of the positive stain with the negative background stain subtracted out. Each slide analyzed consisted of 54,000 to 160,000 cells analyzed depending on the size of the tumor when resected. Significance of the quantitation was analyzed by a two-tailed student's t-test.

Results

Identification of ARA-211, a selective suppressor of P-Erk1/2 levels in MDA-MB-231 breast cancer cells.

Many common genetic alterations in human cancers result in the hyperactivation of the Mek1/2 kinases leading to constitutively phosphorylated Erk1/2(64, 71-73). Because aberrant activation of the Mek1/2/Erk1/2 pathway has been implicated in oncogenesis and tumor survival, we sought to identify molecules that thwart this pathway. To this end, we first used a chemical biology approach by screening a 2,000 small molecule compound library (NCI diversity set, <http://dtp.nci.nih.gov/>) from the National Cancer Institute for pharmacological agents capable of suppressing the high levels of P-Erk1/2 in the human breast cancer cell line MDA-MB-231. Treatment of MDA-MB-231 cells with compounds from the NCI diversity set (96 well plate assay (25 plates total), 1 compound per well – see Figure 4) and subsequently processing the plates for a cyto blot using an antibody specific for P- Erk1/2, resulted in several compounds that suppress P- Erk1/2 levels. PD-98059, a Mek kinase inhibitor was used as a positive control for inhibition of Erk1/2 phosphorylation. MDA-MB-231 cells were treated with the hits from the assay to confirm the anti-P-Erk1/2 activity. Three

compounds from the screen were identified as inhibitors of Erk activation (Table 1). The IC₅₀ for each compound was obtained from dose response treatment on 231 cells, resulting in IC₅₀ values of 8, 10, and 500 nM for inhibition of Erk1/2 phosphorylation (Table 2). ARA-211 also suppressed P-Mek1/2 levels but not P-C-Raf, P-JNK, P-p38, P-Akt or P-STAT3 (Figure 5). These results demonstrated that ARA-211 is selective for disrupting the Mek1/2/Erk1/2, but not other oncogenic and tumor survival pathways.

Figure 4. High throughput screening of the NCI Diversity Set by cyto blot analysis reveals three inhibitors of Erk1/2 activation

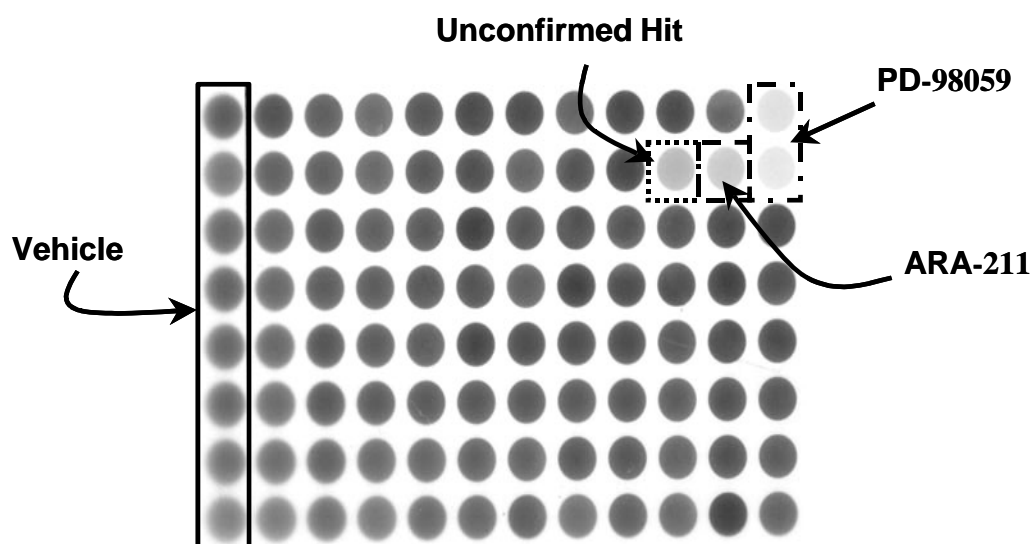


Figure 4. High throughput screening identifies ARA-211. MDA-MB-231 cells were plated in twenty-five 96-well plates, treated with vehicle (8 wells), PD-98059 (2 wells) or 2000 compounds (1 compound/well) from the NCI diversity set, and the plates processed for immunocyto blotting with an anti-phospho-Erk1/2 antibody as described under Materials and Methods. Plate #23 is shown with wells treated with vehicle as well as those treated with the Mek inhibitor PO98059.

Table 1. Chemical structures of the compounds identified from the NCI Diversity Set as inhibitors of P-Erk1/2 levels

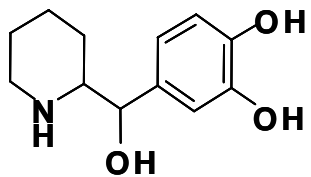
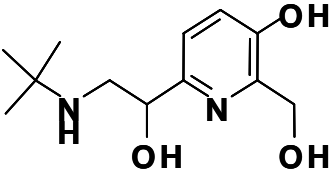
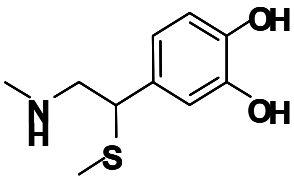
		
NSC #: 289336	NSC #: 355078	NSC #: 39215
Plate #: ERKi-2067	Plate #: ERKi-23211	Plate #: ERKi-624
ARA-67	ARA-211	ARA-624

Table 1. Cytoblot screen reveals three structurally similar chemical compounds that lower anti-P-Erk1/2 levels.

Figure 5. ARA-family of compounds selectively inhibit P-Erk1/2 levels in MDA-MB-231 breast cancer cells

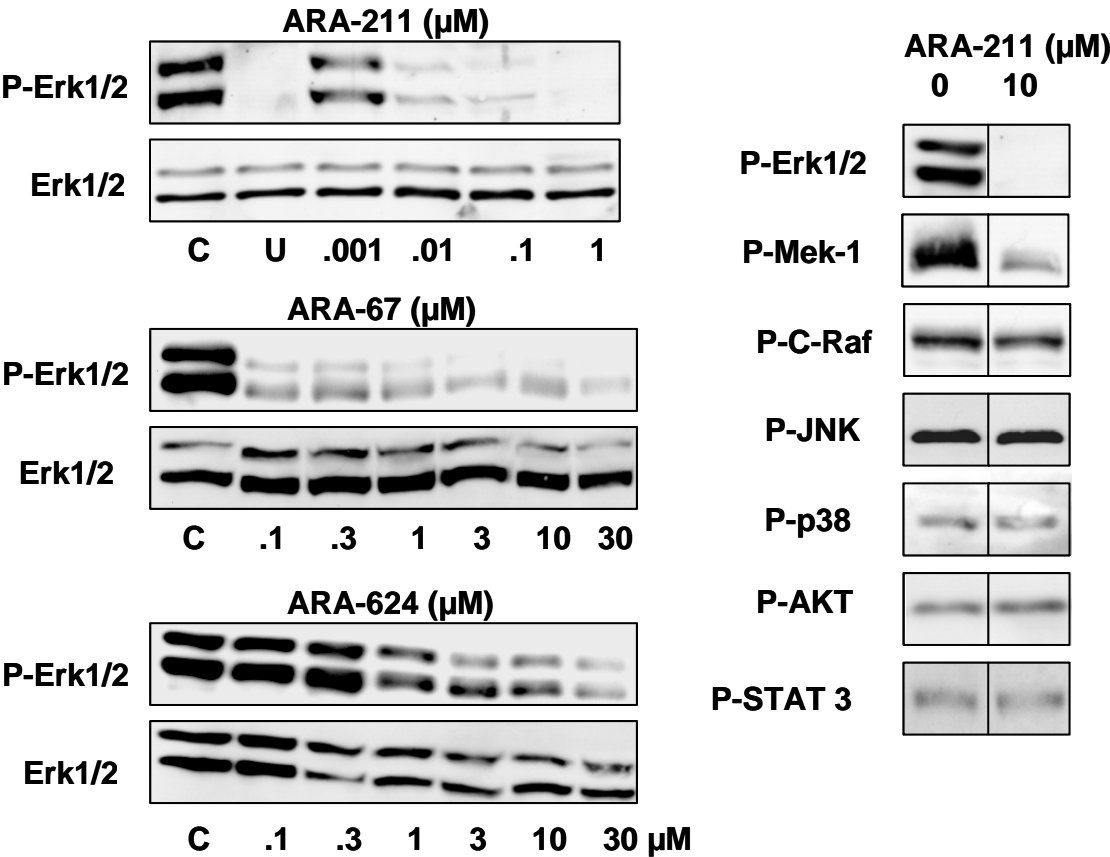


Figure 5. Validation of ARA-211 as selective suppressor of P-Erk1/2 levels in MDA-MB-231 breast cancer cells. ARA-211 treatment of MDA-MB-231 cells and Western blotting were performed as described under Materials and Methods, and resulted in suppression of P-Erk1/2 and P-Mek1/2 but not C-Raf, P-JNK, P-p38, P-Akt and P-STAT3 levels.

The fact that ARA-211 suppressed the levels of P-Mek1/2 and P- Erk1/2 suggested that it might be a C-Raf kinase inhibitor. *In-vitro* incubation of C-Raf and Mek1, immunoprecipitated from MDA-MB-231 cells, with ARA-211 did not inhibit C-Raf and Mek1 kinase activities (Figure 6). As expected, the C-Raf kinase inhibitor (Rki, Calbiochem) and the Mek1 inhibitor (U-0126, EMD Biosciences, San Diego, CA) blocked C-Raf and Mek1 kinase activities *in vitro*, respectively (Figure 6). In contrast to the *in vitro* studies, C-Raf and Mek1 kinase activities were blocked by ARA-211 when intact MDA-MB-231 cells were first treated with ARA-211, prior to cell lysis and immunoprecipitation of C-Raf and Mek1 (Figure 6). As expected only Rki but not U-0126 inhibited C-Raf kinase whereas both Rki and U-0126 inhibited Mek1 kinase when whole cells were treated. Contrary to the effects on C-Raf kinase activity, B-Raf kinase activity was not affected upon stimulation of cells with ARA-211.

Figure 6. C-Raf, but not B-Raf, kinase activity is inhibited upon ARA-211 treatment of whole cells, but not *in-vitro*

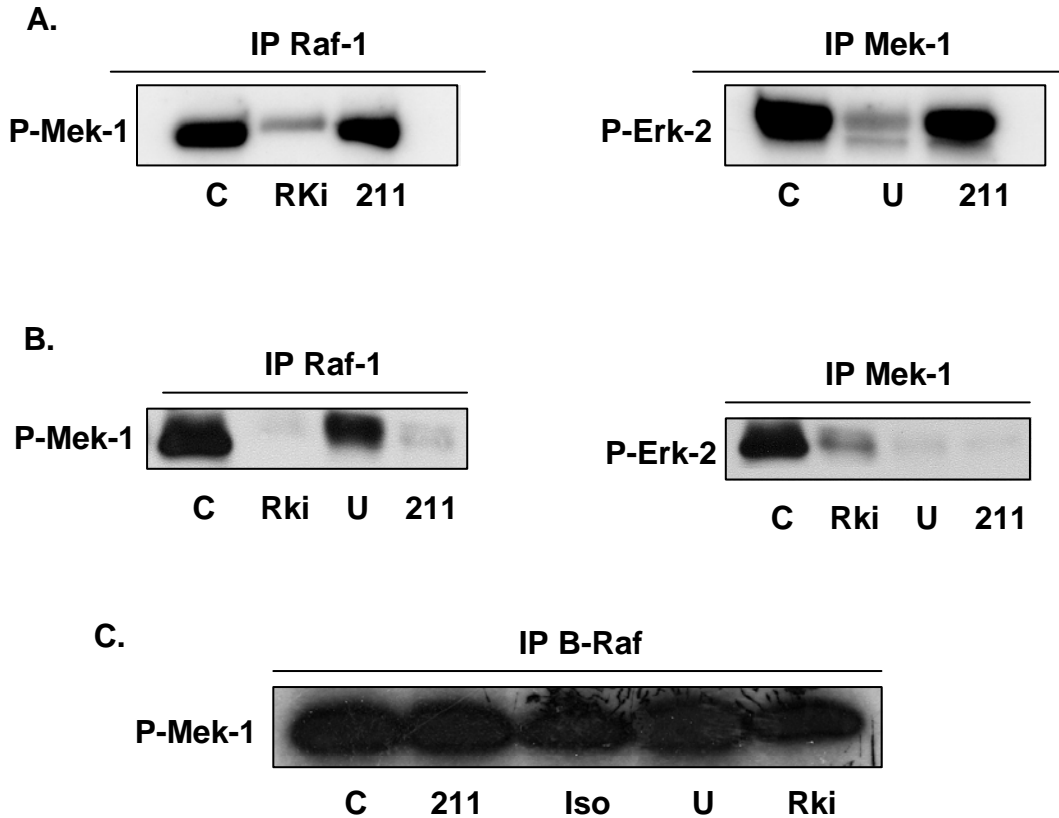


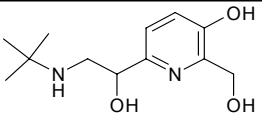
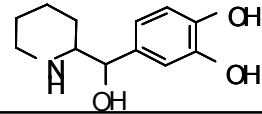
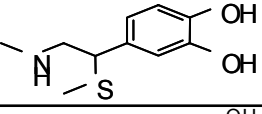
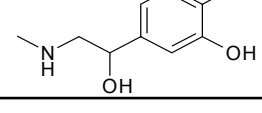
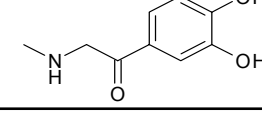
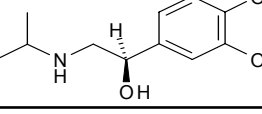
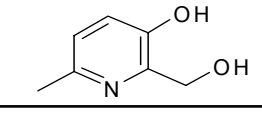
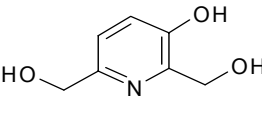
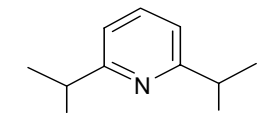
Figure 6. Raf-1, but not B-Raf, kinase activity is inhibited upon ARA-211 treatment of whole cells, but not *in vitro*. A. Raf-1 and Mek-1 were immunoprecipitated from MDA-MB-231 cells and treated *in vitro* with ARA-211, Rki or U-0126 and kinase assays followed by SDS-PAGE were performed as described in Materials and Methods. B. and C. Intact cells were first treated with ARA-211, then C-Raf and Mek-1 (B.) and B-Raf (C.) were immunoprecipitated and processed as for A. Only in cells treated with ARA-211 is Raf-1 kinase inhibited. *In vitro* only the Raf kinase inhibitor (RKi) and Mek kinase inhibitor (U-0126) blocked MAPK signaling.

ARA-211 is a selective β 2 adrenergic receptor agonist that inhibits P-Erk 1/2 levels by increasing cAMP

The fact that ARA-211 inhibits C-Raf and Mek1 kinase activities when intact cells are treated but not in vitro suggested that the target for this compound is upstream of C-Raf kinase. A chemical similarity search identified ARA-211 as pirbuterol, and resulted in many analogues of the beta adrenergic receptor agonist family. Table 2 depicts structural analogues of the ARA compounds that were located using SciFi-Scholar, a program linked to the American Chemistry Society registry of chemical compounds. The commercially available compounds were ordered and first screened at 10 μ M for inhibition of activation of Erk1/2 in MDA-MB-231 cells. Epinephrine, Isoproterenol, and Adrenalone showed inhibition of ERK 1/2 activation; while 2,6-Lutidine- α ,3-diol, 1-(6-(1-Hydroxyethyl)-Pyridin-2-Yl)-Ethanol, and 3-Hydroxy-2,6-Pyridinedimethanol-HCl did not inhibit the activation of ERK 1/2 in MDA-MB-231 cells. The active compounds were then tested in MDA-MB-231 cells in a dose response manner to better characterize each compound. IC50 values of epinephrine and adrenalone were found to be 5 and 10nM respectively, while Isoproterenol demonstrated an IC50 of .01 nM (Table 2). Comparing ARA-211 with 2,6-Lutidine- α ,3-diol & 3-Hydroxy-2,6 Pyridinedimethanol-HCl it can be determined that the tertiary butyl amine group is critical to ARA-211 activity. However, the size of this group appears to

be important as well, with the isopropyl (isoproterenol) being better than the methyl (epinephrine). It can also be determined, by comparing ARA 211 to epinephrine and isoproterenol that the cyclic nitrogen is not significant. Finally, the aliphatic hydroxyl is critical as its replacement with S-methyl results in loss of the ability to lower P-Erk1/2 levels (compare ARA-624 to epinephrine). The main value from the SAR however, was the crucial information that led us to investigate stimulation of the β 2 AR as an event leading to the inhibition of P-Erk1/2 in MDA-MB-231 cells. Based on the chemical structure search we found that the hit that was identified as ARA-211 is pirbuterol, a selective β 2 AR agonist.

Table 2. Structure-activity relationship studies identify the ARA family of inhibitors as analogues of epinephrine, and identifies ARA-211 as pirbuterol

Name	Structure	P-Erk1/2 IC ₅₀ (nM)
ARA-211 (Pirbuterol)		8 ± 5
ARA-67		10 ± 5
ARA-624		500 ± 25
Epinephrine		10 ± 7
Adrenalone		5 ± 15
Isoproterenol		0.01 ± .018
2,6-Lutidine-a,3-diol		>10,000
3-Hydroxy-2,6-Pyridinedimethanol-HCl (HPDM)		>10,000
1-(6-(1-Hydroxyethyl)-Pyridin-2-Yl)-Ethanol (HEPE)		>10,000

To demonstrate that ARA-211 acts as a β_2 adrenergic receptor agonist in MDA-MB-231 cells, and that this results in blockade of the Raf/Mek/Erk pathway, we treated these cells with ARA-211 and first showed that this compound induced the formation of cAMP (Figure 7). We then determined that ARA-211 is highly selective for β_2 adrenergic receptors by determining that only β_2 but not β_1 , α_1 or α_2 receptor antagonists block the ability of ARA-211 to induce cAMP formation (Figure 7). Furthermore, we used isopreterenol, another selective adrenergic receptor agonist and showed that it also stimulates the formation of cAMP and decreases the levels of P-Erk 1/2 (data not shown). Finally, to validate the effects of cAMP signaling on P-Erk1/2 activation MDA-MB-231 cells were pretreated with selective adrenergic antagonists followed by ARA-211 treatment. ARA-211 mediated inhibition of P-Erk1/2 levels was abrogated only when β_2 adrenergic signaling was blocked (Figure 8). Treatment of MDA-MB-231 cells with a β_1 selective, dobutamine, and a β_3 selective agonist CI316243, did not inhibit P-Erk 1/2 levels (data not shown). Furthermore, to demonstrate that the effects of P-Erk1/2 inhibition was due to cAMP mediated signaling we stimulated adenylyl cyclase to produce cAMP directly by forskolin treatment. Forskolin inhibited P-Erk1/2 levels with an IC₅₀ of 10 nM, similar to the ARA-211 induced inhibition (Figure 8). Taken together these data demonstrate that ARA-211 is a β_2 -selective adrenergic receptor agonist that suppresses P-Erk1/2 by increasing cAMP levels.

Figure 7. ARA-211 stimulates cAMP selectively through β 2 adrenergic receptor activation

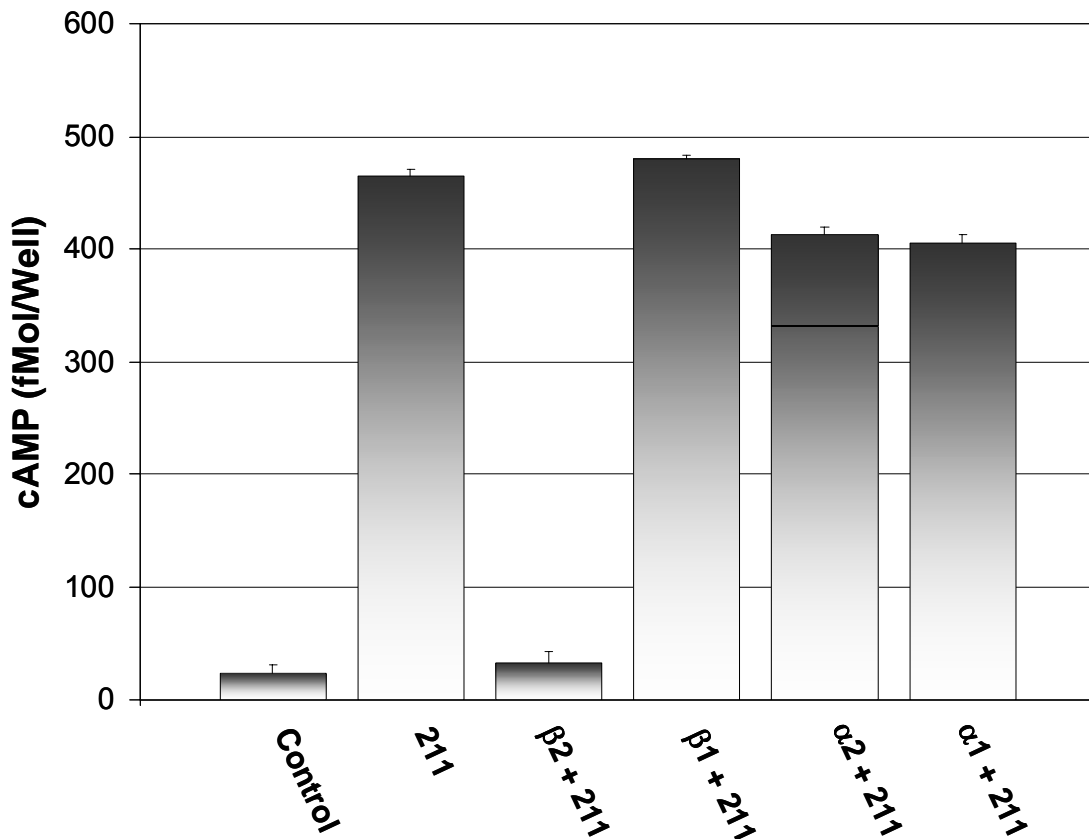


Figure 7. ARA-211 is a selective β 2 adrenergic receptor agonist. MDA-MB-231 cells were treated with ARA-211 alone or in the presence of β 1, β 2, α 1 or α 2 adrenergic receptor antagonists and the levels of cAMP were determined as described under Materials and Methods. Only pre-treatment with a β 2 selective adrenergic receptor antagonist blocked the ability of ARA-211 to stimulate cAMP in MDA-MB-231 cells.

Figure 8. ARA-211-mediated cAMP stimulation through β 2 adrenergic receptor activation results in inhibition of P-Erk1/2

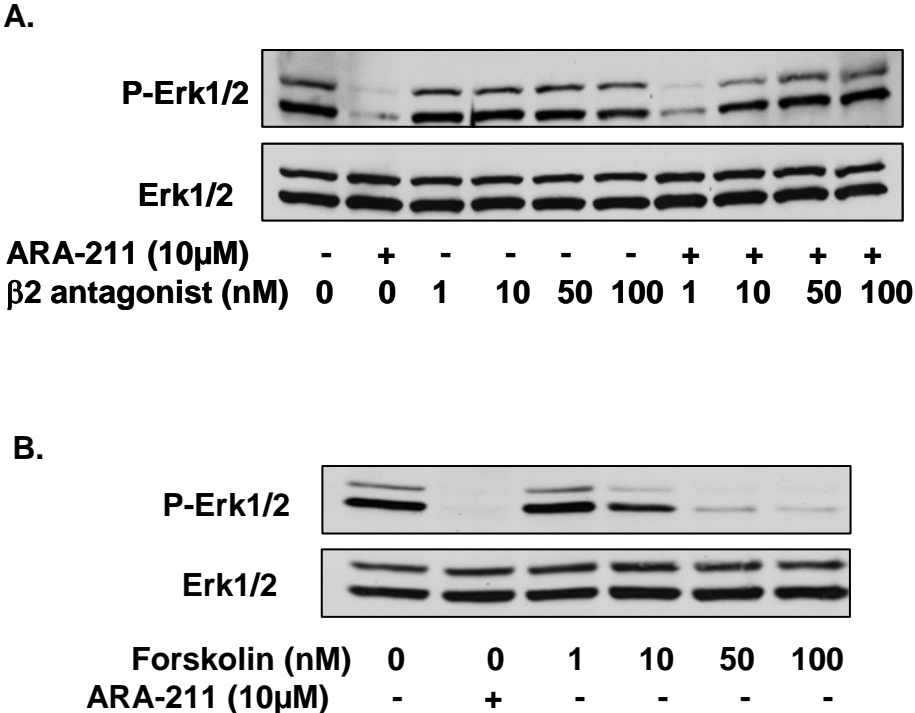


Figure 8. ARA-211 is a selective β 2 adrenergic receptor agonist that inhibits P-Erk 1/2 levels by increasing cAMP. A. MDA-MB-231 cells were treated with ARA-211 alone or in the presence of β 1, β 2, α 1 or α 2 adrenergic receptor antagonists and the levels of P-Erk1/2 were determined as described under Materials and Methods. B. Similarly, direct activation of cAMP by forskolin also results in inhibition of P-Erk1/2 activation.

ARA-211 inhibits P-Erk 1/2 levels by PKA but not EPAC activation

The data from Figures 7 and 8 demonstrated that ARA-211 stimulates the production of cAMP, which in turn suppresses the C-Raf/Mek1/2/Erk1/2 pathway. Previous studies primarily in normal cells have shown that the Ras-Erk pathway can be regulated by the ability of cAMP and PKA to modulate growth factor signaling via C-Raf and B-Raf. PKA, which is activated by cAMP, has been shown in some normal cells to interfere with Ras-C-Raf binding, downregulating MAPK-Erk signaling. This occurs through the PKA-dependant activation of the small G-protein Rap-1. Rap-1 competes with C-Raf for binding to GTP-Ras, resulting in a smaller amount of activated C-Raf available to activate Mek1/2. Alternatively, Rap1 can be activated by cAMP independently of PKA. Exchange Proteins Activated by cAMP (EPACs) are guanosine nucleotide exchange factors (GEFs) that are activated by cAMP and modulate the GTP loading of Rap1. Other studies have shown that if a cell line expresses high levels of B-Raf that PKA can activate B-Raf in a Ras-independent fashion. Active B-Raf is then free to phosphorylate and activate Mek-2, which activates Erk1/2. Therefore, the ARA-211 cAMP-dependent decrease in P-Erk1/2 levels could be modulated by cAMP-activation of either PKA or EPAC. In addition, PKA could either inactivate C-Raf directly, or through activation of Rap-1. Based on these possibilities, we next examined whether cAMP suppresses the P-Erk1/2 levels by activating the protein kinase A (PKA) or by activating the Rap1 guanine exchange factor EPAC. To this end, we treated MDA-MB-231 cells either with the EPAC activator 8-CPT-

2'-O-Me-cAMP, which would mimic the effects of ARA-211 on P-Erk1/2 levels, or the PKA kinase inhibitor H-89, which would block the effects of ARA-211. Figure 9 demonstrates that treatment with the EPAC activator did not affect P-Erk1/2 levels. In contrast, treatment with the PKA inhibitor prevented ARA-211 from suppressing the levels of P-Erk1/2. These results suggest that ARA-211-induced decrease in p-Erk1/2 levels is mediated through a cAMP-dependent PKA activation, but not a cAMP-activation of EPAC. If this is the mechanism involved then ARA-211 would be expected to activate PKA, and PKA siRNA would be expected to inhibit ARA-211 from decreasing the P-Erk1/2 levels. Therefore, to further strengthen this suggestion, we first determined if ARA-211 is able to activate PKA. Figure 10 shows that ARA-211 treatment of MDA-MB-231 cells activated PKA kinase activity, and that H-89 prevented ARA-211 from activating PKA. siRNA to the alpha catalytic subunit of PKA was then used to further validate the necessity of PKA activation for ARA-211 mediated inhibition of Erk1/2 phosphorylation. Figure 10 demonstrates that as PKA protein levels are diminished the effects of ARA-211 on P-Erk1/2 are rescued. A dose response of PKA α -cat siRNA of 5, 50 and 100 nM were used to demonstrate a linear signaling correlation between PKA α catalytic subunit protein levels and P-Erk1/2 phosphorylation.

Figure 9. ARA-211-mediated cAMP stimulation (through β 2 adrenergic receptor activation) results in inhibition of P-Erk1/2 through PKA activation, not EPAC activation of Rap1

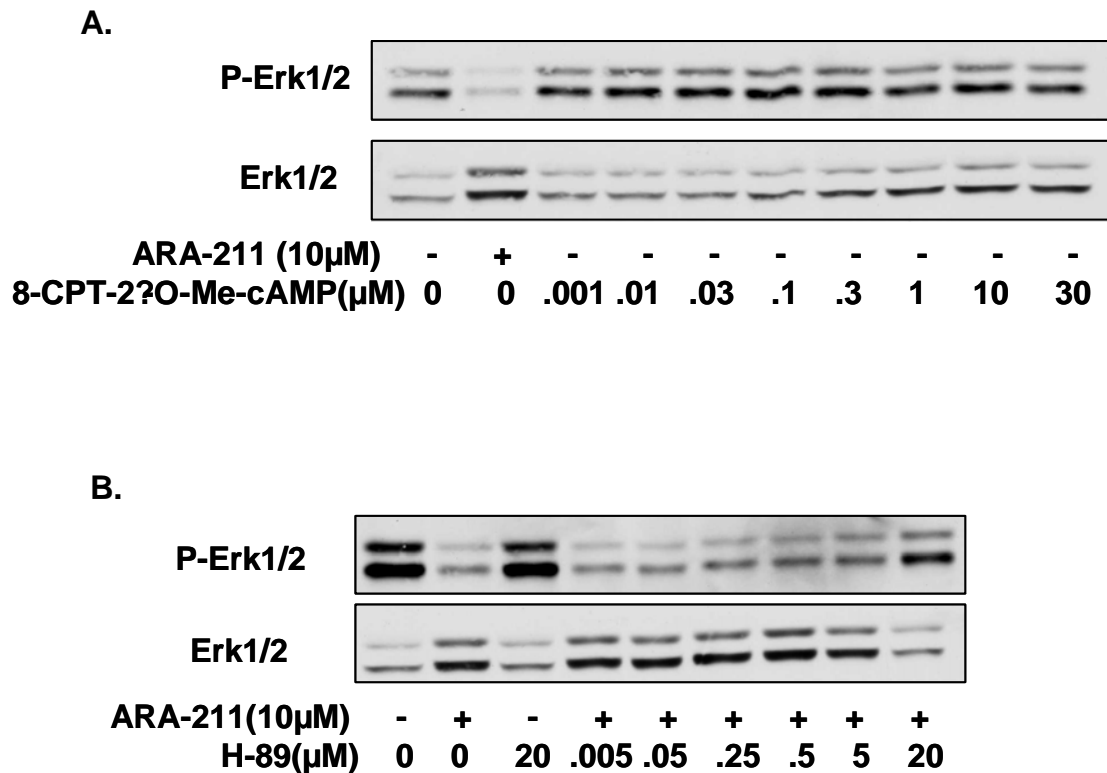


Figure 9. ARA-211 inhibits P-Erk1/2 levels by PKA but not EPAC activation. MDA-MB-231 cells were treated either with ARA-211, the EPAC activator 8CPT-2'-O-Me-cAMP (A.), the PKA inhibitor H-89 (B.), or ARA-211 and H-89 (B.). Direct activation of EPAC did not inhibit P-Erk1/2 levels, while blockade of PKA kinase activity by H89 abrogated ARA-211-mediated inhibition of P-Erk1/2

Figure 10. siRNA and kinase assays validate that ARA-211-mediated cAMP stimulation results in inhibition of P-Erk1/2 through PKA activation

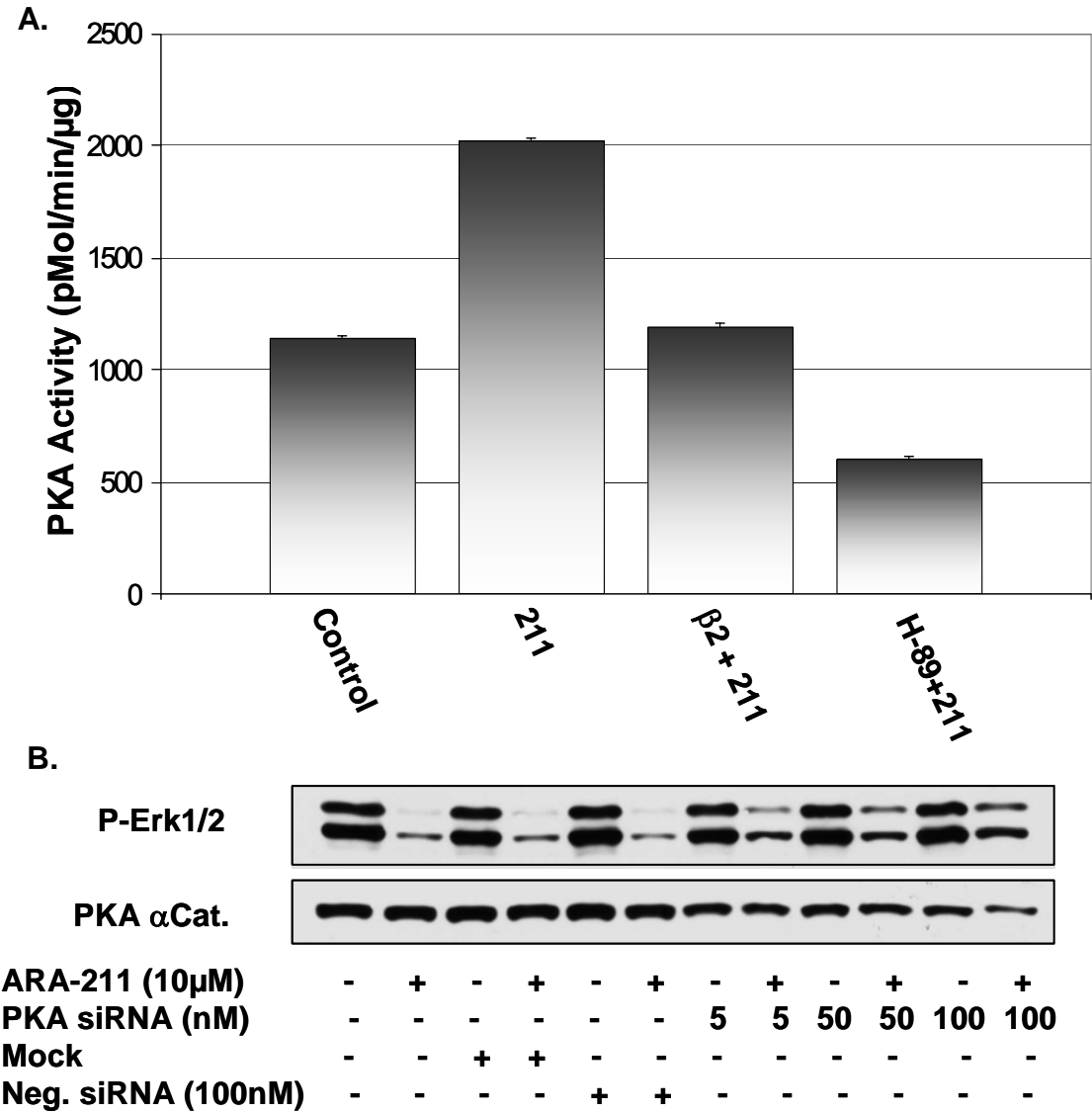


Figure 10. ARA-211 inhibits P-Erk1/2 levels by PKA but not EPAC activation. A. PKA kinase assays show ARA-211 stimulates PKA, which is blocked by pre-treatment with a β2 antagonist as well as PKA kinase inhibitor H89. B. siRNA to PKA demonstrates that as PKA expression decreases the ability of ARA-211 to inhibit P-Erk1/2 levels also diminishes.

ARA-211 inhibits tumor cell proliferation by β 2AR-stimulation of cAMP and inhibition of Mek1/2

The data from the previous figures demonstrated that stimulation of the β 2 AR with ARA-211 suppresses the C-Raf/Mek1/2/Erk1/2 pathway by a cAMP-dependent activation of PKA but not EPAC. Whether stimulation of the β 2 AR and subsequent inhibition of Raf/Mek/Erk causes tumor suppression is not known. Therefore, we next determined whether activation of the β 2 adrenergic receptor, which leads to inhibition of the C-Raf/Mek1/2/ Erk1/2 pathway, results in inhibition of tumor cell growth and survival of human cancer cells. Figure 11 demonstrates that ARA-211 inhibits the proliferation of MDA-MB-231 cells in a dose dependent manner, and requires the ability of ARA-211 to bind the β 2 adrenergic receptor. MTT and Alamar Blue assays were used to determine the effects of ARA-211 on cell proliferation. The proliferation of cells that were pretreated with β 2 AR antagonist was not affected by ARA-211, in contrast to cell treated with ARA-211 alone. Western blotting from cells from the Alamar Blue proliferation assay demonstrated that pre-treatment with the β 2 AR antagonist rescued from the ARA-211 induced inhibition of Erk1/2 phosphorylation (Figure 11). Likewise, forskolin was used to directly stimulate adenylyl cyclase to determine if β 2 AR stimulation resulting in cAMP production is a necessary step in the inhibition of cell proliferation. Figure 12 shows that forskolin indeed inhibits MDA-MB-231 cell proliferation with an IC₅₀ of approximately 50 nM.

Figure 11. ARA-211 inhibition of MDA-MB-231 cell proliferation requires β 2 AR activation and inhibition of P-Erk1/2

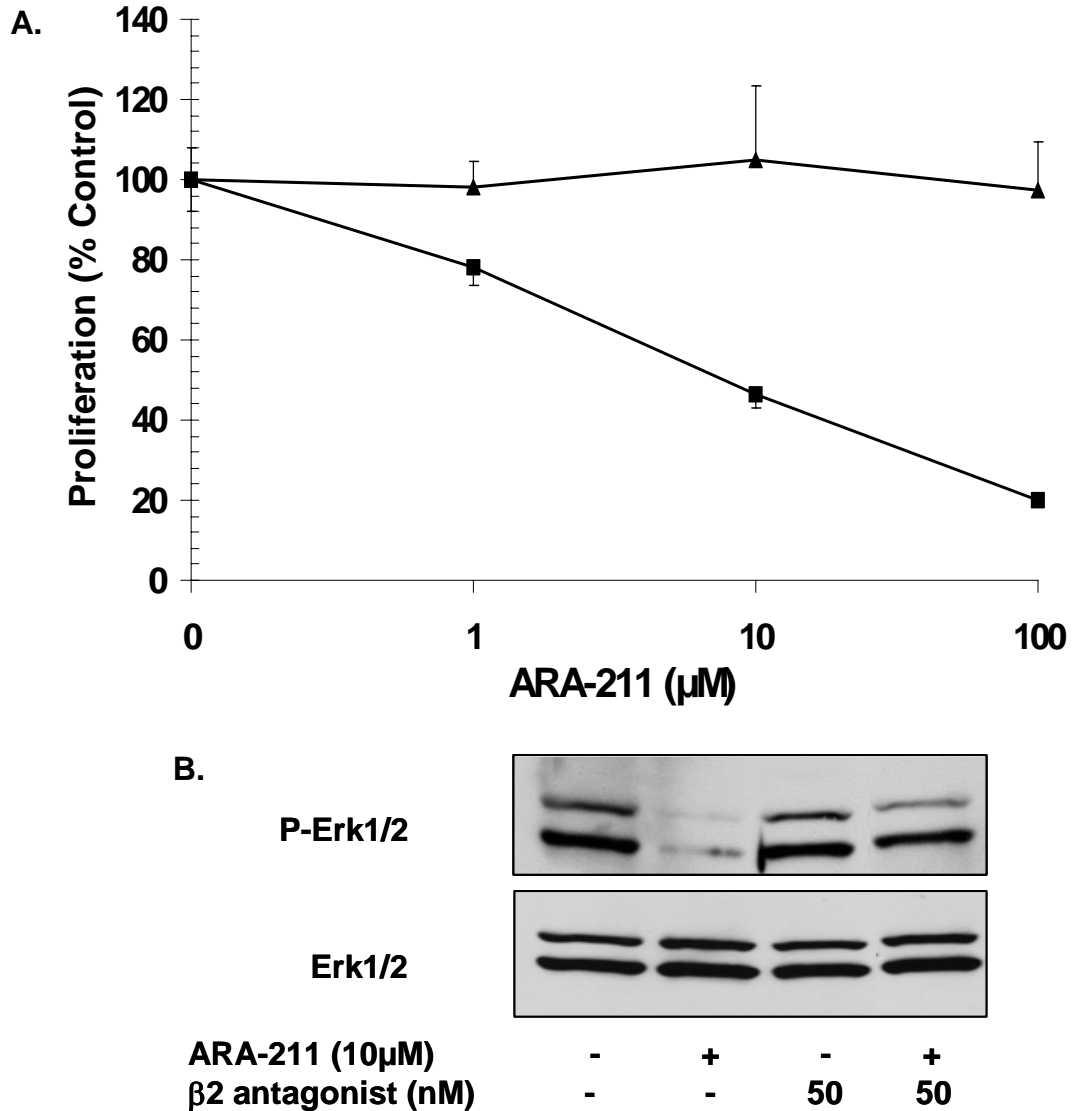


Figure 11. ARA-211 inhibition of MDA-MB-231 cell proliferation requires β 2 AR activation and inhibition of P-Erk1/2. MDA-MB-231 cells were treated with ARA-211 alone (square) or in the presence of the β 2AR antagonist ICI 118.551 (triangle) and the effects of treatment on tumor cell growth (A.) and P-Erk1/2 levels (B.) were determined as described under Materials and Methods.

Figure 12. Direct activation of adenylyl cyclase by forskolin inhibits the proliferation of MDA-MB-231 cells

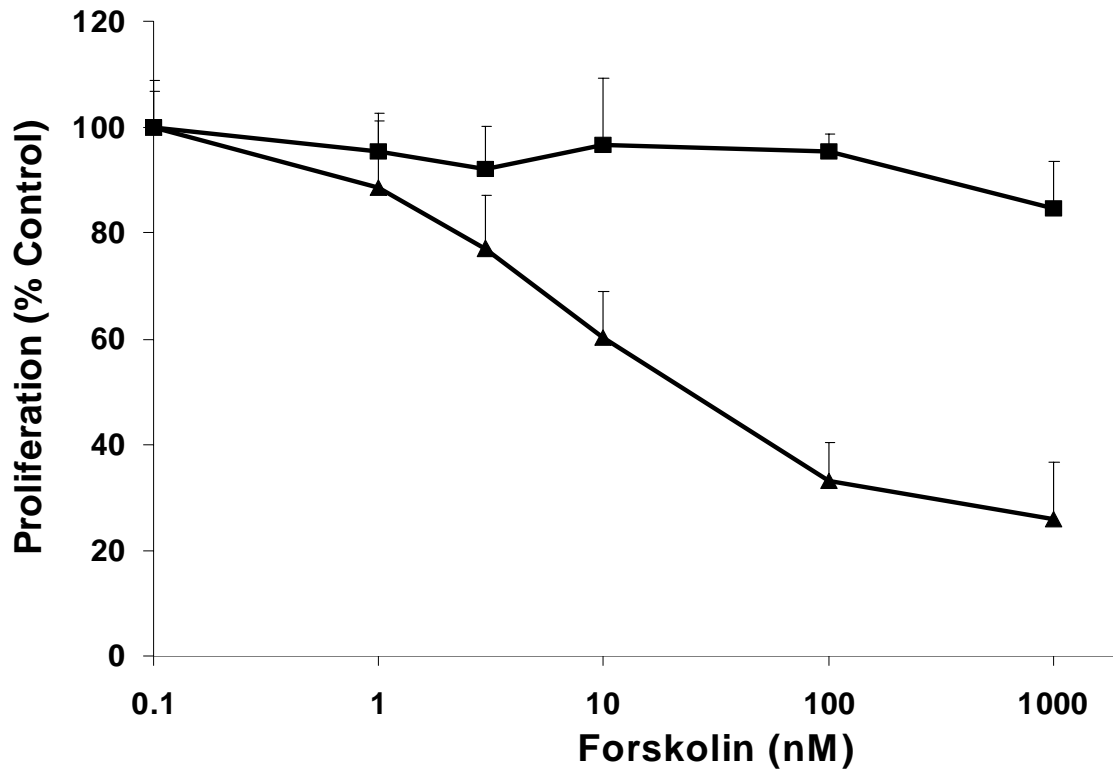


Figure 12. Forskolin inhibits MDA-MB-231 cell proliferation correlating with inhibition of P-Erk1/2. MDA-MB-231 cells were treated with vehicle (square) or Forskolin (triangle) and the effects on tumor cell growth determined.

The above data clearly demonstrated that the ability of ARA-211 to disrupt the C-Raf/Mek1/2/Erk1/2 pathway and to inhibit tumor cell growth and survival depends on its ability to stimulate the β 2 adrenergic receptor and produce cAMP. However, the ability of ARA-211 to inhibit tumor cell growth could be due to its ability to affect cellular events other than those leading to decreased P-Erk1/2. Therefore, we next determined whether the inhibition of tumor cell growth by ARA-211 requires its ability to inhibit the C-Raf/Mek1/2/Erk1/2 pathway. We reasoned that if suppression of C-Raf and Mek1/2 were critical to ARA-211 inhibition of tumor growth then ectopically expressing constitutively active Mek1/2 would rescue human cancer cells from the effects of ARA-211. Figure 13 shows that MDA-MB-231 cells that ectopically express constitutively active Mek1/2 (CA-Mek) are resistant to ARA-211 inhibition of P- Erk1/2 and inhibition of tumor cell growth. Mek1/2 levels clearly show a dramatic induction of expression with transfection of CA-Mek plasmid. Likewise, downstream signaling through Erk1/2 activation is also increased. Finally, P-Erk1/2 inhibition mediated by ARA-211 is rescued in the cells over expressing CA-Mek. This demonstrates that ARA-211 inhibits proliferation of MDA-MB-231 cells through inhibition of Mek/Erk signaling.

Figure 13. ARA-211-mediated inhibition of MDA-MB-231 cell proliferation is dependent on the ability to inhibit Mek1/2 and to decrease P-Erk1/2 levels

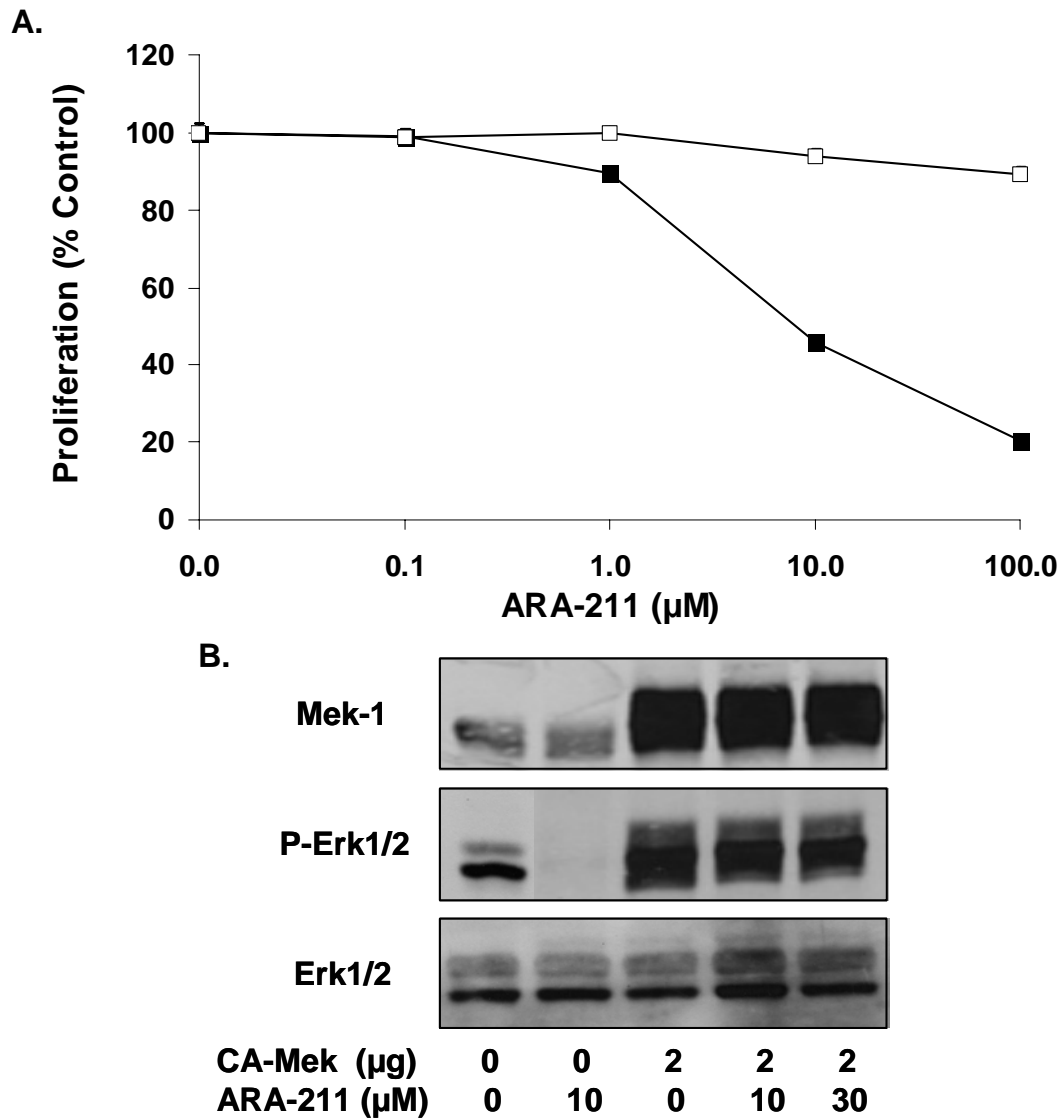


Figure 13. Inhibition of proliferation by ARA-211 is dependent on Mek1/2/Erk1/2 signaling. MDA-MB-231 cells were treated with ARA-211 alone (open square) or in the presence of CA-Mek (closed square) and the effects of treatment on tumor cell growth (A.) and P-Erk1/2 levels (B.) were determined as described under Materials and Methods.

Screening of NCI 60 cell line panel leads to discovery of ARA-211 sensitive and insensitive cell lines

So far we have demonstrated that ARA-211 binds the $\beta 2$ AR, stimulates cAMP, and inhibits Erk1/2 phosphorylation through a PKA dependent mechanism leading to inhibition of cell proliferation in MDA-MB-231 cells. While these findings have not been reported previously and therefore are novel, it is critical that we determine whether this mechanism of tumor suppression is relevant to other human tumors, or if it is unique to the MDA-MB-231 breast cancer cell line. To this end we searched for cancer cell lines that possess the correct signaling circuitry to respond to $\beta 2$ AR stimulation similarly to the MDA-MB-231 cell line. We hypothesized that cells that express the $\beta 2$ AR and high levels of P-Erk1/2 would be candidates for ARA-211 sensitivity based on the necessity of ARA-211 to bind the $\beta 2$ AR and inhibit P-Erk1/2 to block cell proliferation. Likewise, literature reports suggest that in some normal cells the ratio of C-Raf to B-Raf expression levels may dictate whether $\beta 2$ AR activation inhibits or activates Erk1/2. To reach our goal we determined by western blotting the levels of $\beta 2$ AR, P-Erk1/2, C-Raf and B-Raf in the lysates from the NCI 60 cell line panel. Table 3 summarizes the findings from the western blot analysis shown in Figure 14. A minus (-) sign indicates little to no expression, a plus (+) sign indicates moderate expression, whereas a double plus (++) sign indicates high protein expression (Table 3). Based on the expression analysis, the cell lines that were available

and expressed both the $\beta 2$ AR and P-Erk1/2 were tested for ARA-211 sensitivity. Cells insensitive to treatment based on the ability of ARA-211 to inhibit P-Erk1/2 were denoted by a *, and the cell lines tested that were sensitive to ARA-211 treatment were denoted by a **. Out of 20 lines tested 3, MDA-MB-231, ACHN, and SF-539, were found to be sensitive to ARA-211 treatment. Analysis of the findings from the cell lines tested with ARA-211 compared to C-Raf and B-Raf expression led to the finding that the ratio hypothesis did not hold true. No cell lines tested demonstrated an ARA-211 mediated increase in P-Erk1/2 expression, even when expression of B-Raf was high and C-Raf was low. Similarly, it was found that even though some cells express $\beta 2$ AR, P-Erk1/2, and C-Raf but not B-Raf, the cells were still insensitive to ARA-211 treatment (IGR-OV1, MCF-7, Table 3, Figure 14). It is clear however, that all cell lines that responded to ARA-211 express $\beta 2$ AR and have high levels of P-Erk1/2. Therefore, the sensitive cell lines MDA-MB-231, SF-539, and ACHN, along with insensitive cell lines A549, HCT-116, and SNB-19 were chosen to provide a panel of cell lines to demonstrate that only cells where ARA-211 stimulates cAMP production (which results in decreased levels of P-Erk1/2) are sensitive to ARA-211-induced apoptosis and human tumor suppression.

Table 3. ARA-211 sensitive and insensitive cell lines tested from the NCI 60 cell line panel do not correlate with C-Raf and B-Raf expression levels

Origin	Gel #	Cell Line	β2-AR	pErk ½	C-Raf	B-Raf
Colon	1	*Colo-205	-	+	-	-
	2	HCC-2998	-	-	-	+
	3	HCT-15	+	-	+	+
	4	*HCT-116	++	++	++	+
	5	*HT29	++	-	++	++
	6	KM 12	++	-	++	+
	7	*SW-620	++	+	++	-
CNS	8	SF-268	++	+	++	-
	9	SF-295	++	-	++	-
	10	**SF-539	+	++	+	+
	11	*SNB-19	+	+	++	-
	12	SNB-75	+	+	+	++
	13	*U251	+	++	+	++
Leukemia	14	CCRF-CEM	-	-	+	-
	15	HL-60	++	++	-	++
	16	K562	++	-	++	++
	17	MOLT4				
	18	RPMI-8226	-	-	-	-
	19	SR	++	-	++	+
Lung	20	*A549	+	+	++	-
	21	*EKVX	++	++	-	-
	22	HOP-62	-	-	+	+
	23	HOP-92	++	+	+	-
	24	NCI-H23	-	++	+	++
	25	NCI-H226	-	-	-	++
	26	NCI-H322M	-	++	-	-
	27	NCI-H460	-	-	-	+
Mammary	29	*MCF7	+	+	+	-
	30	MCF7-Adr Res	++	++	+	-
	31	HS 578T	++	-	-	+
	32	**MDA-MB-231	+	++	-	+
	33	*MDA-MB-435	-	++	-	+
	34	BT-549	+	+	-	++
	35	*T-47D	-	-	-	+

Table 3. ARA-211 sensitive and insensitive cell lines tested from the NCI 60 cell line panel do not correlate with C-Raf and B-Raf expression levels

Melanoma	36	LOX IMVI	-	++	-	+
	37	M14	-	++	-	+
	38	MALME-3M	-	+	-	+
	39	SK-MEL-2	-	-	-	-
	40	SK-MEL-28	-	++	-	-
	41	UACC-62	-	-	+	+
	42	UACC-257	+	-	+	-
Ovarian	44	*IGR-OV1	+	++	++	-
	45	*OVCAR-3	+	-	-	-
	46	OVCAR-4	-	-	+	+
	47	*OVCAR-5	-	-	+	++
	48	OVCAR-8	-	-	++	-
	49	SK-OV-3	-	-	-	-
Prostate	50	DU-145	-	-	-	-
	51	*PC-3	-	-	+	+
Renal	52	*786-0	+	-	++	+
	53	A498	-	-	-	++
	54	**ACHN	+	+	-	+
	55	CAKI-1	-	-	++	++
	56	RXF 393	-	+	-	+
	57	*SN 12C	+	+	++	-
	58	TK-10	-	-	+	+
	59	UO-31	-	-	-	-

- = little to no expression
 + = moderate expression
 ++ = high expression

* = ARA-211 and Isoproterenol have no effect on pERK levels
 ** = ARA-211 and Isoproterenol decrease levels of P-Erk1/2

Table. 3 Cell lines from the NCI 60 cell line panel were screened for ARA-211 sensitivity based on P-Erk1/2 inhibition. Likewise, the levels of β 2 AR, P-Erk1/2, C-Raf and B-Raf were analyzed by western blot to determine if sensitivity is conferred by C-Raf versus B-Raf expression levels (Figure 10).

Figure 14. Western blot verification of $\beta 2$ AR, P-Erk1/2, C-Raf and B-Raf expression levels from the NCI 60 cell line panel

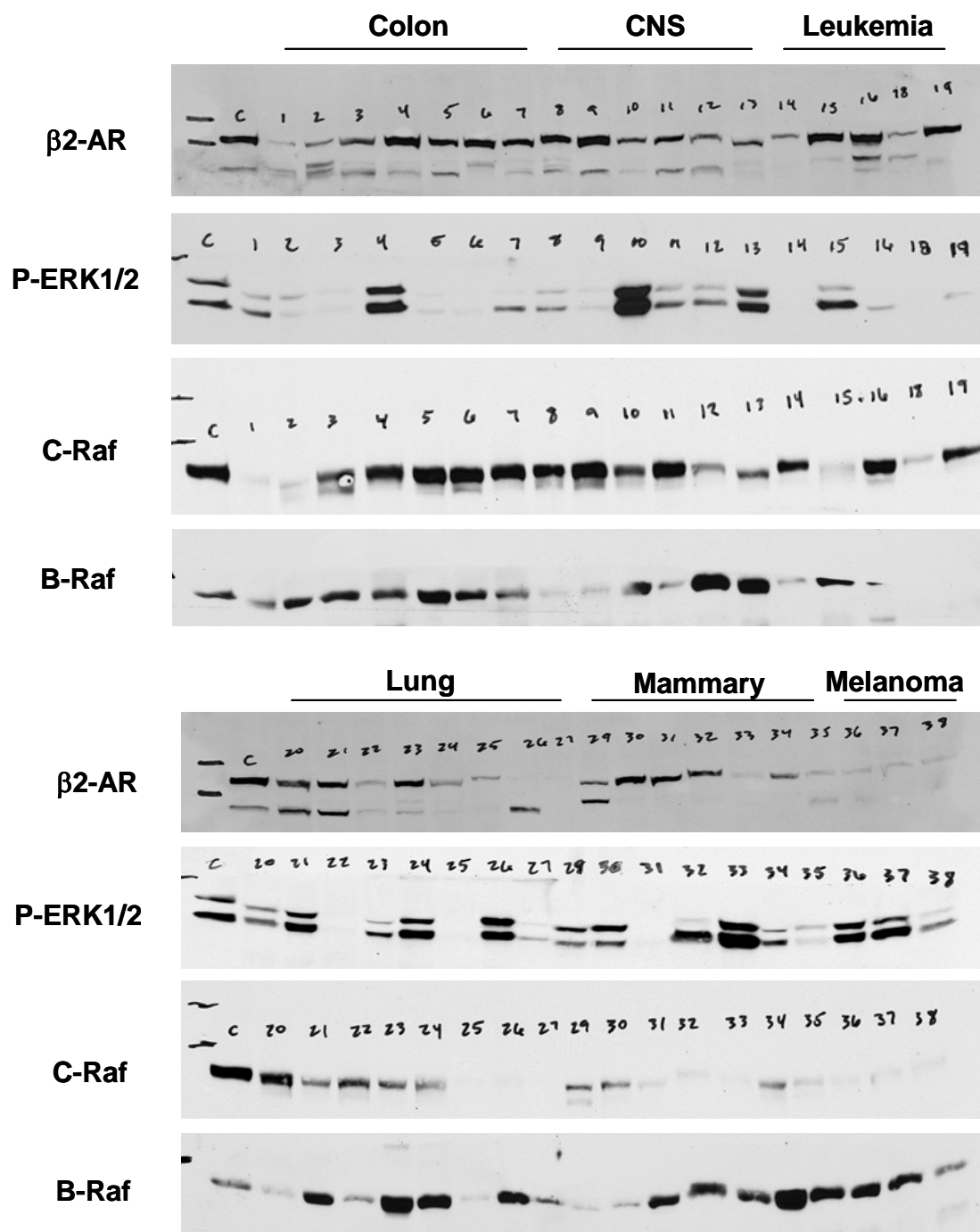


Figure 14 (continued). Western blot verification of β 2 AR, P-Erk1/2, C-Raf and B-Raf expression levels from the NCI 60 cell line panel

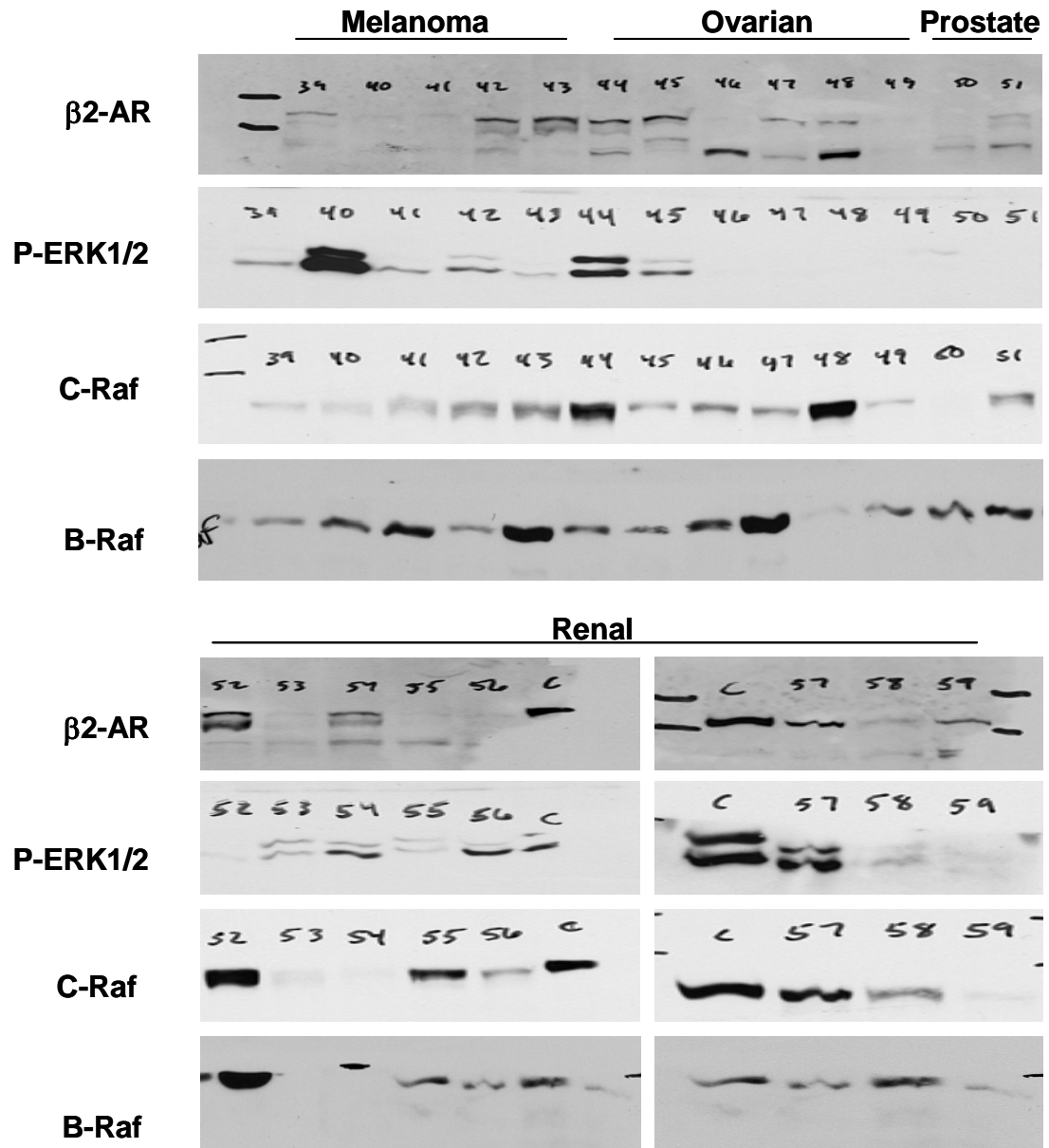


Figure 14. Western blot analysis of β 2 AR, P-Erk1/2, C-Raf and B-Raf expression levels from the NCI 60 cell line panel. Cell lysates were obtained from NCI, and western blot analysis was performed according to Materials and Methods.

ARA-211 inhibits anchorage independent proliferation, induces apoptosis, and suppresses the growth of human tumor xenografts in nude mice only in cell lines where it produces cAMP and inhibits P-Erk1/2 levels

We next determined if ARA-211 suppresses tumor growth only in those cells where it inhibits P-Erk1/2 in a cAMP-dependent manner. To this end, we treated with ARA-211 the 6 cell lines identified above and processed them for assays for cAMP stimulation (ELISA), anchorage-independent proliferation (soft agar growth), apoptosis (TUNEL) and *in-vivo* tumor growth (xenograft). Figure 15 demonstrates the stimulation of cAMP in MDA-MB-231 (breast), SF-539 (cns), and ACHN (renal) tumor cell lines by 16, 13, and 16 fold with 10 μ M ARA-211 stimulation. However, ARA-211 failed to stimulate cAMP in A549 (lung), HCT-116 (colon) and SNB-19 (cns) (summarized in Table 4). In agreement with Table 3, Table 4 also shows that ARA-211 inhibited P-Erk1/2 levels only in cell lines where it induces cAMP formation. Furthermore, Table 4 shows the anchorage-dependent cell proliferation is inhibited in a dose dependent manner with ARA-211 treatment of MDA-MB-231, ACHN, and SF-539, but not of A549, HCT-116, or SNB-19 cells. Inhibition of anchorage-dependent growth at 10 μ M ARA-211 stimulation was 60, 55, and 62 percent for ARA-211 sensitive cell lines versus 9, 6, and 0 percent for insensitive cell lines (Table 4). There was even greater inhibition of anchorage-independent cell proliferation, with sensitive cell lines inhibited by 82, 94, and 97 percent, whereas the insensitive cell lines showed 0, 7, and 5 percent inhibition at 10 μ M (Figure 16, Table 4).

Figure 15. ARA-211 induces cAMP formation in MDA-MB-231, SF-539 and ACHN cells but not in A549, SNB-19 and HCT-116 cells

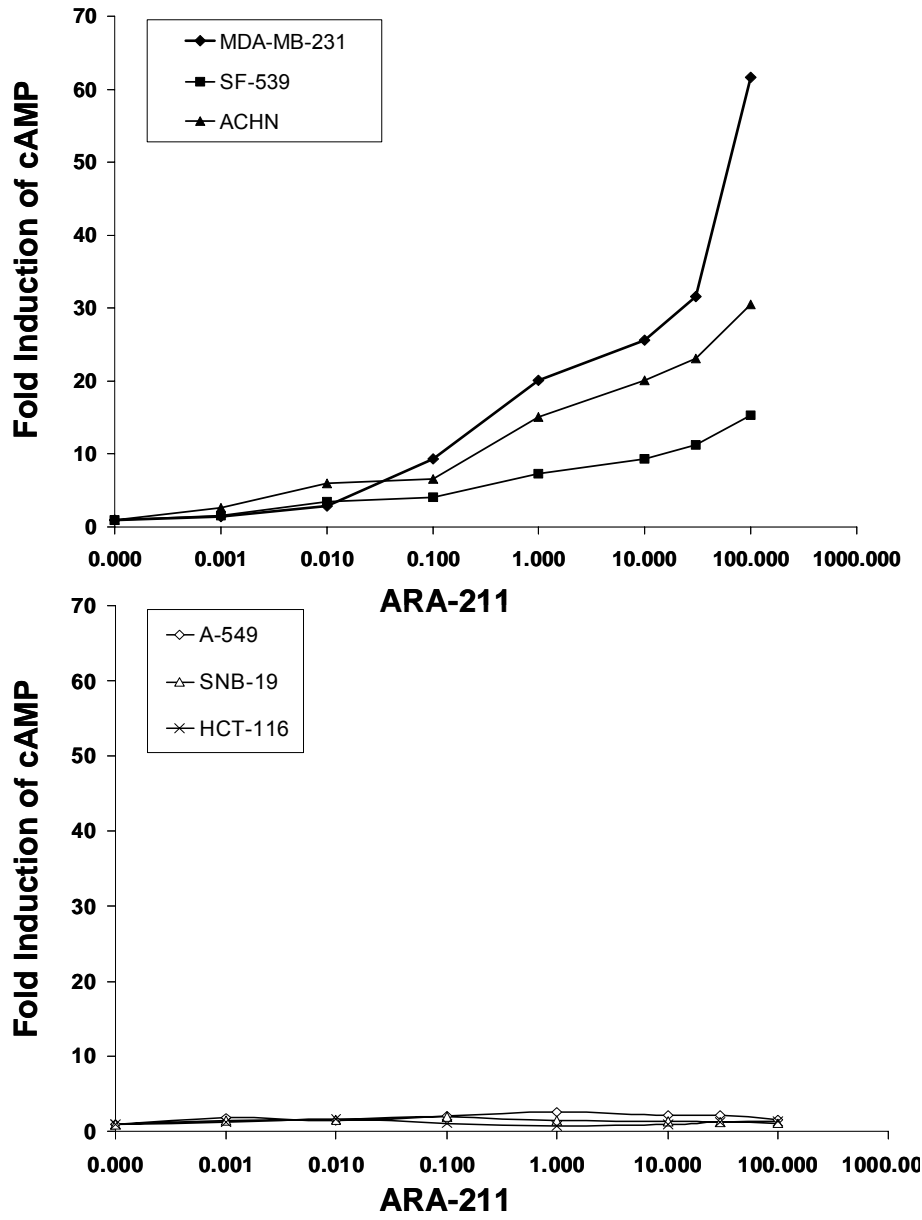


Figure 15. cAMP ELISA assays were used, as described under Materials and Methods, to determine the sensitivity of cell lines to ARA-211 mediated stimulation of cAMP.

Figure 16. ARA-211 inhibits anchorage independent growth in MDA-MB-231, SF-539 and ACHN cells but not in A549, SNB-19 and HCT-116 cells

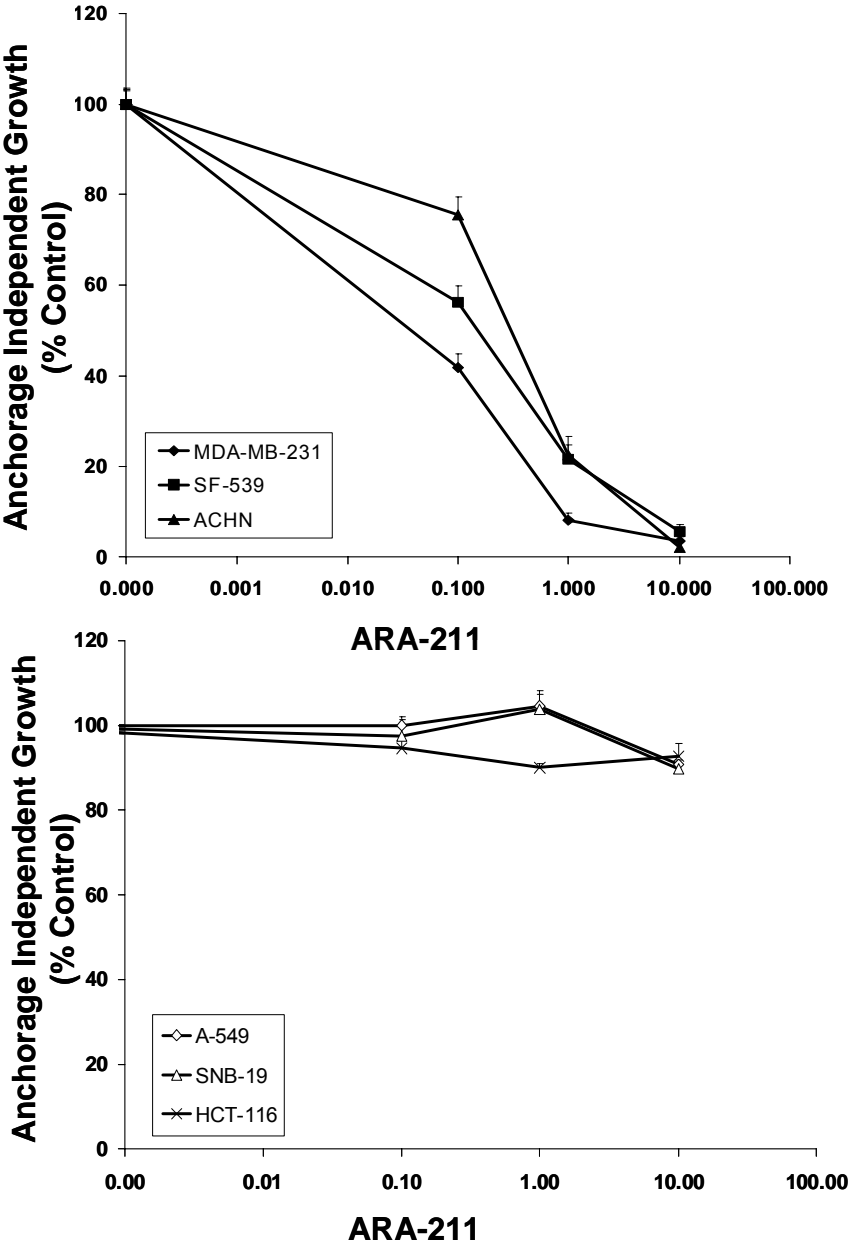


Figure 16. Anchorage-independent growth on soft agar was used, as described under Materials and Methods, to determine the sensitivity of cell lines to ARA-211 mediated stimulation of cAMP.

Figure 17. ARA-211 induces apoptosis in MDA-MB-231, SF-539 and ACHN cells but not in A549, SNB-19 and HCT-116 cells

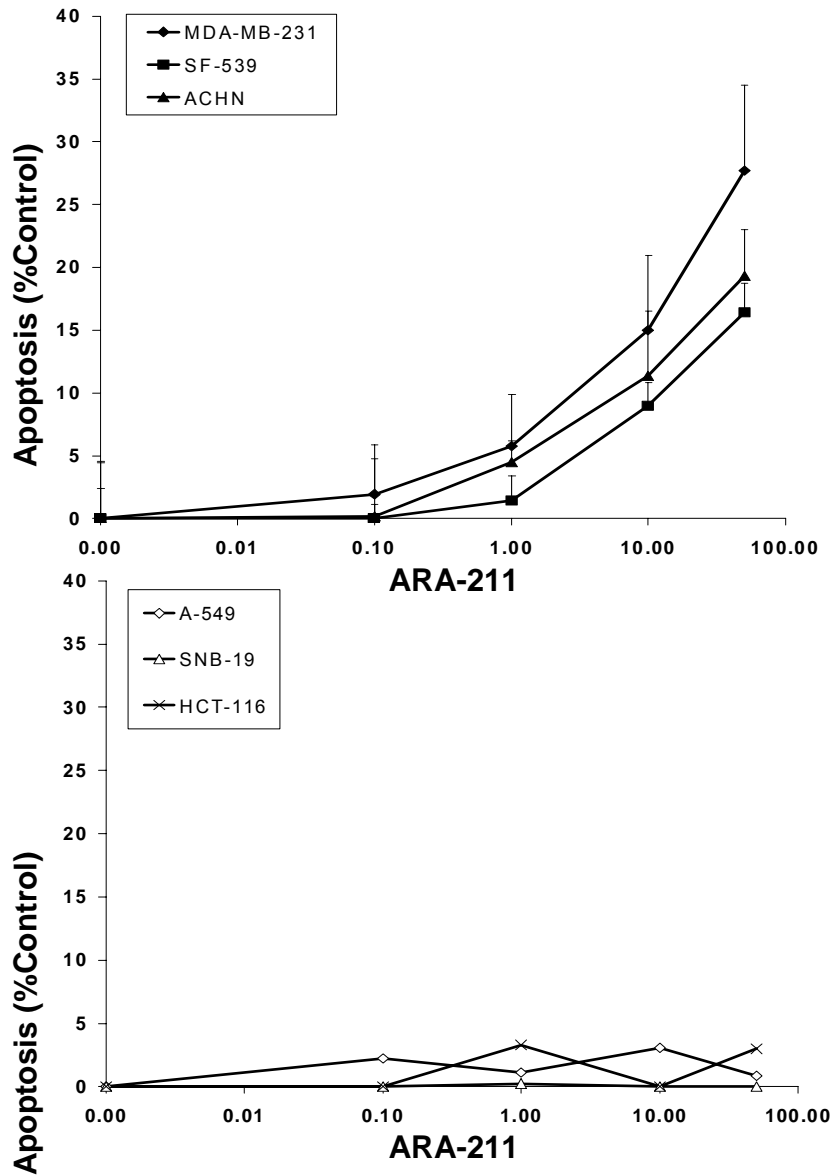


Figure 17. A cell death detection apoptosis ELISA kit was used, as described under Materials and Methods, to determine the sensitivity of cell lines to ARA-211 mediated induction of Apoptosis.

ARA-211 suppresses tumor growth and causes tumor regression

The ability of ARA-211 to inhibit tumor cell growth and induce apoptosis in cultured cells in a β 2 AR and Mek1/2-dependent manner suggested that ARA-211 might induce tumor regression in human cancers where it can induce cAMP and block the C-Raf/Mek1/2/Erk1/2 pathway. Therefore, we determined the ability of ARA-211 to interfere with the growth and progression of nude mice xenografts of the 6 human cancer cell lines described above. Figure 18-19 and Table 4 shows that ARA-211 was only able to suppress tumor growth in human tumors (MDA-MB-231, and ACHN) where β 2AR stimulation occurs but not in those (A-549, SNB-19, and HCT-116) in which it does not. Figure 18 demonstrates that treatment with ARA-211 (i.p.) of mice bearing established MDA-MB-231 breast tumors under the mammary fat pads suppressed growth at 100mpk/day and actually caused tumor regression at 200mpk/day. In the same MDA-MB-231 mammary fat pad model, isopreterenol at 200mpk/day did not cause tumor regression and inhibited tumor growth by 89% (data not shown). After two weeks of treatment with ARA-211 and total tumor regression the mice were taken off of the treatment regiment and monitored for tumor growth for an additional three weeks, during which none of the tumors regrew and remained undetectable (data not shown). Similarly, the growth of ACHN renal tumors was inhibited when the mice were treated i.p. with ARA-211 (75 mpk/day) and tumor growth was blocked at 200 mpk/day (Figure 18, 200 mpk day 12 (see \uparrow)). SF-539 cells did not grow consistently in nude mice, so no in-vivo data was collected.

Figure 18. ARA-211 treatment of MDA-MB-231 xenografts results in tumor regression, and treatment of AHCN xenografts completely inhibits tumor growth in nude mice

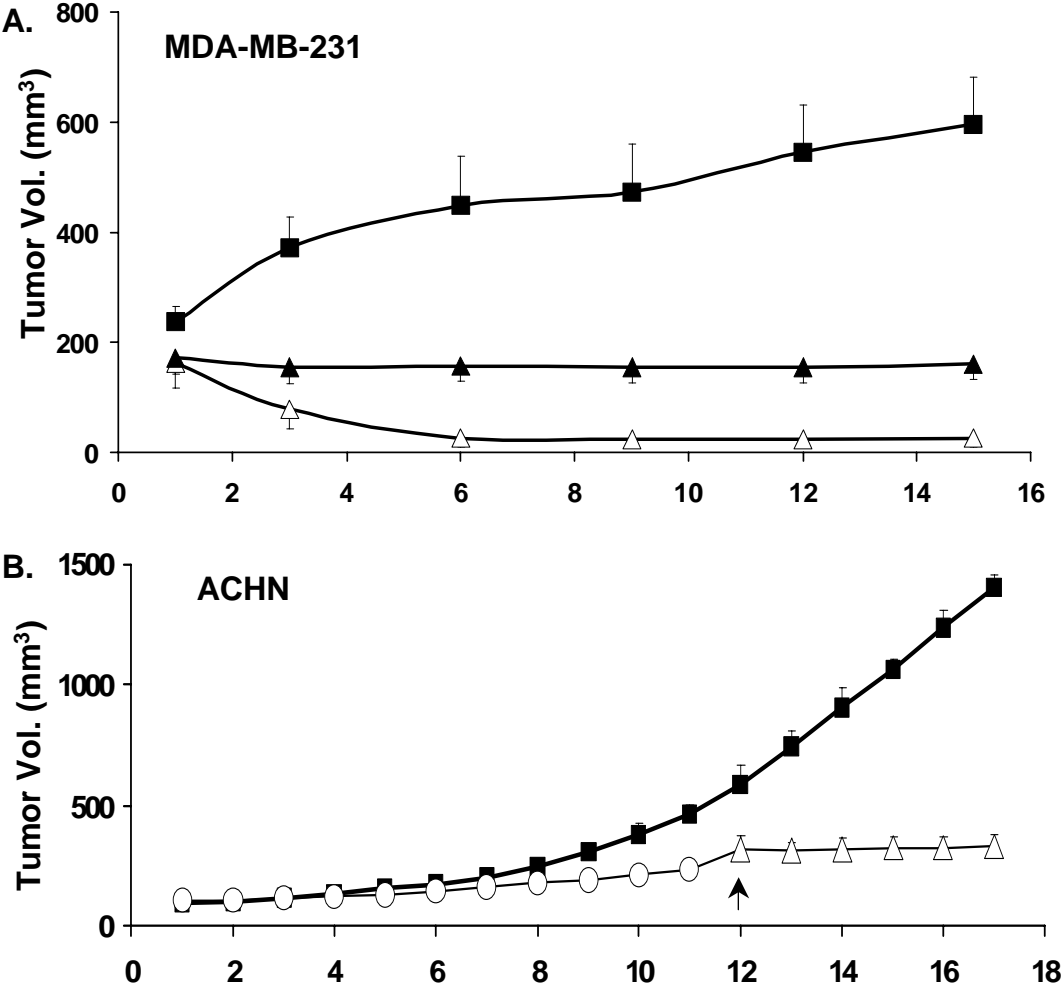


Figure 18. ARA-211 suppresses tumor growth and causes tumor regression. MDA-MB-231 cells were implanted under mammary fat pads (A.), and AHCN were implanted s.c. in nude mice (B.), and the mice treated (i.p.) either with vehicle (square) or ARA-211, 100mpk/day (MDA-MB-231, closed triangle), 200 mpk/day (MDA-MB-231, open triangle), 75mpk/day (ACHN open circle) or 200 mpk/day (ACHN starting day 12, see ?) as described under Materials and Methods.

Figure 19. ARA-211 treatment of mice bearing A549, HCT-116 and SNB-19 xenografts has no effect on tumor growth

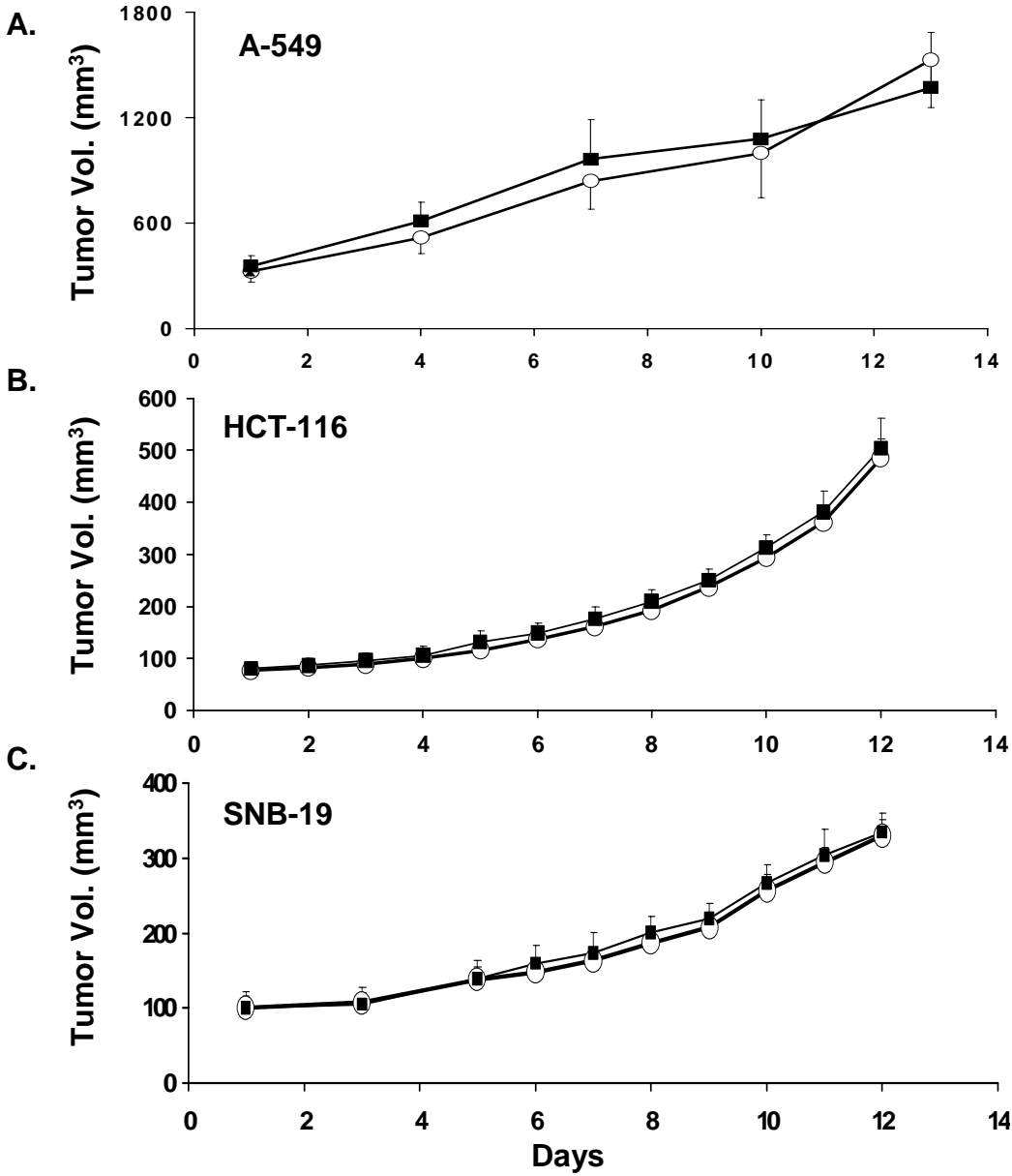


Figure 19. ARA-211 does not inhibit tumor growth in A549, HCT-116 or SNB-19 cell lines. A-549 (A.), HCT-116 (B.) and SNB-19 (C.) were implanted s.c. in nude mice and the mice treated (i.p.) either with vehicle (square) or 75mpk/day (circle) as described under Materials and Methods.

Table 4. ARA-211 inhibits tumor growth and induces apoptosis only in human cancer cell lines where it induces cAMP and lowers P-Erk1/2 levels






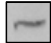


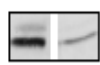
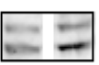
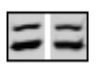
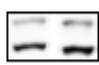
	MDA-MB-231	SE-539	ACHN	A-549	HCT-116	SNB-19
β2-ARExpression						
P-Erk1/2 (% Inhibition)	100 	100 	91 	0 	0 	0 
cAMP (Fold Induction)	16.7±5.4	13.1±3.0	16.5±3.2	1.3±0.3	1.1±0.1	1.2±0.4
Anchorage Dependent Growth (% Inhibition)	60.6±6.5	55±6.9	62±12.7	9.6±6.1	6.5±4.0	0(n=3)
Anchorage Independent Growth (% Inhibition)	82.7±7.9	94.4±1.5	97.9±1.2	0(n=6)	7.3±3.1	5.1±5.0
Apoptosis (% Induction)	15±4.0	9±1.7	11.4±1.9	3.1, 22	0, 1.2	0, 0
Tumor Growth in Mice (% Inhibition)	100	*	100	0	0	0

Table 4. Summary of physiological effects of ARA-211 mediated inhibition of P-Erk1/2 compared to vehicle, β2 AR expression, induction of cAMP and apoptosis, inhibition of anchorage dependent and independent cell growth, and inhibition of tumor growth in nude mice xenografts.

ARA-211 in-vivo treatment suppresses P-Erk1/2 levels, inhibits tumor growth and induces apoptosis in human xenografts in nude mice

Treatment with 200 MPK ARA-211 in the MDA-MB-231 xenograft model resulted in complete tumor regression, which left no tissue available at the end of the study for Immunohistochemical (IHC) evaluation. Therefore, we repeated the xenograft study with 75 MPK to elicit a response to ARA-211 but allow for partial inhibition of tumor growth. Figure 20 shows that treatment of mice with ARA-211 (75 mpk/day) inhibited tumor growth by 63%. Two hours after the final treatment the mice were euthanized, and the tumors were harvested and snap frozen. Tumors from MDA-MB-231 tumor xenografts treated with ARA-211 (75 mpk/day i.p.) or vehicle were analyzed by IHC for inhibition of P-Erk1/2, inhibition of proliferation (Ki-67), and induction of apoptosis (TUNEL). Tumors from ARA-211 treated mice had a significant decrease in cells staining positive for P-Erk1/2 (62%, $p = 0.02$) and Ki-67 (38% $P = 0.007$) along with a significant increase in cells staining positive for TUNEL (6-fold, $P = 0.0045$).

Figure 20. In-vivo treatment with ARA-211 suppresses P-Erk1/2 levels, inhibits tumor cell growth and induces apoptosis in human xenografts in nude mice

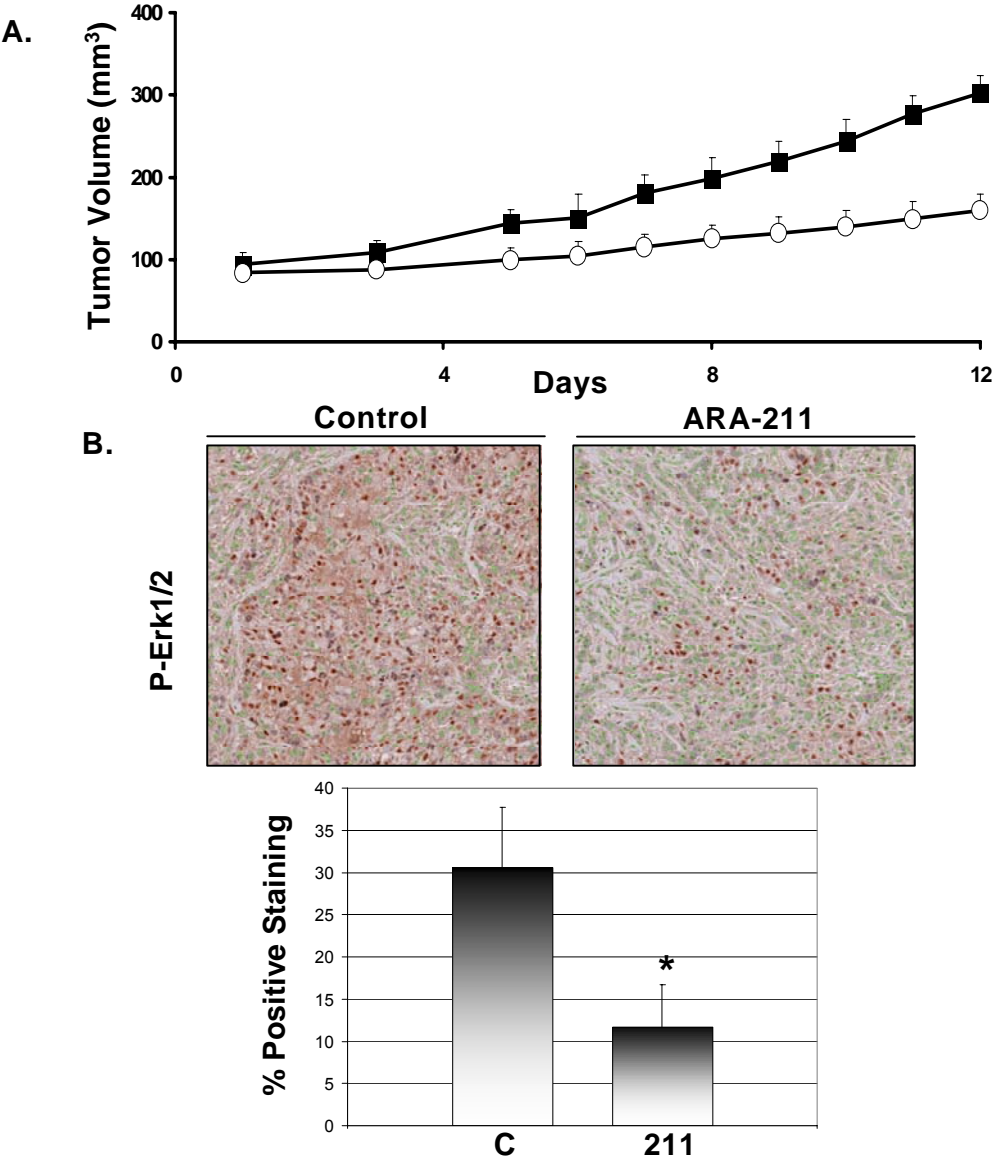


Figure 20. ARA-211 suppresses P-Erk1/2 levels in human xenografts in nude mice. A. MDA-MB-231 cells were implanted under mammary fat pads and the mice treated with vehicle (square) or ARA-211 (circle, 75mpk/day) as described previously. B. Tumors were removed on day 12 and processed for P-Erk1/2 levels (IHC) as described under Materials and Methods. * $p < 0.05$.

Figure 20 (continued). In-vivo treatment with ARA-211 suppresses P-Erk1/2 levels, inhibits tumor cell growth and induces apoptosis in human xenografts in nude mice

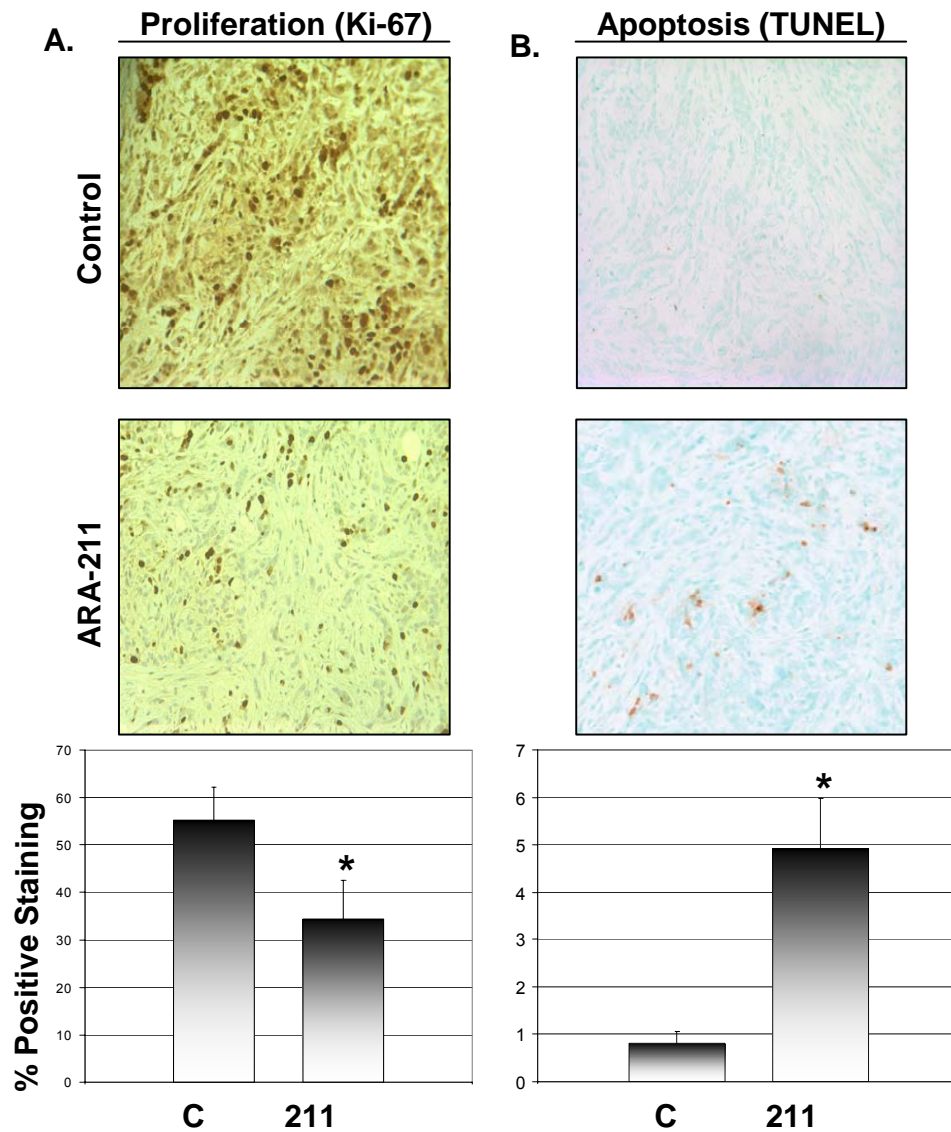


Figure 16. ARA-211 inhibits proliferation and induces apoptosis in human xenografts in nude mice. MDA-MB-231 cells were implanted under mammary fat pads and the mice treated with vehicle (square) or ARA-211 (circle, 75mpk/day) as described previously, tumors removed on day 12 and processed for proliferation (Ki-67) (A.) and apoptosis (Tunel) (B.) as described under Materials and Methods. * p < 0.05.

Discussion

A chemical biology approach was used to interrogate aberrant signal transduction circuits in human cancer cells about the importance of the $\beta 2$ adrenergic receptor in regulating cell division and tumor survival. Our studies clearly demonstrated that activation of the $\beta 2$ adrenergic receptor by ARA-211 results in inhibition of anchorage-dependent and -independent tumor cell growth as well as induction of apoptosis, and tumor regression in human tumors where stimulation of the $\beta 2$ AR results in blockade of the C-Raf/Mek1/2/Erk1/2 pathway. The mechanism by which ARA-211 inhibits the C-Raf/Mek1/2/Erk1/2 involves a cAMP-dependent PKA but not EPAC activation, as shown in Figure 21. This result was surprising in that PKA is traditionally known as a protooncogene. The fact that PKA can modulate C-Raf activity is known, but the mechanism by which PKA regulates C-Raf is controversial(61). Studies using radiolabeled phosphopeptide mapping for C-Raf demonstrated that serine 43 was the major residue directly phosphorylated by PKA *in-vivo*, but did not affect the kinase activity of C-Raf(133). This suggests that PKA either phosphorylates another inhibitory residue on C-Raf, or that PKA indirectly decreases the binding affinity of C-Raf for Ras. Other data suggests that inhibitory phosphorylation of serine 259 by PKA on C-Raf mediates the negative regulatory effects of PKA on the

Raf/Mek/Erk1/2 cascade(112). We investigated the affects of PKA activation by ARA-211 treatment of MDA-MB-231 cells on the phosphorylation of C-Raf on serine 43 and 259 residues, but did not find any changes compared to control treatments. It is possible that another proposed mechanism by which PKA indirectly inhibits C-Raf through activation of Rap-1 leading to competition for binding sites on Ras is occurring in MDA-MB-231 cells. However, we analyzed the levels of GTP-loaded Rap-1 from MDA-MB-231 cells treated with or without ARA-211, but did not find a difference in activated Rap-1 (data not shown). Therefore, our data suggests that the signaling mechanisms by which PKA controls C-Raf kinase activity in these breast cancer cells is more complex and will require more interrogation.

Data obtained from our ARA-211 studies clearly demonstrates that ARA-211-mediated inhibition of tumor cell growth is rescued by β 2 AR antagonists, suggesting that growth inhibition requires β 2 AR signaling. This is consistent with other studies that showed that isoprenaline, cholera toxin, forskolin, and 8-bromo-cAMP inhibit DNA synthesis and cell growth in normal cells(67, 134). However, these studies failed to interrogate the signaling responsible for these inhibitory effects. Increases in cAMP levels have also been shown to inhibit mitosis and MMP expression in MDA-MB-231 cells(67). These data, taken together with others demonstrating the ability of cAMP to regulate MAPK-Erk signaling and proliferation in normal cells, suggest that cAMP signaling may have tumor suppressive effects. However, this thesis work provides the first comprehensive examination of the tumor suppressive effects of cAMP

stimulation by a β 2 AR agonist in multiple cancer cell lines both *in-vitro* and *in-vivo*.

Figure 21. ARA-211 stimulates crosstalk between β 2 AR and Raf/MEK/Erk1/2 resulting in inhibition of P-Erk1/2 through a cAMP-dependent activation of PKA but not EPAC.

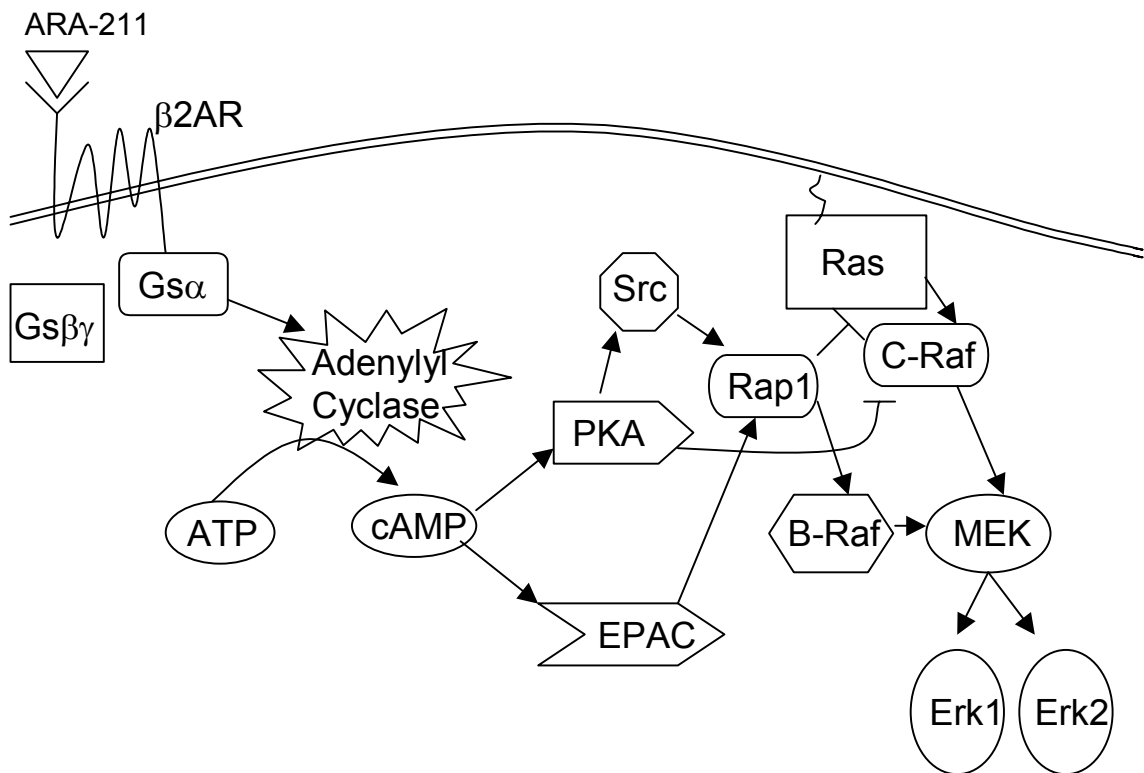


Figure 21. Schematic representation of crosstalk between signaling from ARA-211-stimulated β 2 AR to the Raf/MEK/Erk1/2 pathway through PKA or EPAC intermediates.

Another important finding from our studies is that cAMP induction by ARA-211 treatment induces apoptosis in cancer cells both *in-vitro* and *in-vivo*. Currently we do not have evidence that directly relates the inhibition of the Raf/Mek/Erk kinase cascade with the induction of apoptosis seen with ARA-211 treatment, however there is data in the literature supporting the proapoptotic functions of cAMP. These data include investigations showing cAMP induction resulting in S and G2/M cell cycle arrest, with cells eventually undergoing apoptosis in neuroblastoma and leukemia cell lines(66). Furthermore, another group identified a leukemia cell line that is resistant to cAMP-induced apoptosis based on overexpression of Bcl-2(135). This demonstrates that the apoptosis induced by cAMP may be independent of Erk1/2 inhibition, but other groups showed that inhibition of Erk1/2 could also lead to apoptosis. In melanoma cells it was shown that S6 kinase (S6K), an effector of Erk1/2 downstream, phosphorylates the proapoptotic protein Bad, leading to sequestration in the cytoplasm(136). Therefore, when P-Erk1/2 is inhibited, Bad is not sequestered and can localize to the mitochondrial membrane where it blocks the prosurvival functions of Bcl-2(136, 137). Similar studies have demonstrated that inhibition of Mek/Erk1/2 signaling results in accumulation of Bim, which ultimately associates with Bax, resulting in the induction of apoptosis(138, 139). Aside from inhibition of Mek/Erk1/2 activation, there have been reports of C-Raf modulating apoptosis, however these mechanisms were independent of the kinase activity of C-Raf. This is the case for Raf-related apoptosis through direct binding and influencing of MST2(140). These mechanisms all represent valid ways by which ARA-211

could induce apoptosis. Further work is necessary to elucidate the exact mechanisms causing the ARA-211-mediated induction of apoptosis.

Our studies also demonstrated that constitutively active Mek1/2 rescues from ARA-211 inhibition of tumor cell growth, suggesting that ARA-211 must inhibit C-Raf/Mek1/2/Erk1/2 to induce its antiproliferative effect. This is an important finding as a large number of human cancers harbor genetic alterations that ultimately result in hyperactivation of the C-Raf/Mek1/2/Erk1/2 pathway. For example, it is estimated that 30% of all human cancers contain Ras mutations that lead to hyperactivation of this pathway(9). And yet, some tumors with activated Ras do not have hyperactivactivated Erk1/2 due to activation of MAP kinase phosphatases. Similarly, a great majority of human cancers over express or contain constitutively activated receptor and non-receptor tyrosine kinases and/or growth factor autocrine loops that also result in hyperactivation of the C-Raf/Mek1/2/Erk1/2(141-144). More importantly, hyperactivation of this pathway is critical to the growth and survival of human tumors(72, 77). Finally, thwarting this pathway in human cancers may result in great benefits in the treatment of cancer patients since the genetic aberrations (i.e. Ras mutations, EGFR and ErbB2 overexpression) that result in hyperactivation of the C-Raf/Mek1/2/Erk1/2 pathway have all been associated with poor prognosis, resistance to therapy and shortened patient life(69, 70, 145, 146).

Using β 2 stimulation to cause tumor regression by blocking the C-Raf/Mek1/2/Erk1/2 pathway is a novel and powerful approach that could have a widespread use in cancer therapy. Indeed, tumors activate this pathway with a

broad spectrum of growth factors/cytokines and their receptors. For example, many growth factors such as EGF, PDGF, FGF, VEGF, IGF-1, heregulin and others all activate this pathway(72, 112, 141, 147). Therefore, tumors that express two or more of these growth factors may require a cocktail of anticancer drugs. In contrast, β 2AR stimulation will block activation of the C-Raf/Mek1/2/Erk1/2 pathway when it is driven by several growth factors since they all required Mek to activate Erk1/2(48, 53, 61, 62, 76). For example, we have shown that growth factor (i.e. EGF) stimulation of P-Erk1/2 is blocked by ARA-211 in MDA-MB-231 cells (data not shown).

This approach, however, is limited to those human tumors that express the β 2AR and where stimulation of this receptor results in blockade of C-Raf/Mek1/2/Erk1/2. In normal cells it has been shown that adrenergic stimulation can either stimulate or inhibit P-Erk1/2 and proliferation(34, 35, 48). However, in tumor cells, it is not known if stimulation of the β 2AR can stimulate tumorigenesis. In some normal cells expressing B-Raf, β 2 adrenergic receptors stimulate Erk1/2 by activating B-Raf which in turn activates Mek1/2(33, 148) while in other normal cells, β 2 adrenergic receptors inactivate Erk1/2 by blocking C-Raf(50, 57, 59, 60). Therefore, β 2 adrenergic receptors may also inhibit or stimulate Erk1/2 and proliferation in tumors.

To translate these important results to clinically relevant findings, fresh human tumor biopsies were used to determine the effects of β 2 AR stimulation on P-Erk1/2 levels in β 2 AR expressing tumors, as well as to determine if the ability of β 2 AR stimulation inhibits proliferation and/or induces apoptosis.

Chapter 2 focuses on the effects of ARA211 on fresh human tumor biopsies from the operating rooms at Moffitt Cancer Center. The fact that ARA-211 (pirbuterol) has previously been used orally and locally (149-151) in humans to evaluate its potential as an anti-asthmatic and for the treatment for congestive heart failure will facilitate its testing as an anti-cancer drug in hypothesis-driven clinical trials with patients where β 2AR stimulation is predicted to block C-Raf/Mek1/2/Erk1/2.

Chapter 2

**Determining the Prevalence of β 2 AR expression and P-Erk1/2 Activation in
Fresh Biopsies: ARA-211 Ex-vivo Studies**

Abstract

In Chapter 1 of this thesis we have demonstrated that stimulation of the $\beta 2$ AR with ARA-211 induced tumor suppression by a mechanism involving a cAMP-dependent activation of PKA, which in turn inhibited C-Raf and its downstream effectors Mek1/2 and Erk1/2. While this is an important finding, its benefit to patients will depend on confirming that $\beta 2$ AR has tumor suppressor activity in patient tumors. Furthermore, based on our data in human cancer cell lines, it is anticipated that only certain patients whose tumors express the appropriate markers will benefit from this novel therapeutic approach. Therefore, it is critical that fresh patient biopsies first be examined for the levels of $\beta 2$ AR as well as activation of Erk1/2, and that we determine whether the treatment of these fresh biopsies with ARA-211 ex-vivo leads to tumor growth suppression. In this chapter we determined by tissue array as well as fresh biopsies from Moffitt Cancer Center that approximately 25% of human tumors express both P-Erk1/2 and $\beta 2$ AR. Furthermore, ARA-211 treatment ex-vivo of these fresh patient samples followed by immunohistochemical staining of the tissue for P-Erk1/2, $\beta 2$ AR, Ki-67 for proliferation, and TUNEL for apoptosis, revealed that the effects are highly variable and need to be confirmed by xenograft studies of fresh biopsies.

Introduction

Recently the adrenergic receptor/trimeric G-protein/Adenyl Cyclase/cAMP pathway was shown to crosstalk to the RTK/Ras/Raf/Mek/Erk pathway in a tissue specific manner in normal cells. Both α and β isoform subtypes have been shown to crosstalk with MAP kinase cascade via $G\alpha_s$, $G\alpha_i$, and $\beta\gamma$ activation(49, 152, 153). In some normal cell types such as adipocytes, endothelial cells, fibroblasts, smooth muscle cells, hepatocytes, pancreatic acinar cells (AR42J), and bone cells (MG63), β_2 AR stimulation of cAMP production results in inhibition of the Ras/Raf/Mek/Erk pathway (60). The mechanism by which β_2 AR-mediated formation of cAMP blocks the Raf/Mek/Erk pathway is not well understood. For example, some reports have suggested a cAMP-dependent activation of PKA, which phosphorylates C-Raf and inactivates it. Other reports described a cAMP/PKA activation of Rap1, which binds Ras and inhibits its binding to C-Raf (60). Finally, others have shown that cAMP can activate the guanine nucleotide exchange factors EPAC1/2 that activate Rap1, which binds Ras and inhibits binding and activation of C-Raf (36, 37). In these cells where β_2 AR stimulation shuts down the Ras/Raf/Mek/Erk pathway, normal cell proliferation is inhibited.

On the contrary, in normal cells such as cardiac myocytes, rat thyroid cells, bone cells (ATDC5, MC4), prostate (PC12) and, sertoli cells, granulosa

cells, preadiposities, neuronal, and pituitary cells (GH4C1/GH3 cells), β 2AR stimulation of cAMP formation results in activation of the B-Raf/Mek/Erk pathway enhancing cell proliferation, inducing differentiation, or protection from apoptosis (32, 34, 126). Unlike the normal cells where cAMP production results in inhibition of C-Raf, in these normal cells cAMP production appears to be stimulating B-Raf. Here again, several mechanisms have been proposed by which the increase of cAMP results in the activation of B-Raf. One of these proposes a cAMP activation of EPAC, which activates Rap1 to activate B-Raf by an as yet unknown mechanism. Another reported mechanism involves cAMP activation of PKA, which activates Src, in turn activating Rap1 to activate B-Raf(34). Here PKA directly phosphorylates Src on serine 17, leading to activation of Rap-1 through exchange factors activated indirectly by Src(109).

In contrast to normal cells, little is known about the role of β 2AR stimulation in tumor growth and survival. The previous chapter demonstrated that activation of the β 2 AR in tumor cell lines MDA-MB-231, ACHN, and SF-539 resulted in induction of cAMP and subsequent stimulation of PKA kinase activity resulting in inhibition of C-Raf, but not B-Raf, kinase activity and inhibition of anchorage-dependent and -independent cell proliferation, induction of apoptosis, and inhibition of tumor growth in nude mice. It was also shown that these physiological effects were dependent on cAMP activation of PKA, but not EPAC, that resulted in the inhibition of Erk1/2 phosphorylation. However, these results relied only on cell lines, and we felt that translating these important findings to the clinic is critical. In order to do this we first needed to confirm our results and

conclusions in fresh human biopsies. There were several questions we needed to address; these are: 1. What is the prevalence of β 2AR expression and P-Erk1/2 levels in fresh human biopsies? 2. Are there certain tumor types that express these important markers, whereas others do not express these markers? 3. Are tumors that express β 2AR and P-Erk1/2 more sensitive to ARA-211 than those that do not, as we have seen in cell lines? 4. Are there any human tumors where ARA-211 may actually stimulate proliferation?

In this chapter we describe our work where we examined fresh tumor biopsies from patients from Moffitt Cancer Center for expression of β 2AR and P-Erk1/2, as well as the effects of ARA-211 ex-vivo treatment of these fresh biopsies on P-Erk1/2 levels, tumor cell proliferation, and apoptosis to answer these questions. In this chapter we determined by tissue array as well as fresh biopsies from Moffitt Cancer Center that approximately 25% of human tumors express both P-Erk1/2 and β 2 AR. Furthermore, ARA-211 treatment ex-vivo of these fresh patient samples followed by immunohistochemical staining of the tissue for P-Erk1/2, β 2 AR, Ki-67 for proliferation, and TUNEL for apoptosis, revealed that the effects are highly variable and need to be confirmed by xenograft studies of fresh biopsies.

Materials and Methods

Human Tissue Array

Using stage oriented human cancer tissue microarrays (Imgenex, Inc., San Diego, CA, catalogue # MB2 60), 56 tumor samples were analyzed for β 2 AR and MAPK expression by immunohistochemistry (four cores revealed no evidence of tumor). The tumors included invasive ductal carcinomas from breast (8); medullary carcinoma of breast (2); hepatocellular carcinomas (10); transitional cell carcinomas of the bladder (9); mucinous adenocarcinoma of urachal remnant (1); papillary serous cystadenocarcinomas of the ovary (9), mucinous cystadenocarcinoma of the ovary (1); pancreatic duct adenocarcinomas (10); prostatic adenocarcinomas (6). The patients had an average age of 59 years (range 16 to 85). Thirty were male and 26 were female. The tumors were staged according to the TNM system, following the recommendations of the American Joint Committee on Cancer, 5th Edition. The stage of the tumors was as follow: 4 patients had stage I, 9 stage II, 28 stage III, and 15 stage IV disease.

Immunohistochemistry.

Anti- β_2 Adrenergic Receptor (β_2 -AR) rabbit polyclonal antibody (H-73; sc-9042, Santa Cruz Biotechnology, Inc., dilution: 1: 400) and phospho ERK1/2 rabbit monoclonal antibody (20G11; Cell Signaling Technology, Inc., dilution 1:200) were applied to 3 μ M sections from formalin fixed, paraffin embedded tissue specimens, using the avidin-biotin-peroxidase complex method (Vectastatin Elite ABC Kit, Vector, Burlingame, CA), following the manufacturer's instructions. Slides were blocked with normal serum for 20 minutes, followed by incubation with the Anti- β_2 Adrenergic Receptor and the p-ERK 1/2 primary antibodies, at the dilution given, for 60 min. After rinsing with PBS for 5 minutes, sections were incubated with a biotinylated secondary antibody for 20 min. Following washing with PBS for 5 minutes, slides were incubated with avidin-biotin complex for 30 minutes and washed again. Chromogen was developed with 10 mg of 3,3 diaminobenzidine tetrahydrochloride (Sigma, St. Louis, Mo) diluted in 12 mL of Tris buffer, pH 7.6 for 2 minutes. All samples were lightly counterstained with Mayer's hematoxylin for 30 seconds before dehydration and mounting. Positive controls (cell line and non-stained tissue) and non-immune protein-negative controls were used for each section. No antigen retrieval was performed. The stain was semi-quantitatively examined by a board certified molecular pathologist. The positive reactions of each of the antibodies were scored into four grades according to the intensity of the staining: 0, 1+, 2+, and 3+. The percentages of β_2 -AR, and p-ERK1/2 positivity in the tumor cells were also

scored into four categories: 0 (0%), 1 (1% to 25%), 2 (26% to 50%), 3 (51% to 75%), 4 (76% to 100%) as determined by pathological scoring. The sum of the intensity and percentage scores was used as the final staining score. The final staining pattern of the tumors is defined as follows: 0 to 1, negative; 2 to 3, weak; 4 to 5, moderate; 6 to 7, strong.

Treatment of Patient Samples *Ex-vivo*

Fresh human tumor tissue samples were taken from biopsies or resections at Moffitt Cancer Center and immediately placed in RPMI media containing 20% calf serum. Samples were cut into thin sections using a surgical scalpel and placed in 24 well plates with media completely covering the tissue. Samples were treated with vehicle (0.1% DMSO) or ARA-211 at 100 μ M for 2 and 18 hours. These time points were selected to minimize the potential for tissue necrosis to occur. Tissue was collected at these time points and fixed in 10 % neutral buffered formalin for at least 48 hours. Fixed samples were taken to the histology core facility at the University of South Florida College of Medicine for immunohistochemical staining for P-Erk1/2, β 2 AR, Ki-67 and TUNEL. Staining analysis and slide quantitation was provided by the Moffitt Cancer Center Pathology Core Facility.

Results

Tissue arrays and fresh human biopsies reveal human tumor samples that express β 2 AR and have activated Erk1/2

To determine if patients could benefit from ARA-211 therapy for cancer we first determined if human tumor tissue expressed the β 2 AR, which is necessary for ARA-211 to induce cAMP through adenylyl cyclase activation, as well as whether they contained persistently active hyper-phosphorylated Erk1/2. To this end, we first determined the levels of β 2 AR in a human tumor tissue array that contained tumor specimens from breast, liver, bladder, ovary, prostate and pancreatic tissue (Figures 22-27, Table 5). Strong to moderate cytoplasmic β 2 AR immunostaining (final score between 4 and 7), was observed in 100% of prostate (6/6) (Figure 27) and breast (10/10) (Figure 22) carcinomas, independently of the tumor subtype; 80% of ovarian carcinomas (8/10) (Figure 25); 70% of pancreatic cancers (7/10) (Figure 26); 55% of bladder tumors (5/9) (Figure 24), and in only 30% of hepatocellular carcinomas (3/10) (Figure 23). One of the two ovarian tumors with low final β 2 AR score (3) was a mucinous cystadenocarcinoma. Six (60%) of the hepatocellular carcinomas, 4 (44%) bladder transitional cell carcinomas, and 1 (10%) of the pancreatic cancers

demonstrated no $\beta 2$ AR expression (final score 0). Moderate to strong P-Erk1/2 reactivity (final score between 4 and 7) was observed in 50% of the ovarian tumors (5/5) (Figure 25); 2 of 10 bladder tumors (20%) (Figure 24); 2 of 6 prostate cancers (33%) (Figure 27); 2 of 10 breast cancers (20%) (Figure 22), and in only 1 of 10 pancreatic tumors (10%) (Figure 26). All of the other tumors examined were found to be P-ERK1/2 negative (final score 0). The P-Erk1/2 immunostain localized to both nucleus and cytoplasm of the tumor cells, in the majority of the positive cases. In general, $\beta 2$ AR was more commonly expressed in this array than P-Erk1/2. $\beta 2$ AR was expressed in all breast and ovarian samples and in 90% and 75% of pancreatic and prostate samples. A significant inverse correlation between $\beta 2$ AR and P-Erk1/2 staining was observed in 31 of 56 cases (55%). All together the data from the tissue array demonstrated that even with a small sample size we were able to identify human tumors that express both the $\beta 2$ AR as well as P-Erk1/2. In fact, approximately 20 percent of the tissue analyzed expressed both protein markers. Furthermore, ovarian cancer appears to have the highest frequency of expression of both markers (50%), followed by prostate (25%) and breast (20%). On the other hand, liver, bladder and pancreas tissues have the lowest with 0, 10 and 10%, respectively. These findings suggest that there may be patient populations whose tumors express both $\beta 2$ AR and high levels of P-Erk1/2 which may respond favorably to ARA-211 therapy.

Figure 22. Tissue array identifies human breast tumor samples that express β 2 AR and P-Erk1/2

<u>Tissue Array Sample</u>	<u>P-Erk1/2</u>	<u>β2 AR</u>
Breast infiltrating duct carcinoma II		
Breast infiltrating duct carcinoma III		
Breast infiltrating duct carcinoma III		
Breast infiltrating duct carcinoma III		
Breast infiltrating papillary carcinoma III		

Figure 22 (continued). Tissue array identifies human breast tumor samples that express β 2 AR and P-Erk1/2

Tissue Array Sample	P-Erk1/2	β 2 AR
Breast infiltrating duct carcinoma III		
Breast mixed infiltrating duct and lobular carcinoma III		
Breast medullary carcinoma II		
Breast atypical medullary carcinoma II		
Breast infiltrating duct carcinoma III		

Figure 23. Tissue array identifies human liver tumor samples that express β 2 AR and P-Erk1/2

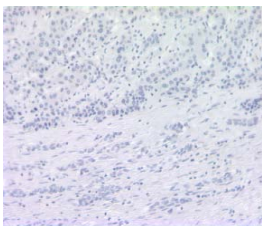
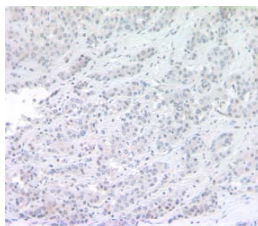
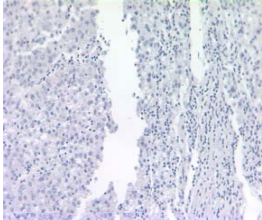
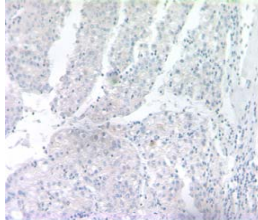
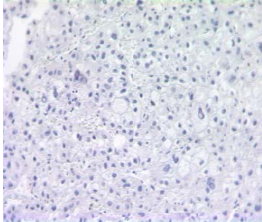
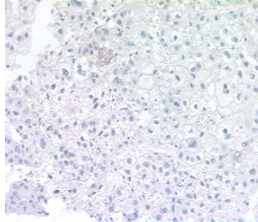
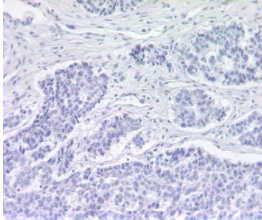
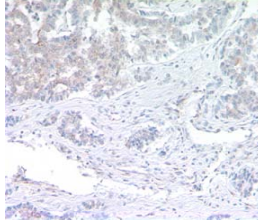
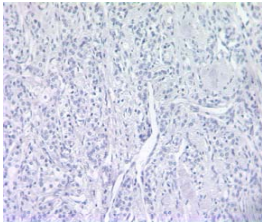
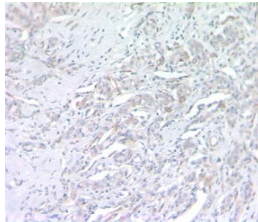
Tissue Array Sample	P-Erk1/2	β2 AR
Liver combined hepatocellular and cholangiocarcinoma III		
Liver hepatocellular carcinoma III		
Liver hepatocellular carcinoma II		
Liver hepatocellular carcinoma IV		
Liver hepatocellular carcinoma II		

Figure 23 (continued). Tissue array identifies human liver tumor samples that express β 2 AR and P-Erk1/2

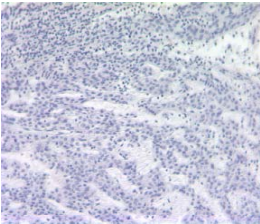
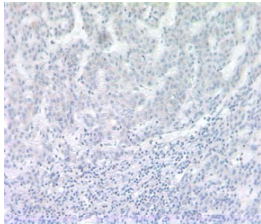
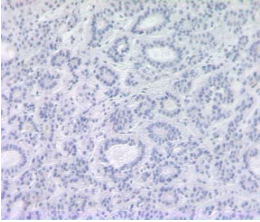
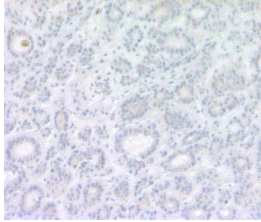
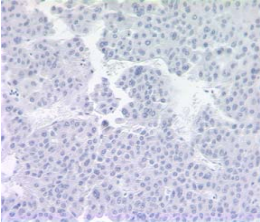
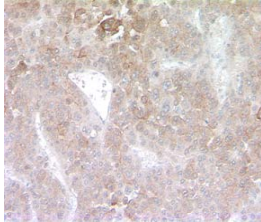
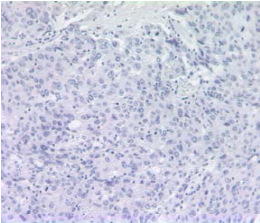
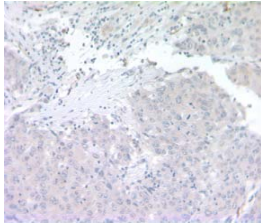
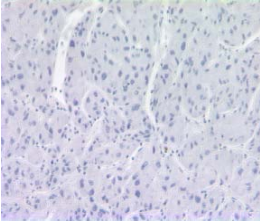
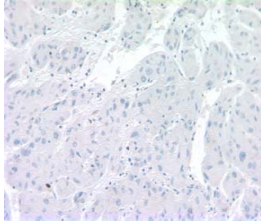
Tissue Array Sample	P-Erk1/2	β 2 AR
Liver hepatocellular carcinoma II		
Liver hepatocellular carcinoma II		
Liver hepatocellular carcinoma III		
Liver combined hepatocellular and cholangiocarcinoma III		
Liver hepatocellular carcinoma III		

Figure 24. Tissue array identifies human bladder tumor samples that express β 2 AR and P-Erk1/2

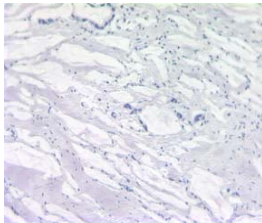
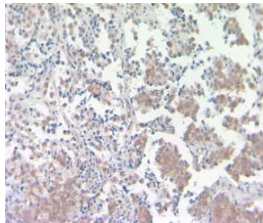
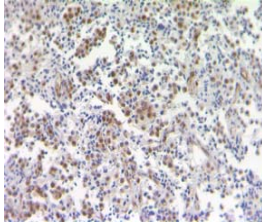
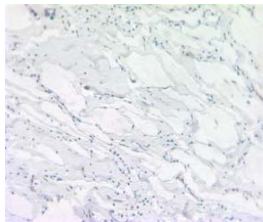
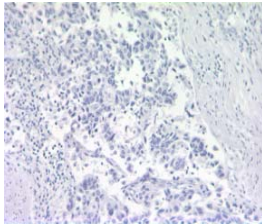
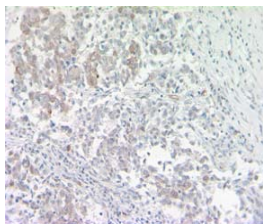
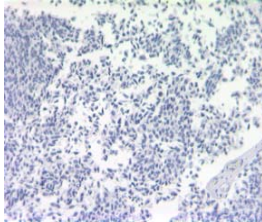
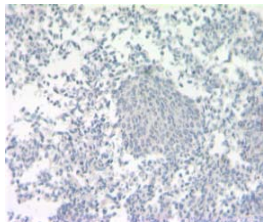
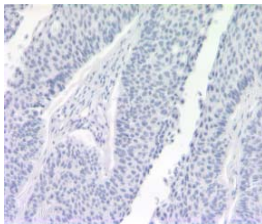
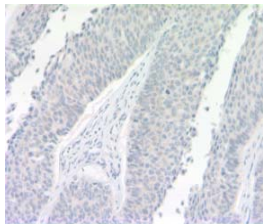
Tissue Array Sample	P-Erk1/2	β2 AR
Urinary bladder mucinous adenocarcinoma		
Urinary bladder transitional cell carcinoma IV		
Urinary bladder transitional cell carcinoma IV		
Urinary bladder transitional cell carcinoma IV		
Urinary bladder papillary transitional cell carcinoma IV		

Figure 24 (continued). Tissue array identifies human bladder tumor samples that express $\beta 2$ AR and P-Erk1/2

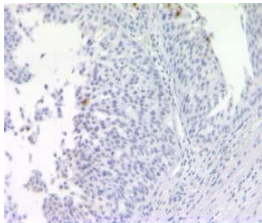
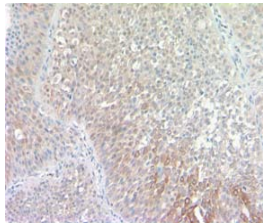
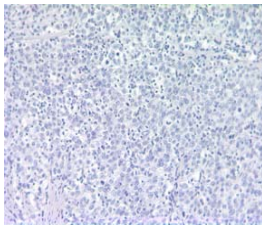
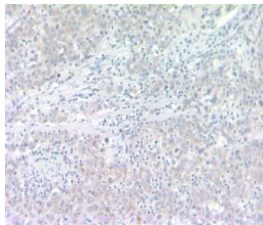
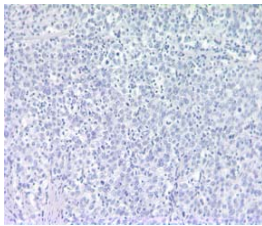
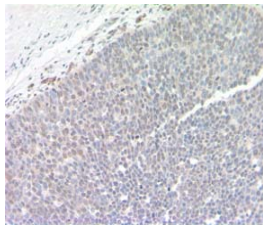
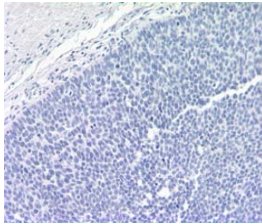
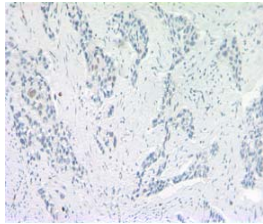
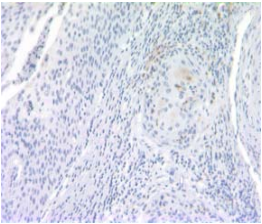
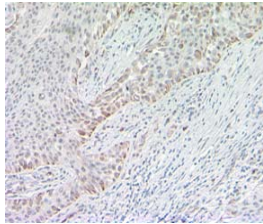
Tissue Array Sample	P-Erk1/2	$\beta 2$ AR
Urinary bladder papillary transitional cell carcinoma IV		
Urinary bladder transitional cell carcinoma III		
Urinary bladder papillary transitional cell carcinoma I		
Urinary bladder transitional cell carcinoma III		
Urinary bladder transitional cell carcinoma III		

Figure 25. Tissue array identifies human ovarian tumor samples that express β 2 AR and P-Erk1/2

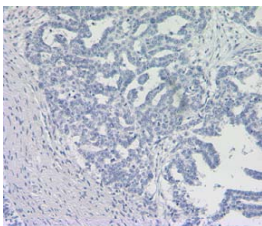
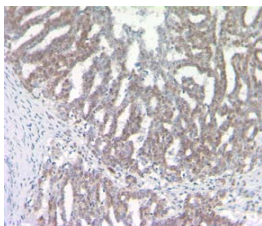
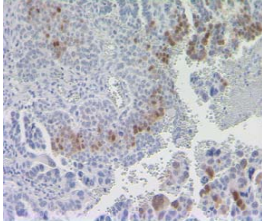
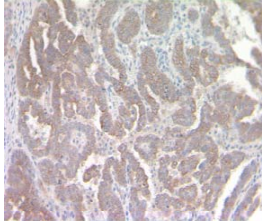
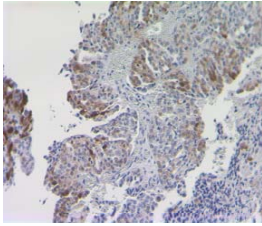
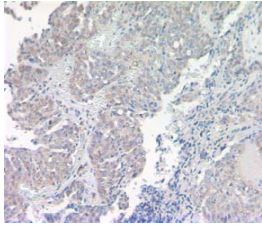
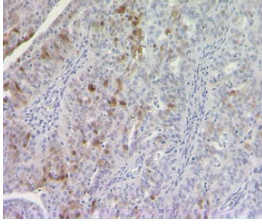
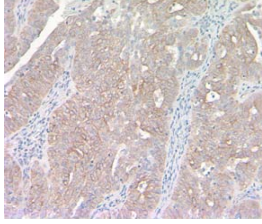
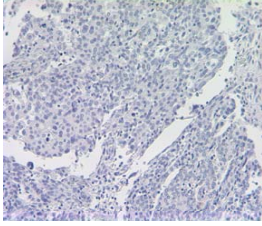
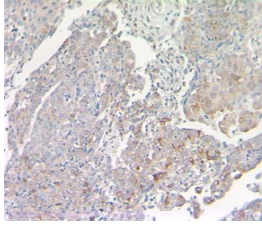
Tissue Array Sample	P-Erk1/2	β 2 AR
Ovary papillary serous cystadenocarcinoma		
Ovary papillary serous cystadenocarcinoma		
Ovary papillary serous cystadenocarcinoma I		
Ovary papillary serous cystadenocarcinoma		
Ovary papillary serous cystadenocarcinoma		

Figure 25 (continued). Tissue array identifies human ovarian tumor samples that express β 2 AR and P-Erk1/2

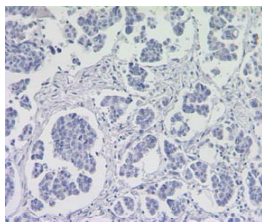
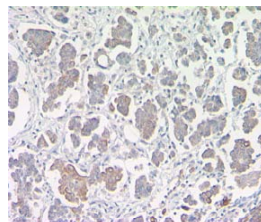
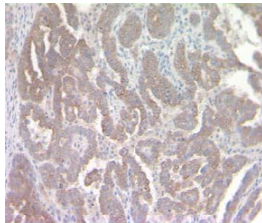
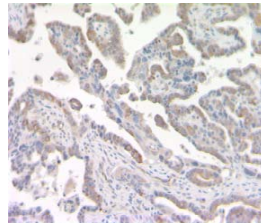
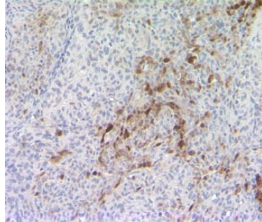
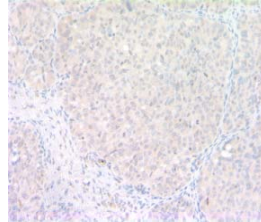
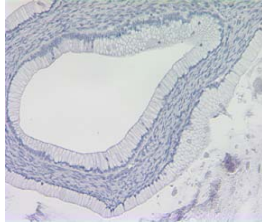
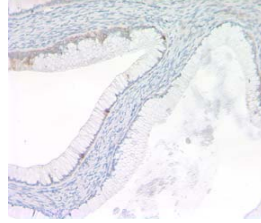
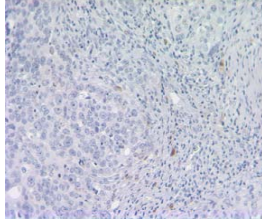
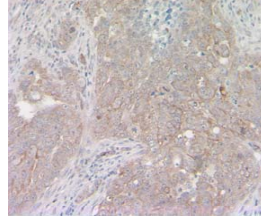
<u>Tissue Array Sample</u>	<u>P-Erk1/2</u>	<u>β2 AR</u>
Ovary papillary serous cystadenocarcinoma		
Ovary papillary serous cystadenocarcinoma I		
Ovary papillary serous cystadenocarcinoma III		
Ovary mucinous cystadenocarcinoma		
Ovary serous cystadenocarcinoma		

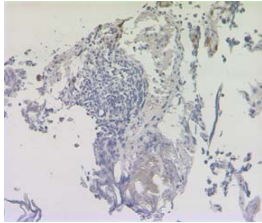
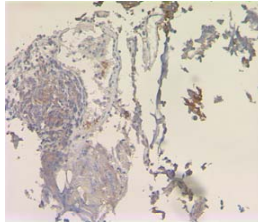
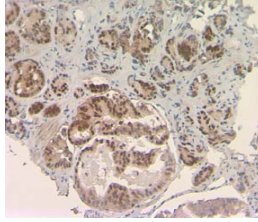
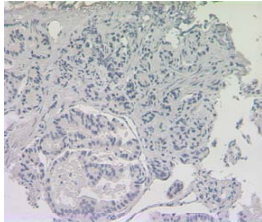
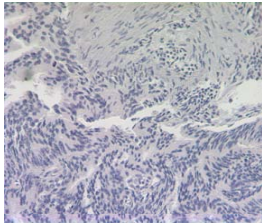
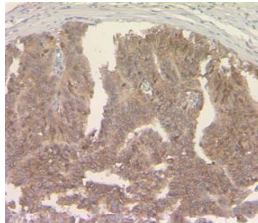
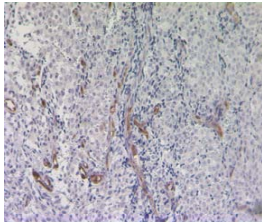
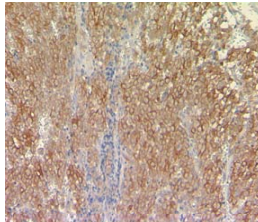
Figure 26. Tissue array identifies human pancreatic tumor samples that express β 2 AR and P-Erk1/2

<u>Tissue Array Sample</u>	<u>P-Erk1/2</u>	<u>β2 AR</u>
Pancreatic ductal adenocarcinoma I		
Pancreatic ductal adenocarcinoma II		
Pancreatic ductal adenocarcinoma III		
Pancreatic ductal adenocarcinoma I		
Pancreatic ductal adenocarcinoma I		

Figure 26 (continued). Tissue array identifies human pancreatic tumor samples that express $\beta 2$ AR and P-Erk1/2

<u>Tissue Array Sample</u>	<u>P-Erk1/2</u>	<u>$\beta 2$ AR</u>
Pancreatic ductal adenocarcinoma III		
Pancreatic ductal adenocarcinoma V		
Pancreatic ductal adenocarcinoma III		
Pancreatic ductal adenocarcinoma III		
Pancreatic ductal adenocarcinoma III		

Figure 27. Tissue array identifies human prostate tumor samples that express β 2 AR and P-Erk1/2

Tissue Array Sample	P-Erk1/2	β 2 AR
Prostate adenocarcinoma		
Prostate adenocarcinoma	ND	
Prostate adenocarcinoma		ND
Prostate adenocarcinoma		
Prostate adenocarcinoma		

ND = Not Determined

Figure 27 (continued). Tissue array identifies human prostate tumor samples that express $\beta 2$ AR and P-Erk1/2

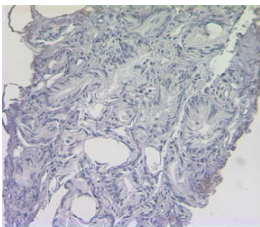
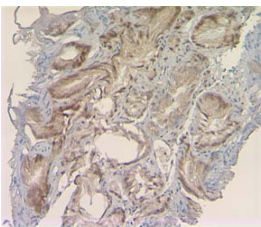
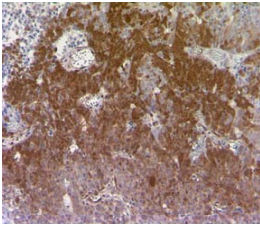
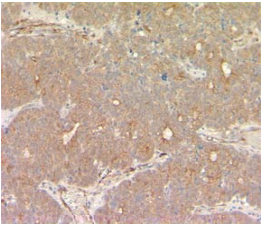
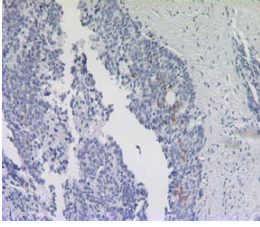
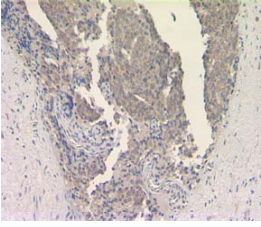
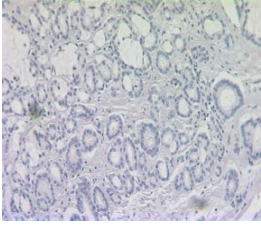
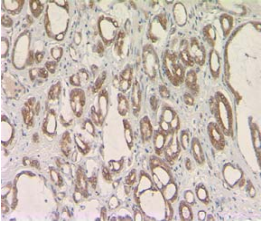
<u>Tissue Array Sample</u>	<u>P-Erk1/2</u>	<u>$\beta 2$ AR</u>
Prostate adenocarcinoma III		
Prostate adenocarcinoma		
Prostate adenocarcinoma		
Prostate adenocarcinoma I		

Table 5. Summary of tissue array staining results for β 2 AR and P-Erk1/2

Tissue Type	β2 AR ^a	P-Erk1/2 ^b	β2 AR & P-Erk1/2 ^c
Breast (n =10)	100	20	20
Liver (n =10)	40	0	0
Bladder (n =10)	60	10	10
Ovary (n =10)	100	50	50
Pancreas (n =10)	90	10	10
Prostate (n =9)	75	25	25

a - % of tumors positive for β 2 AR

b - % of tumors positive for P-Erk1/2

c - % of tumors positive for both

Fresh human tumor biopsies from Moffitt Cancer Center were obtained to extend the findings of the tissue array to fresh samples. The tissues were then fixed in 10% neutral buffered formalin and stained for expression of $\beta 2$ AR and P-Erk1/2. Results obtained from these tissues were similar to the tissue array in that approximately 28 percent of the tissues stained positive for both $\beta 2$ AR as well as P-Erk1/2 (Table 6). Figure 28 demonstrates the typical staining patterns of both $\beta 2$ AR and P-Erk1/2 in the fresh human tumor biopsies. P-Erk1/2 staining is localized to both the nucleus and cytoplasm, whereas $\beta 2$ AR staining is seen mostly in the cytoplasm and somewhat around the plasma membrane. Table 6 further characterizes the staining percentages seen in the tumor biopsies collected from all tissue types. Results from the fresh biopsy samples differed from those of the tissue array in that tumors from the liver, colon and pancreas demonstrated the highest percentage of co-staining for the $\beta 2$ AR and P-Erk1/2 at 50%. Interestingly, 100% of the liver, retroperitoneal and pancreatic tumor tissues showed moderate to strong staining for $\beta 2$ AR, however even in some tissues that expressed high $\beta 2$ AR levels there were still high levels of P-Erk1/2 co-expressed. This suggests that either the activating ligands for the $\beta 2$ AR are not present, or that $\beta 2$ AR signaling does not result in inhibition of the C-Raf/Mek/Erk pathway in these tissues. Ultimately, 56% of all tumor types tested showed $\beta 2$ AR staining. In contrast to the tissue array staining results in which $\beta 2$ AR staining was more prevalent than P-Erk1/2, the samples collected from Moffitt Cancer Center demonstrated similar staining percentages for P-Erk1/2 at

57%, compared to $\beta 2$ AR at 56%. The differences in staining between the two sets of tissues may be due to the wider variety cancer tissues obtained from Moffitt Cancer Center, compared to the 6 tumor types from the array. 100% of the sarcomas, brain tumors, and mediastinum tumors demonstrated staining for P-Erk1/2, although the sample size for these tissues were low. Likewise, 50% of the tumors tested for 12 of the 15 tumor types showed expression of P-Erk1/2. These findings confirm that there may be a patient population whose tumors express both $\beta 2$ AR and high levels of P-Erk1/2, however we do not know if stimulation of the $\beta 2$ AR in these tumors will result in decreases in P-Erk1/2, inhibition of cell proliferation or induction of apoptosis.

Figure 28. Fresh patient samples from Moffitt Cancer Center express β 2 AR and P-Erk1/2

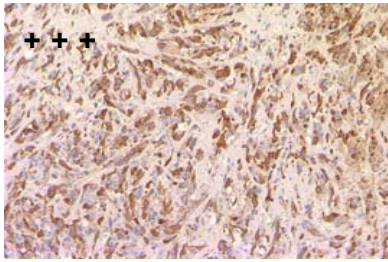
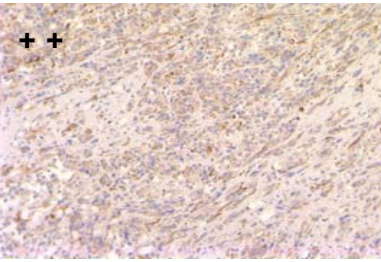
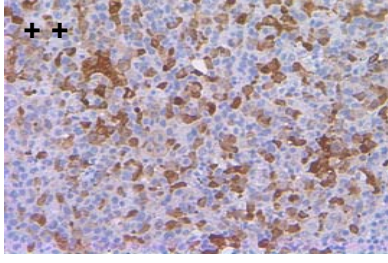
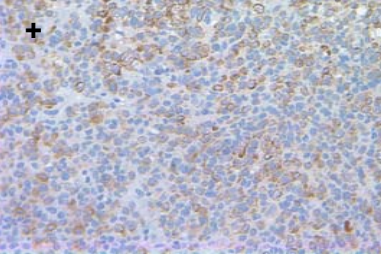
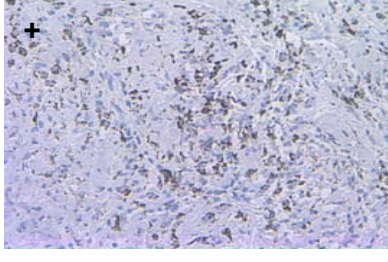
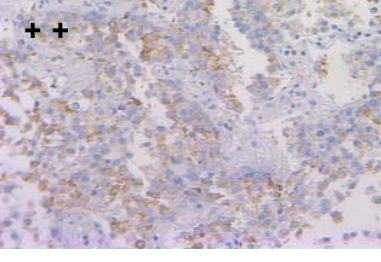
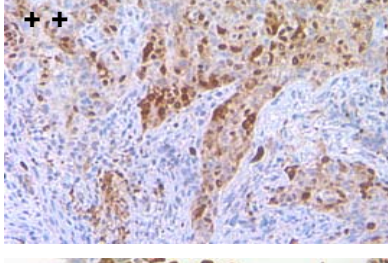
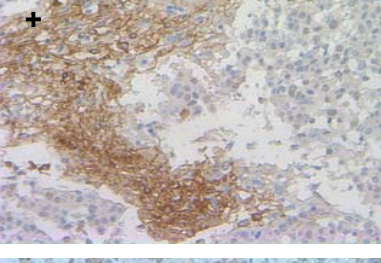
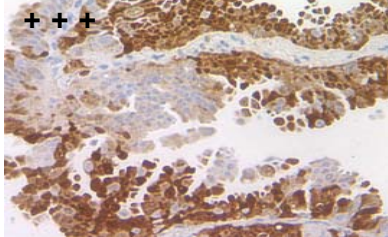
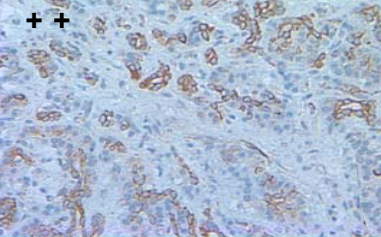
Pt Sample	P-Erk1/2	β 2AR
Liver	+++ 	++ 
Lung	++ 	+ 
Lung	+ 	++ 
Mediastinum	++ 	+ 
Pancreas	+++ 	++ 

Table 6. Summary of fresh human tumor biopsy staining results for β 2 AR and P-Erk1/2

Tumor Type	β2 AR^a	P-Erk1/2^b	β2 Ar & P-Erk1/2^c
Liver (n=6)	100	50	50
Breast (n=5)	60	60	20
Lung (n=5)	60	60	40
Kidney (n=5)	60	60	40
Colon (n=4)	50	75	50
Retro-peritoneal (n=3)	100	66	33
Sarcoma (n=3)	33	100	33
Stomach (n=3)	33	33	0

a - % of tumors positive for β 2 AR

b - % of tumors positive for P-Erk1/2

c - % of tumors positive for both

Table 6 (continued). Summary of fresh human tumor biopsy staining results for β 2 AR and P-Erk1/2

Tumor Type	β2 AR^a	P-Erk1/2^b	β2 Ar & P-Erk1/2^c
Pancreas (n=2)	100	50	50
Head and Neck (n=2)	50	50	0
Lymph Node (n=2)	50	0	0
Omentum (n=2)	50	50	0
Brain (n=1)	0	100	0
Thyroid (n=1)	0	0	0
Mediastinum (n=1)	100	100	100

a - % of tumors positive for β 2 AR

b - % of tumors positive for P-Erk1/2

c - % of tumors positive for both

Table 6. Summary of fresh human tumor biopsy staining results for β 2 AR and P-Erk1/2 as described under Materials and Methods.

Fresh human tumor samples treated ex-vivo demonstrate variable efficacy of ArA-211

The results described under Figures 22-28 and Tables 5 and 6 demonstrated that about 1/4 (~ 25%) of human tumors analyzed express both $\beta 2$ AR and have activated Erk1/2. We next attempted to determine whether the expression of these 2 markers predicts sensitivity to ARA-211 in fresh human biopsies treated ex-vivo. We therefore hypothesized that at least some of the human tumors that express both $\beta 2$ AR and P-Erk1/2 will respond to ARA-211 treatment ex-vivo, as shown by decreased P-Erk1/2 levels (IHC) and proliferation (Ki-67 staining), and increased apoptosis (TUNEL staining). To test this hypothesis we prepared the fresh biopsies in a variety of ways to optimize preserving the human cancer cells as well as to avoid necrosis, independent of drug treatments. The first cohort of samples was processed by mincing the tissue to increase the exposure to ARA-211. Treatments were done in a time course of 0.5, 2, 6, 18, and 24 hours at 20 μ M to determine the best time point to harvest the tissue and analyze expression of P-Erk1/2, $\beta 2$ AR, Ki-67 and TUNEL. Prior to ex-vivo treatment a portion of the sample was taken as a pre-treatment sample and analyzed for $\beta 2$ AR and P-Erk1/2 expression. Analysis of the treated tumor samples revealed severe necrosis induced by mincing, which rendered the data obtained uninterpretable.

The second cohort of samples was subsequently collected and prepared for ex-vivo treatment by cutting the tissue into thin slices, and increasing the

concentration of ARA-211 from 20 μM to 100 μM to increase the tissue exposure to the drug. Vehicle treated samples were exposed for 24 hours, while ARA-211 treated samples were exposed for 2, 6, and 24 hours. Specimens were collected and analyzed for P-Erk1/2 and $\beta 2$ AR expression, along with proliferation and apoptosis by Ki-67 and TUNEL staining, respectively. Upon further examination of the results it was determined that the 24 hour time point for the vehicle treated sample was too distant from the 2 hour time point to analyze P-Erk1/2 and $\beta 2$ AR expression. In each case, the vehicle treated samples demonstrated a loss of expression of both P-Erk1/2 and $\beta 2$ AR compared to the pre-treatment samples collected before ex-vivo treatments. Due to the loss of expression in the 24 hour vehicle sample we were unable to determine the efficacy of ARA-211 to inhibit P-Erk1/2.

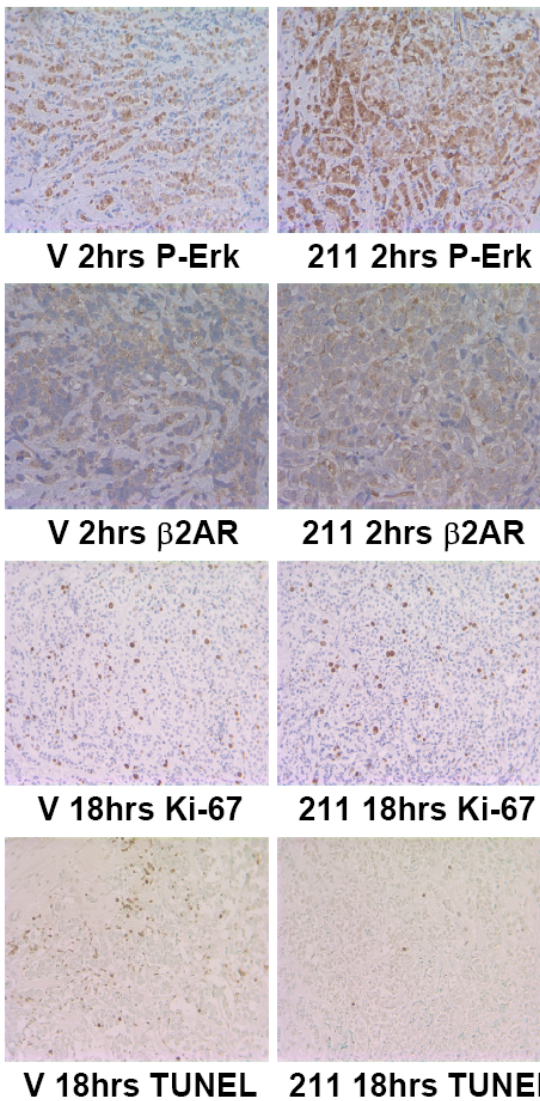
Finally, 2 hour and 18 hour time points were used for both vehicle and ARA-211 treated samples for the third cohort of patient samples collected. Aside from this difference the samples were treated just as they were in cohort two. In this case 20 fresh biopsies were collected and treated *ex-vivo*. Pathological analysis determined that interpretable data was obtained using this procedure as necrosis was minimized and interfered in only 4 of the 20 samples. However, in some samples necrosis was induced in the ARA-211 treated samples, but not the vehicle-treated samples. Necrosis was determined by pathological analysis of HE staining morphology, indicating overall intactness of the tissue before and after ex-vivo treatment. From the remaining samples in the absence of ARA-211 treatment there were 6 tumors that expressed both $\beta 2$ AR and P-Erk1/2, 6

tumors expressed only the $\beta 2$ AR, 2 tumors expressed only P-Erk1/2, and 1 tumor expressed neither $\beta 2$ AR or P-Erk1/2. The majority of the *ex-vivo* treated samples did not demonstrate changes in P-Erk1/2 or $\beta 2$ AR upon ARA-211 treatment. In 2 samples, Lung I and Kidney IV, P-Erk1/2 decreased 25% and 3%, respectively. These changes did not change staining by Ki-67, but resulted in a 15% and 5% increase in TUNEL staining, respectively. However, pathological analysis determined that the TUNEL background staining was high for several samples and additional apoptosis markers such as caspase 3 are needed. *Ex-vivo* treatment resulted in increases in P-Erk1/2 in 4 samples (Colon, Lung I, Kidney II, Omentum II), but with no other changes except for a 50% increase in the Ki-67 staining of the Omentum II sample from 15% to 30%. However, in the Lung I sample ARA-211 treatment increased TUNEL staining from 5% to 45%, but at 18 hours the sample also exhibited 90% necrosis. The $\beta 2$ AR staining remained fairly constant at the 2 hour treatment time point among most of the samples treated *ex-vivo*. An increase in $\beta 2$ AR expression was seen in 4 samples and a decrease was noted in only 2 samples, where the expression did not change among the remainder of the 14 samples. Likewise, the Ki-67 staining for proliferation exhibited little changes in these samples as well. Only 3 samples demonstrated a decrease in Ki-67 positive cells, while 1 sample showed an increase. No correlation was noted between decreases in Ki-67 and decreases in P-Erk1/2. In fact, 2 of the samples in which Ki-67 decreased there was no P-Erk1/2 expression, and in 1 sample the P-Erk1/2 staining increased by 15% while the Ki-67 staining decreased by 30%. Taken together, based on the

limited sample size of 20 and the variability of the results, it is not possible to determine whether expression of $\beta 2$ AR and P-Erk1/2 predicts response to ARA-211. Indeed, only 6 samples expressed both $\beta 2$ AR and P-Erk1/2. Furthermore, the necrosis observed not only interfered with the quality of the data, but also made it difficult to interpret the data. This led us to question whether slices of tumor biopsies were the best approach to answer the questions we posed. Therefore, our conclusion is that an alternative approach must be utilized. To this end, perhaps using fresh tumor biopsies that have been passaged in nude mice to select for tumors that grow *in-vivo* is a better approach(154).

Figure 29. Ex-Vivo treatment of fresh human tumor tissue demonstrates variable efficacy of ARA-211 to inhibit P-Erk1/2, inhibit proliferation and induce apoptosis

Breast Tumor :



Liver Tumor :

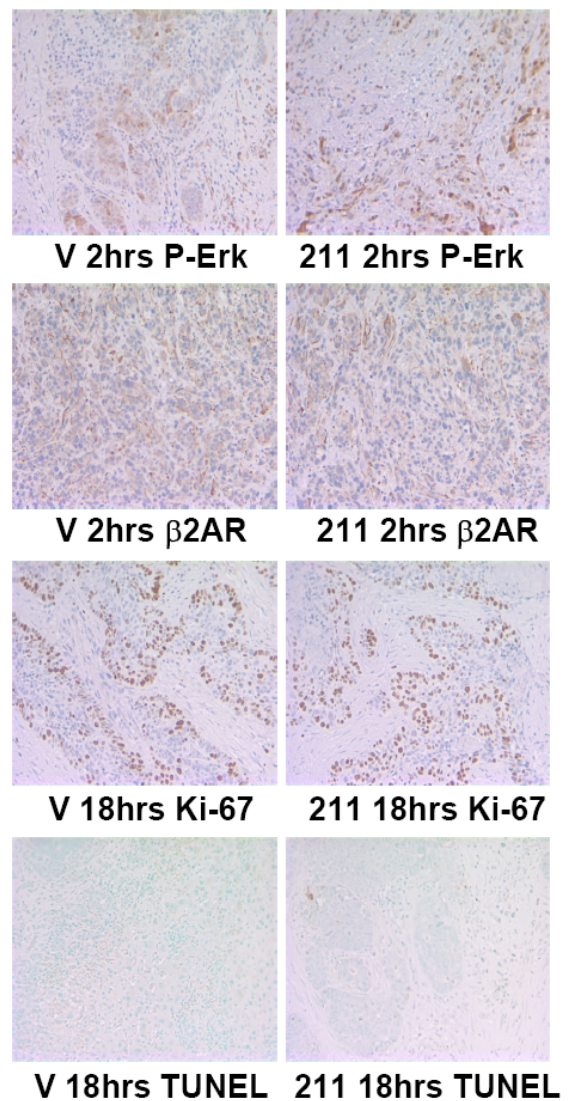


Figure 29 (continued). Ex-Vivo treatment of fresh human tumor tissue demonstrates variable efficacy of ARA-211 to inhibit P-Erk1/2, inhibit proliferation and induce apoptosis

Retro-Peritoneal Tumor :

Colon Tumor :

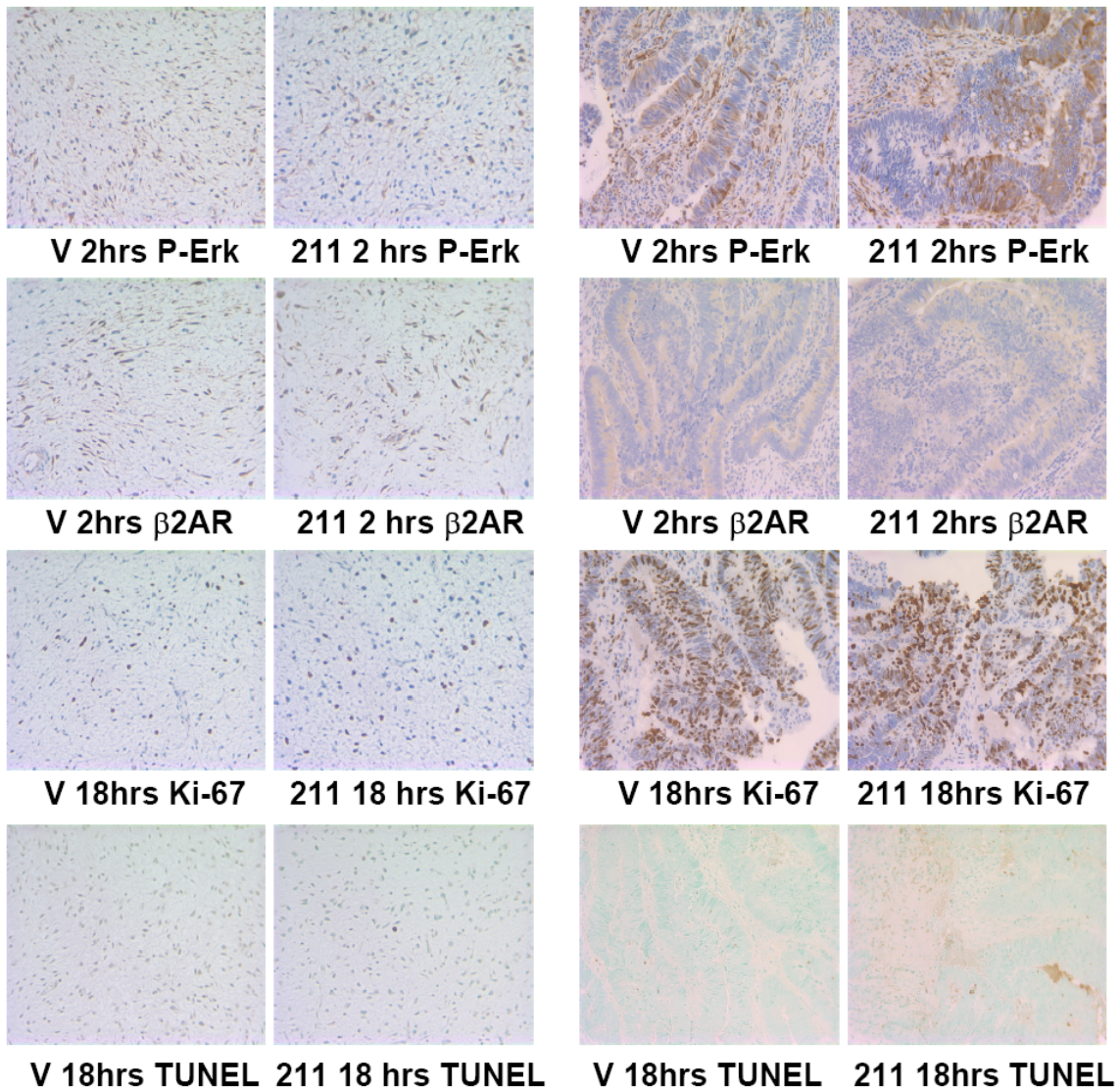
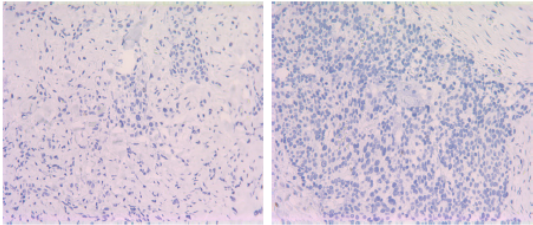


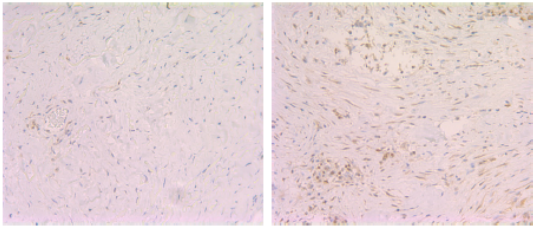
Figure 29 (continued). Ex-Vivo treatment of fresh human tumor tissue demonstrates variable efficacy of ARA-211 to inhibit P-Erk1/2, inhibit proliferation and induce apoptosis

Lymph Node Tumor :



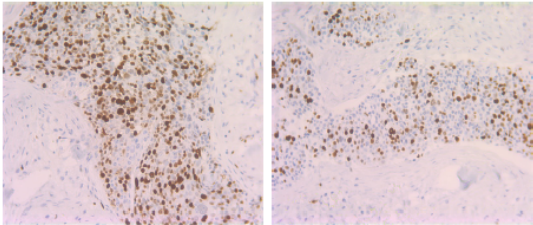
V 2hrs P-Erk

211 2hrs P-Erk



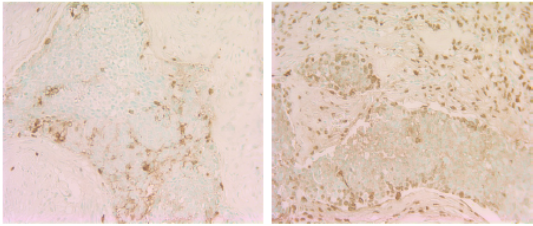
V 2hrs beta2AR

211 2hrs beta2AR



V 18hrs Ki-67

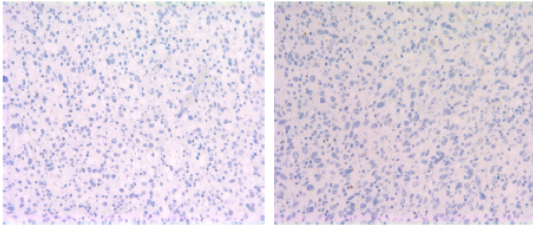
211 18hrs Ki-67



V 18hrs TUNEL

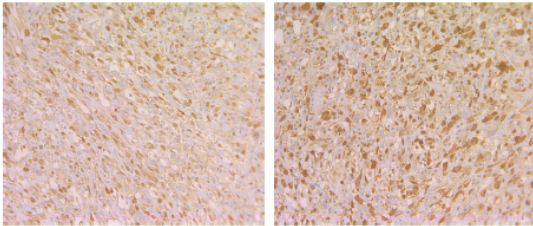
211 18hrs TUNEL

L Thigh Sarcoma Tumor :



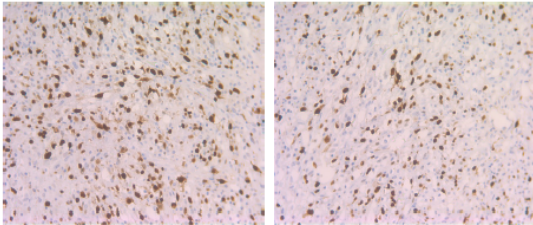
V 2hrs P-Erk

211 2hrs P-Erk



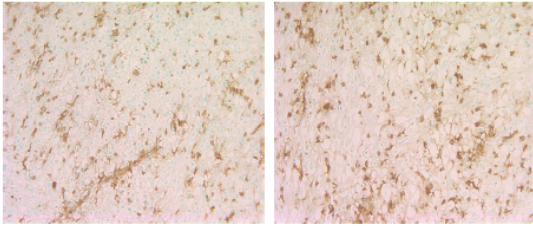
V 2hrs beta2AR

211 2hrs beta2AR



V 18hrs Ki-67

211 18hrs Ki-67

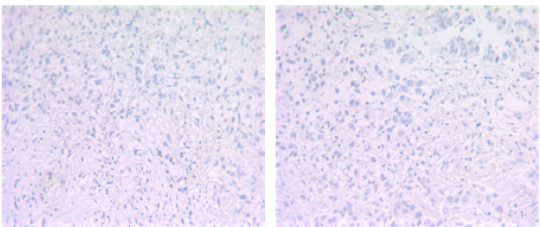


V 18hrs TUNEL

211 18hrs TUNEL

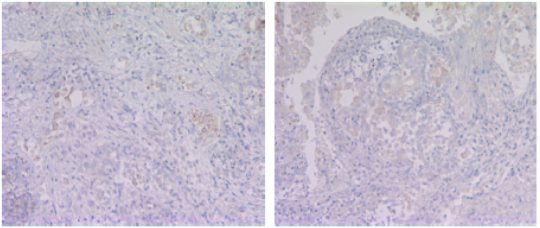
Figure 29 (continued). Ex-Vivo treatment of fresh human tumor tissue demonstrates variable efficacy of ARA-211 to inhibit P-Erk1/2, inhibit proliferation and induce apoptosis

Lung Tumor I :



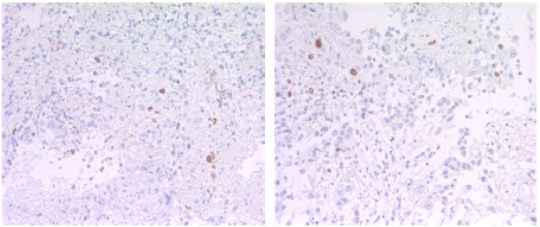
V 2hrs P-Erk

211 2hrs P-Erk



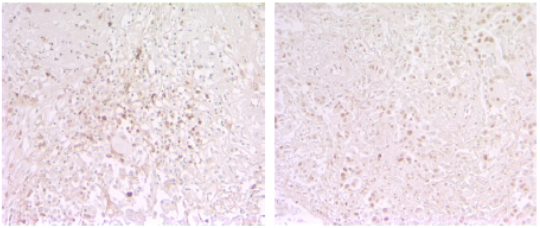
V 2hrs beta2AR

211 2hrs beta2AR



V 18hrs Ki-67

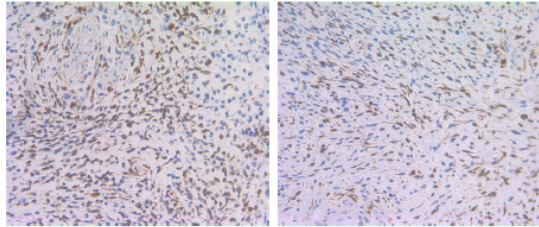
211 18hrs Ki-67



V 18hrs TUNEL

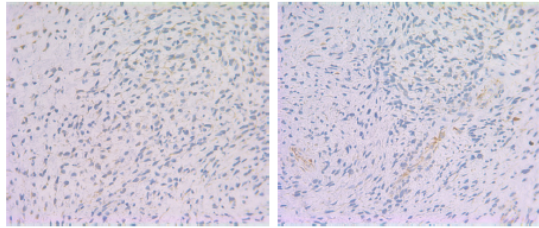
211 18hrs TUNEL

Lung Tumor II :



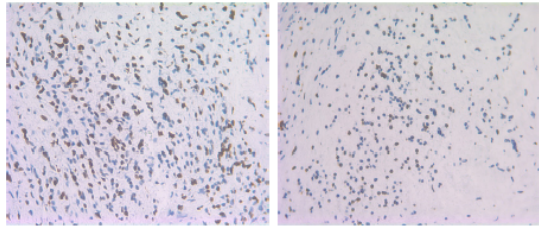
V 2hrs P-Erk

211 2hrs P-Erk



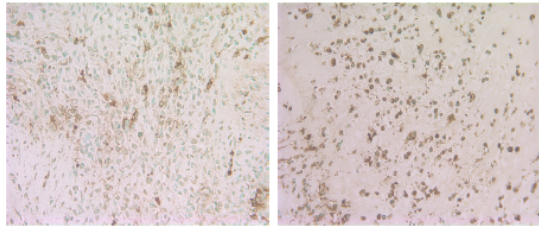
V 2hrs beta2AR

211 2hrs beta2AR



V 18hrs Ki-67

211 18hrs Ki-67

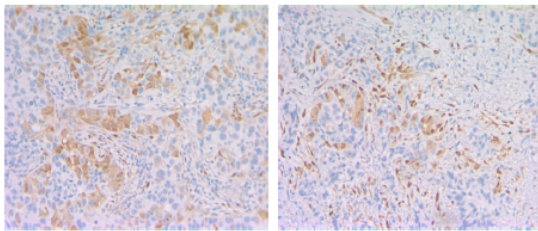


V 18hrs TUNEL

211 18hrs TUNEL

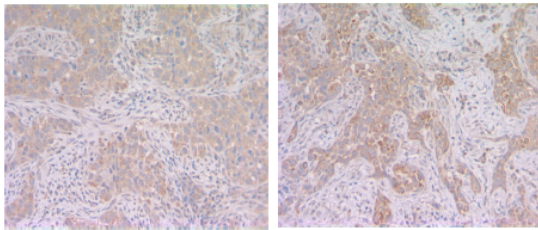
Figure 29 (continued). Ex-Vivo treatment of fresh human tumor tissue demonstrates variable efficacy of ARA-211 to inhibit P-Erk1/2, inhibit proliferation and induce apoptosis

Lung Tumor III :



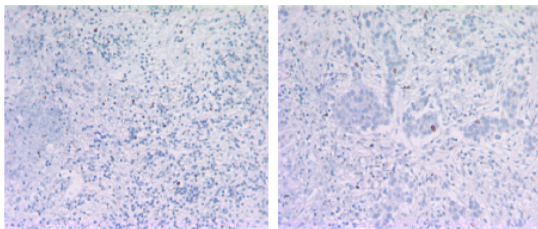
V 2hrs P-Erk

211 2hrs P-Erk



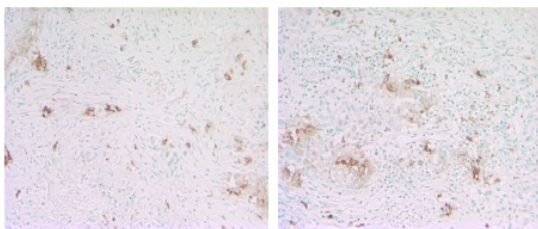
V 2hrs β2AR

211 2hrs β2AR



V 18hrs Ki-67

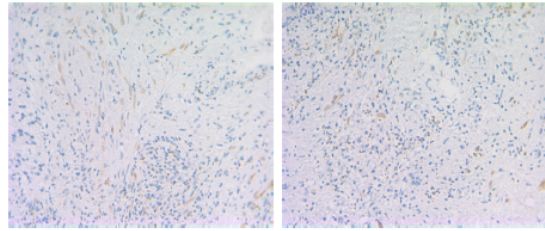
211 18hrs Ki-67



V 18hrs TUNEL

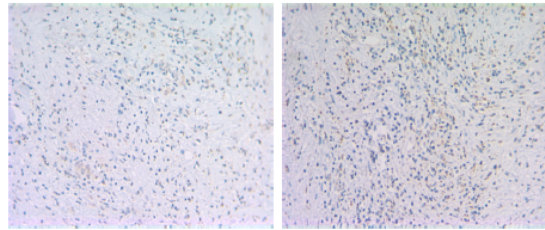
211 18hrs TUNEL

Kidney Tumor I :



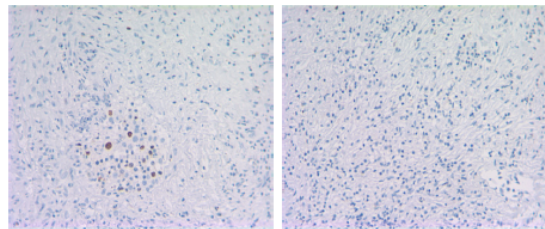
V 2hrs P-Erk

211 2hrs P-Erk



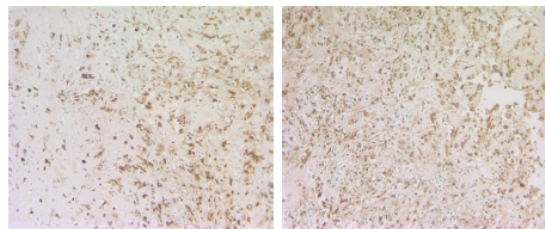
V 2hrs β2AR

211 2hrs β2AR



V 18hrs Ki-67

211 18hrs Ki-67



V 18hrs TUNEL

211 18hrs TUNEL

Figure 29 (continued). Ex-Vivo treatment of fresh human tumor tissue demonstrates variable efficacy of ARA-211 to inhibit P-Erk1/2, inhibit proliferation and induce apoptosis

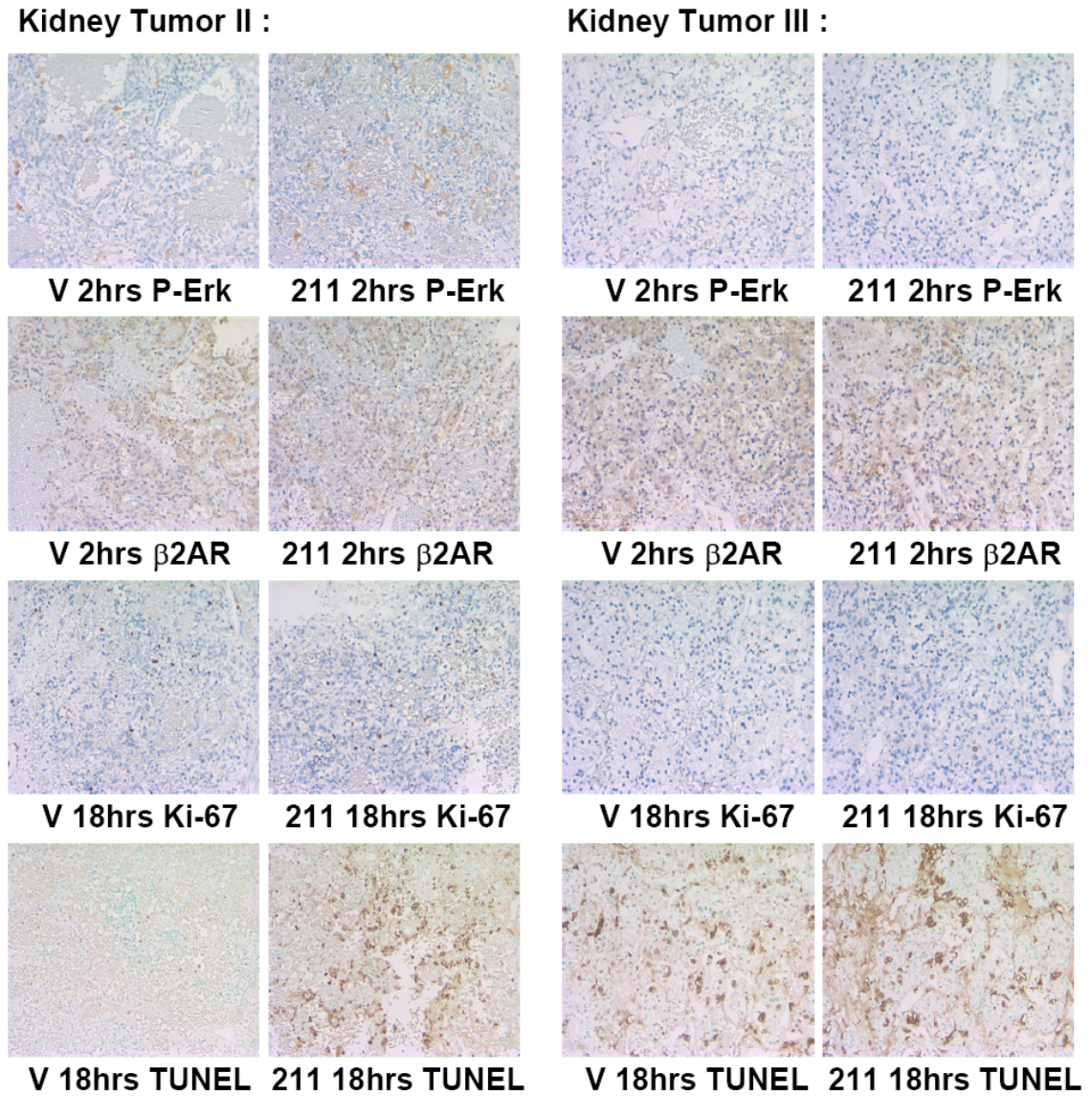
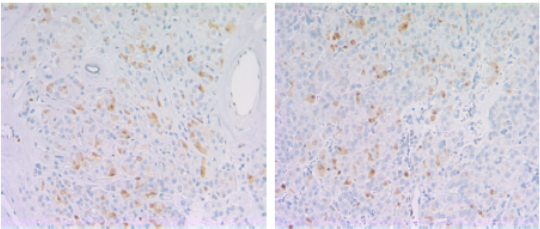


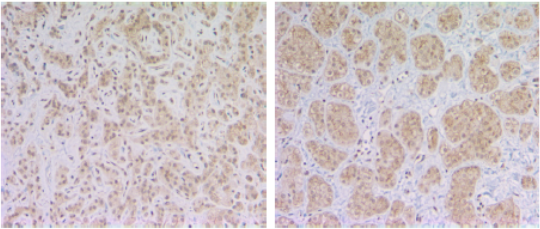
Figure 29 (continued). Ex-Vivo treatment of fresh human tumor tissue demonstrates variable efficacy of ARA-211 to inhibit P-Erk1/2, inhibit proliferation and induce apoptosis

Kidney Tumor IV :



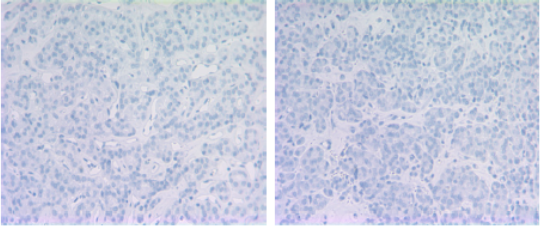
V 2hrs P-Erk

211 2hrs P-Erk



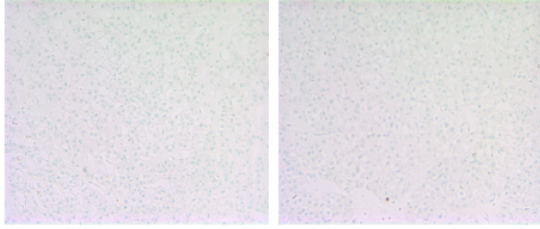
V 2hrs β 2AR

211 2hrs β 2AR



V 18hrs Ki-67

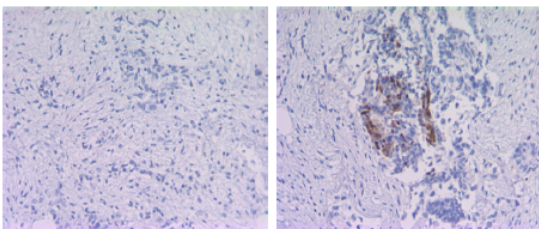
211 18hrs Ki-67



V 18hrs TUNEL

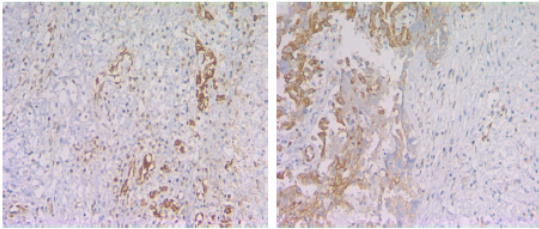
211 18hrs TUNEL

Omentum Tumor :



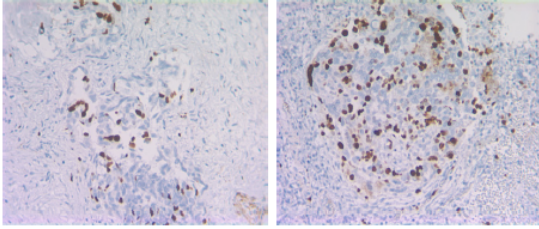
V 2hrs P-Erk

211 2hrs P-Erk



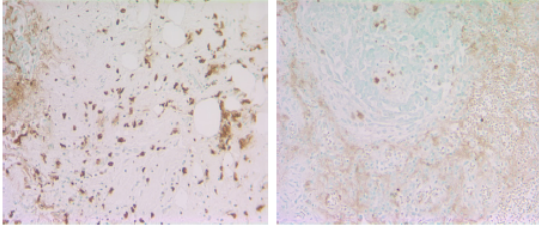
V 2hrs β 2AR

211 2hrs β 2AR



V 18hrs Ki-67

211 18hrs Ki-67



V 18hrs TUNEL

211 18hrs TUNEL

Proposed method of selecting patients for evaluating the efficacy of ARA-211 clinically

Ultimately, the goal of treating patient samples *ex-vivo* is to determine which, if any, patients would benefit from ARA-211 therapy for cancer. To this end we have proposed a flow chart for the identification of patients who may be candidates for ARA-211 therapy (Figure 25). Patient samples that have been archived in the tissue bank at Moffitt Cancer Center will be screened for expression of P-Erk1/2 and β 2 AR expression. Those that do not express both protein markers will be considered off study, while those that express both markers will have a tumor biopsy done to confirm the current expression levels. These biopsies will also be used for *ex-vivo* treatment to determine the sensitivity of the samples to ARA-211 treatment. Those samples in which treatment decreases the levels of P-Erk1/2, decreases proliferation by Ki-67 staining, or increases apoptosis by TUNEL staining will be considered on study for treatment with ARA-211. Those *ex-vivo* treated samples that exhibit no change or an increase in P-Erk1/2, Ki-67 or a decrease in TUNEL will be off study.

Figure 30. Patient treatment with ARA-211 requires pre-determination of $\beta 2$ AR and P-Erk1/2 expression, as well as ex-vivo treatment to determine efficacy to inhibit proliferation and induce apoptosis

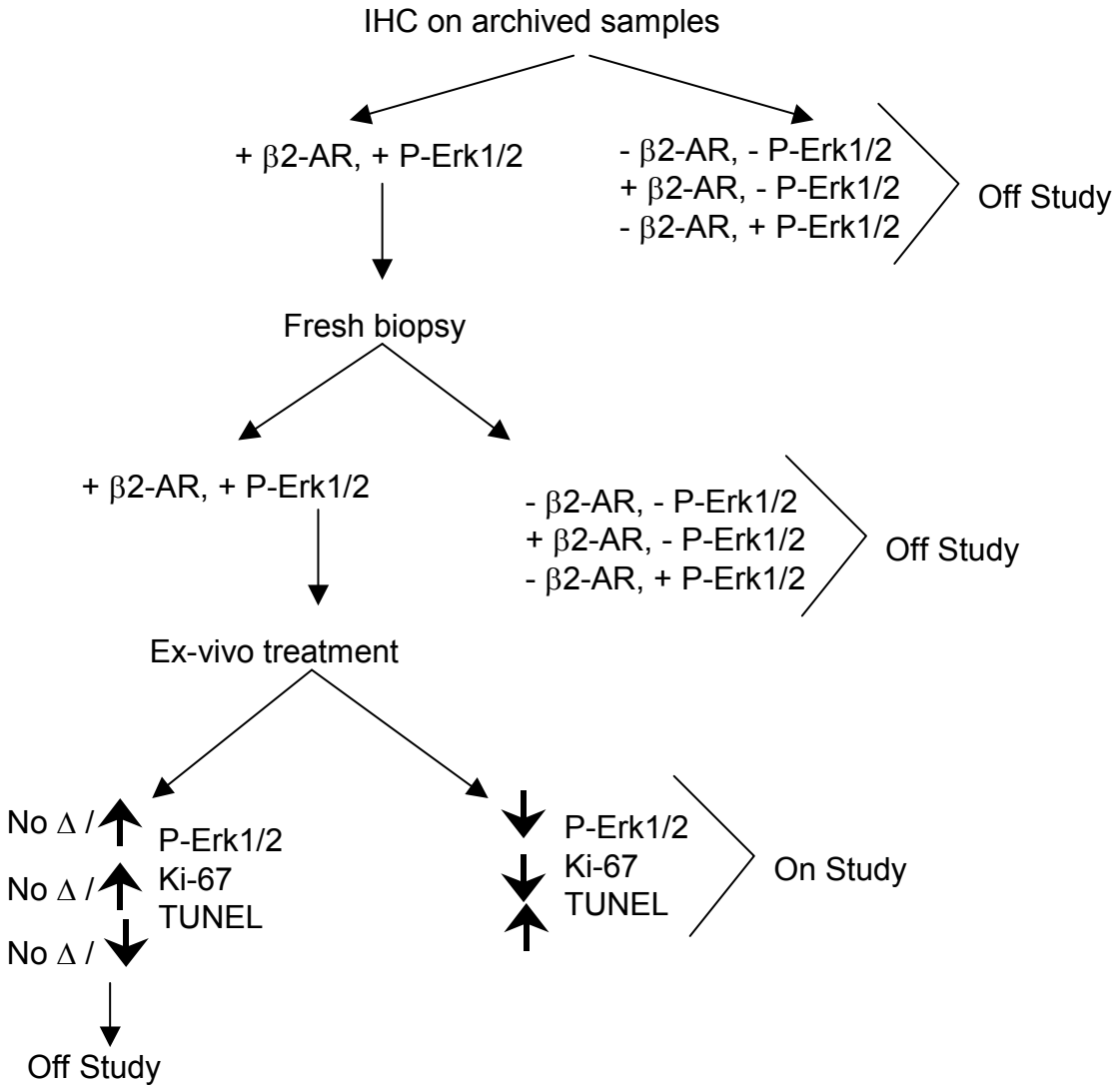


Figure 30. Flow chart schematic for selection of patients whose tumor may be susceptible to ARA-211 therapy.

Discussion

The use of pirbuterol for cancer therapy is a realistic goal given the preclinical data demonstrated in Chapters 1 and 2 of this thesis as well as the extensive clinical data in the literature for the broncho- and vaso-dilatation properties of pirbuterol as a specific β_2 adrenergic receptor agonist. In fact, pirbuterol was approved by the FDA as an anti-asthmatic delivered by nebulizer. Because of this, pirbuterol has been tested extensively in animals and humans, and the toxicity profiles along with the pharmacokinetics and pharmacodynamics are well defined. In order to effectively treat cancer though, we first need to determine which tumors are most likely to respond to pirbuterol by inhibiting proliferation and inducing apoptosis. Previous data from Chapter 1 demonstrated that the antitumor effect of pirbuterol depends on its ability to bind the β_2 AR and to inhibit Erk1/2 phosphorylation. Therefore, we hypothesized that patient samples must express the β_2 AR along with high levels of P-Erk1/2 for the treatment to be effective. Until now there was not much known about expression of the β_2 AR in human tumors, and the link between β_2 AR and P-Erk1/2 signaling was only demonstrated in certain cells in vitro. This led us to first investigate the expression of these protein markers in tissue arrays from human tumors. To our surprise we discovered that the β_2 AR is ubiquitously

expressed in all tumor types, with 100% of ovarian and breast tissues staining positive. Furthermore, 90% and 75% of the pancreas and prostate tumors tested expressed $\beta 2$ AR, based on the tissue array results. It was also surprising that the localization of the $\beta 2$ AR was in the cytoplasm and not in the plasma membrane. One possible explanation for this mislocalization is that the antibody concentration used to stain the tissue was too high. Non-specific staining could account for false positive staining in areas such as the nucleus and cytoplasm. Better characterization of the antibody, and optimization of staining concentrations should be done for future studies using IHC to identify $\beta 2$ AR expression in human tumor biopsies.

In contrast to $\beta 2$ AR, P-Erk1/2 levels were found in only 10-50% of pancreas, bladder, breast, prostate and ovarian cancer samples, and none of the liver cancer samples tested stained positive for P-Erk1/2, based on the tissue array results. With regards to the tissue that expressed both $\beta 2$ AR and P-Erk1/2, we found tissue from ovarian cancer having the highest frequency (50%) followed by prostate (25%), breast (20%), bladder (10%) and pancreas (10%). On average 20% of the tissues from all tumor types stained positive for both $\beta 2$ AR and P-Erk1/2. These data suggest that about 20% of human tumors may be susceptible to pirbuterol therapy. However, as discussed in the introduction to Chapter 2, in some normal cells $\beta 2$ AR stimulation leads to an increase in P-Erk1/2 levels resulting in stimulation of cell proliferation through B-Raf activation. In our human cancer cell line studies in Chapter 1, $\beta 2$ AR stimulation did not

result in stimulation of proliferation in any of the cell lines used; whether this occurs in fresh biopsies is not known. It is therefore critical that the studies of Chapter 1 in human cancer cell lines be extended to fresh human biopsies. It is anticipated that $\beta 2$ AR stimulation will result in inhibition of P-Erk1/2, but clearly any patient whose tumor responds to pirbuterol by increasing P-Erk1/2 would not be a candidate for $\beta 2$ AR agonist treatment. In order to determine how human tumors respond to pirbuterol we treated patient fresh biopsies *ex vivo*, and utilized IHC, Ki-67 and TUNEL staining to determine the ability of pirbuterol to inhibit P-Erk1/2, and cell proliferation and to induce apoptosis. From the studies we have carried out we conclude that treating fresh biopsies in tissue culture poses challenges that were not overcome. Primarily, the biggest obstacle was the inability to preserve the viability of the tumor tissues and stop the necrosis that led to lack of consistency among the responses to treatment. For example, the expression of P-Erk1/2 did not change much following ARA-211 treatment in most samples, whereas in some the expression increased and in others it decreased. Aside from the technical setbacks, analysis of the limited numbers of samples where the staining was clean did not reveal a correlation between inhibition of P-Erk1/2 and inhibition of proliferation or induction of apoptosis. Furthermore, tumor cell proliferation rates increased in a few samples that did not even appear to express the $\beta 2$ AR. Another issue that was not totally overcome by the third cohort of samples was the necrosis in some biopsies that occurred after as little as 18 hours of incubation. Even more surprising was the data that showed that there was more necrosis induced in the treated samples than the

vehicle samples *ex-vivo*. ARA-211-induced necrosis was not seen in tissue culture, as the primary cause of cell death was determined to be apoptosis by TUNEL staining (Chapter 1). TUNEL results for apoptosis may have been masked in the *ex-vivo* studies due to high background staining, most likely due to the necrosis seen in the samples.

Further research needs to be done in the area of *ex-vivo* treatment of patient samples to determine the efficacy of pirbuterol treatment in order to push β 2 AR therapy into the clinic. One way to deal with the issue of necrosis is to implant small pieces of the patient fresh tumor biopsies into the flanks of athymic nude mice, and then treat the mice with ARA-211. Effects of the drug *in vivo* can be determined by measuring the tumor growth in the presence and absence of treatment. Furthermore, the tissue can be harvested from the mice after treatment and stained for P-Erk1/2, β 2 AR, Ki-67 and TUNEL. Although, generally human tumor fresh biopsy explants in mice have a very low take rate, and it may take as many as 10 passages to get enough tumors for antitumor efficacy studies, recent studies however, demonstrated that these explants retain the majority of their initial characteristics as judged by gene expression profiling(154).

Chapter 3

RhoB, but not RhoA Overexpression Delays ErbB2-Mediated Mammary Tumor Onset and Reduces Tumor Multiplicity in Transgenic Mice

All of the work in this Chapter was performed by Adam Carie except for the transgene construct generation, which was performed by Cassandra Martin and Kun Jiang

Abstract

Ras-homologous (Rho) proteins are GTPases that play essential roles in regulating cellular functions such as cell cycle progression, actin cytoskeletal rearrangement, cell motility, and have a strong link to oncogenic transformation and metastasis. The RhoA-like family of Rho GTPases are very interesting in that two of the family members, RhoA and RhoC, are implicated in cell proliferation, invasion and metastasis, whereas the third member RhoB has been implicated in tumor suppression and induction of tumor apoptosis. Furthermore, RhoB expression was found to significantly decrease as tumors progress in head and neck cancer as well as tumors from lung cancer patients. Although in cultured cells, ectopic expression of RhoB antagonizes malignant transformation driven by oncogenes such as receptor tyrosine kinases, Ras and Akt, evidence for this in-vivo is lacking. Therefore, we have developed transgenic mouse models in which wild type RhoB or RhoA is over expressed in the mammary fat pads under the control of the mouse mammary tumor virus (MMTV) promoter. The transgenic mice were then crossed with wild type MMTV-ErbB2 over expressing mice to determine the effects of RhoB and RhoA on ErbB2-mediated mammary oncogenesis. In this chapter of the thesis, we show that overexpression of RhoB, but not RhoA, is sufficient to delay the tumor onset of

ErbB2 mediated tumorigenesis. Furthermore, we demonstrate that RhoB, but not RhoA overexpression results in a decrease in tumor multiplicity compared to the ErbB2 or ErbB2/RhoA animals. This work provides validation of the tumor suppressive effects of RhoB in a transgenic mouse model, which is lacking in the literature to date. Furthermore, this provides us with the means to dissect out the signaling pathways that are affected by tumor suppressive effects of RhoB. Also, the generation of the RhoA and RhoB transgenic mice will allow for the determination of physiological events that RhoA and RhoB may play in the normal proliferation, differentiation and/or apoptotic events that mammary ductal epithelial cells undergo during the pregnancy cycle.

Introduction

Ras-related low molecular weight GTPases of the Rho subfamily act as molecular switches to transduce signals to mediate adhesion, morphology, motility, and cell cycle progression(155, 156). On/off cycling of these switches are dependent on guanosine nucleotide exchange factors (GEFs) and GTPase activating proteins (GAPs) which control the rate of GTP loading and hydrolysis(157). GEFs can be activated by growth factors and cytokines through stimulation of receptors upstream, leading to exchange of GDP-bound for GTP-bound Rho proteins(156, 158). Under normal physiological conditions Rho GTPases are under tight regulation by both guanosine dissociation inhibitors (GDIs) and reliance on post-translational modification. Rho-GDI inhibits spontaneous nucleotide exchange and intrinsic GTPase activity, as well as masking of the lipid modification required for localization(159-162). Sub-cellular localization of activated Rho family members is crucial for the downstream activation of cellular effectors(163). Membrane localization is achieved through post-translational modification of the C-terminal cysteine with a lipid prenyl group(163, 164). Further regulation of some Rho family members (such as RhoB) is achieved through additional modification of C-terminal cysteine motifs by palmitoylation. This also affects sub-cellular localization by preventing

association with Rho-GDI resulting in a more robust activation(165). Many of the Rho family members have high sequence homology, so localization plays an important role in each member's physiological function. RhoB is unique among the RhoA-like family members in that it can be modified by both farnesyl (F) and geranylgeranyl (GG) lipid groups(163). Prenylation of endogenous RhoB was found to be approximately equal, with half of the protein farnesylated and localized to the plasma membrane, while geranylgeranylated RhoB was found in endosomal compartments(166). Further studies demonstrated that when farnesylated RhoB was inhibited by FTI treatment, the population of geranylgeranylated RhoB increased and localized to late endosomal compartments(167). However, the changes in prenylation induced by FTI treatment did not result in differences in the antitumor properties of RhoB. Both RhoB-F and RhoB-GG inhibit anchorage-dependent and -independent growth, induce apoptosis, inhibit constitutive activation of Erk and insulin-like growth factor-1 stimulation of Akt, and suppress tumor growth in nude mice(168).

The Rho family of proteins can be divided into six distinct sub-families based on amino acid sequence and biological function. These proteins modulate many similar biological effects, including growth and cell cycle promotion, regulation of gene expression, and induction of actin cytoskeleton reorganization(169, 170). Many of these family members, such as RhoA, Rac1 and cdc42, have been implicated in malignant transformation, invasion and metastasis, and drug resistance(87, 171, 172). One intriguing family of Rho-GTPases is the RhoA-related proteins, which is comprised of RhoA, RhoB, and

RhoC. Although the three members of this family share an amino acid sequence homology of 85%, share GEFs and effectors, and stimulate actin-myosin contractility, there are glaring functional differences that may be dictated by distinct sub-cellular localization(155, 163, 173, 174). Despite the amino acid similarity, RhoB contrasts with RhoA and RhoC in regulation and in physiological effects. RhoB is tightly regulated at the transcriptional, translational and post-translational levels. The half-life (30-120 minutes) of RhoB mRNA and protein is much shorter than that of other Rho proteins (18-24 hours). RhoB expression is induced by growth factors, UV-irradiation and many chemical agents. RhoB is also up-regulated during G1 and S phases of the cell cycle(175). RhoB, but not RhoA or RhoC, has been shown to exist within cells in both farnesylated (F) as well as geranylgeranylated (GG) forms, and is also modified by the fatty-acid palmitoyl group(163). Similarly, RhoB has been shown to be crucial for stress-induced apoptosis and anti-neoplastic activity (22, 176). As opposed to RhoA, RhoB has been suggested to have tumor suppressive activity. This is based on data demonstrating that over-expression leads to inhibition of cancer cell proliferation, induction of apoptosis, and inhibition of tumor growth in a nude mouse xenograft model(168, 177, 178). Furthermore, RhoB has been shown to negatively regulate NF κ B gene transcription, leading to apoptosis in response to genotoxic stress(179). Support for the anitneoplastic role of RhoB has been sustained clinically by studies demonstrating suppression of RhoB expression in invasive carcinoma from head and neck tumors, and loss of RhoB expression during human lung cancer progression(22, 23).

As opposed to RhoB, RhoA and RhoC expression correlates with tumor progression, invasiveness and metastasis(180-183). RhoA has been implicated in activation of STAT3 and STAT5 leading to cell migration, proliferation, and epithelial-to-mesenchymal transition (EMT)(184, 185). Similarly, siRNA to RhoA and RhoC inhibits the proliferation and invasiveness of human gastric carcinoma by modulating the PI3K/Akt pathway(186). Microarray analysis of transformation by RhoA(Q63L) in NIH3T3 cells demonstrates up-regulation of AP1, E2F and c-Myc through Rock and other effectors(14). Likewise, microarray studies in MCF10A cells demonstrate that over-expression of RhoC results in up-regulation of genes involved in cell proliferation, invasion/adhesion, and angiogenesis(183). Similarly, over-expression of RhoA results in up-regulation of proliferative genes such as cyclin D1, cyclin-dependent kinase 8, cyclin A2 and HMGI-C(183, 187). It is clear from the studies described in the literature from our lab and others that though RhoA and RhoB are highly homologous, they play opposing roles in oncogenesis, with RhoA having tumor promoting whereas RhoB having tumor suppressive activities. However, these conclusions are based on correlative studies in cell culture, nude mice, and human paraffin-embedded biopsies. To gain direct evidence in support of the tumor suppressive and tumor promoting activities of RhoB and RhoA, respectively, we created RhoB and RhoA transgenic mice under the transcriptional control of the mammary-specific promoter, MMTV. We then crossed these mice with transgenic mice that aberrantly express the receptor tyrosine kinase ErbB2, also under the control of the MMTV promoter. These mice were generated to determine the effects of

RhoA and RhoB on ErbB2-mediated breast oncogenesis; specifically tumor onset, growth rate and multiplicity. Furthermore, little is known about the role of RhoA or RhoB on normal mammary gland morphogenesis. Therefore, we will also use the RhoA and RhoB transgenic mice we have generated to investigate the role of these GTPases on the morphological changes that the mammary fat pads undergo during pregnancy. The major stages of mammary gland development occur at puberty, from 3 weeks to 3 months of age, and during pregnancy, where epithelial cells proliferate, differentiate, and eventually undergo involution by apoptosis. Initial development occurs during and just after puberty, where the ductal structures lengthen and branch out filling the mammary fat pads. The rapid onset of ductal epithelial cell proliferation leads to glands that are prepared to sustain differentiation and produce milk for the pregnancy stages to come(188). In the early stage of pregnancy the ductal branches undergo another round of substantial cell proliferation and the alveolar buds begin to form for milk production(189). Differentiation begins in the second half of pregnancy, characterized by the lobuloalveolar phase of growth leading to the cleavage of alveolar buds that will become milk-secreting lobules at lactation(190). This stage nears completion by D18 pregnancy, where the alveolar epithelial cells produce milk proteins and lipids. The final stages of gland morphological changes occur at involution; after weaning the glands undergo massive apoptosis and remodeling(191). The majority of epithelial cells will undergo apoptosis between day 2 and 3 of involution, leading to collapsing of alveolar structures and significant remodeling of the glands beginning around day 6 of

involution, and lasting until as long as day 21(192, 193). By utilizing these known morphological changes we can identify the stages at which RhoA or RhoB have physiological effects on proliferation, differentiation or apoptosis.

In summary, based on the body of literature supporting contrasting roles for RhoA and RhoB, we set out to validate in this chapter our hypothesis that RhoB has tumor suppressive activity using transgenic mouse models comparing the effects of RhoA and RhoB expression on breast tissue proliferation, differentiation and apoptosis, as well as breast tissue neoplasia. To this end we have created transgenic mice that express RhoA or RhoB under the mouse mammary tumor virus (MMTV) promoter to determine the physiological and morphological effects of these Rho proteins on normal breast tissue. Furthermore, we have created bitransgenic mice that express the ErbB2 proto-oncogene in the mammary fat pads in combination with RhoA or RhoB to determine the effects of each Rho protein on the ErbB2-mediated spontaneous tumor onset, growth rate and multiplicity.

Materials and Methods

cDNAs and Gene Subcloning

To generate the constructs for human RhoB and RhoA containing plasmids under the MMTV promoter, approximately 2 μ g MMTV-containing human TGF-alpha gene (Figure 31) along with pcDNA3-HA-RhoB and pcDNA3-HA-RhoA plasmids were all digested using EcoRI restriction endonuclease in its appropriate NEB buffer. The Mouse Mammary Tumor Virus (pMMTV- β globin) vector containing the human TGF-alpha gene was supplied by Dr. Richard Jove's lab at Moffitt Cancer Center. The gene for human RhoB was a gift from Dr. Gilles Favre. The human RhoA gene was a gift from Dr. Channing Der at the Lineberger Comprehensive Cancer Center, University of North Carolina at Chapel Hill. This restriction endonuclease digestion resulted in the removal of the TGF-alpha gene sequence and linearization of all 3 plasmids. Following digestion, the MMTV vector was treated with calf intestinal alkaline phosphatase (CIP) in order to increase ligation efficiency. The RhoB insert, RhoA insert and MMTV vector were then isolated via agarose gel (1.5%) electrophoresis (Figure 32). The desired bands were then removed from the gel and purified with Bio101 GeneClean gel extraction kit following the protocol provided in the kit. EcoRI,

XhoI, BglI, SgrAI, XbaI, PvuI and KpnI restriction endonucleases as well as calf intestinal alkaline phosphatase (CIP) and T4 DNA ligase were all purchased from New England Biolabs (Beverly, MA). The NotI, BglII and EcoRV restriction endonucleases were purchased from Promega (Madison, WI). The GeneClean gel extraction kit was purchased from Bio 101 (Carlsbad, CA).

Figure 31. MMTV-TGF α construct linearized by EcoRI digestion for insertion of human RhoA and RhoB genes

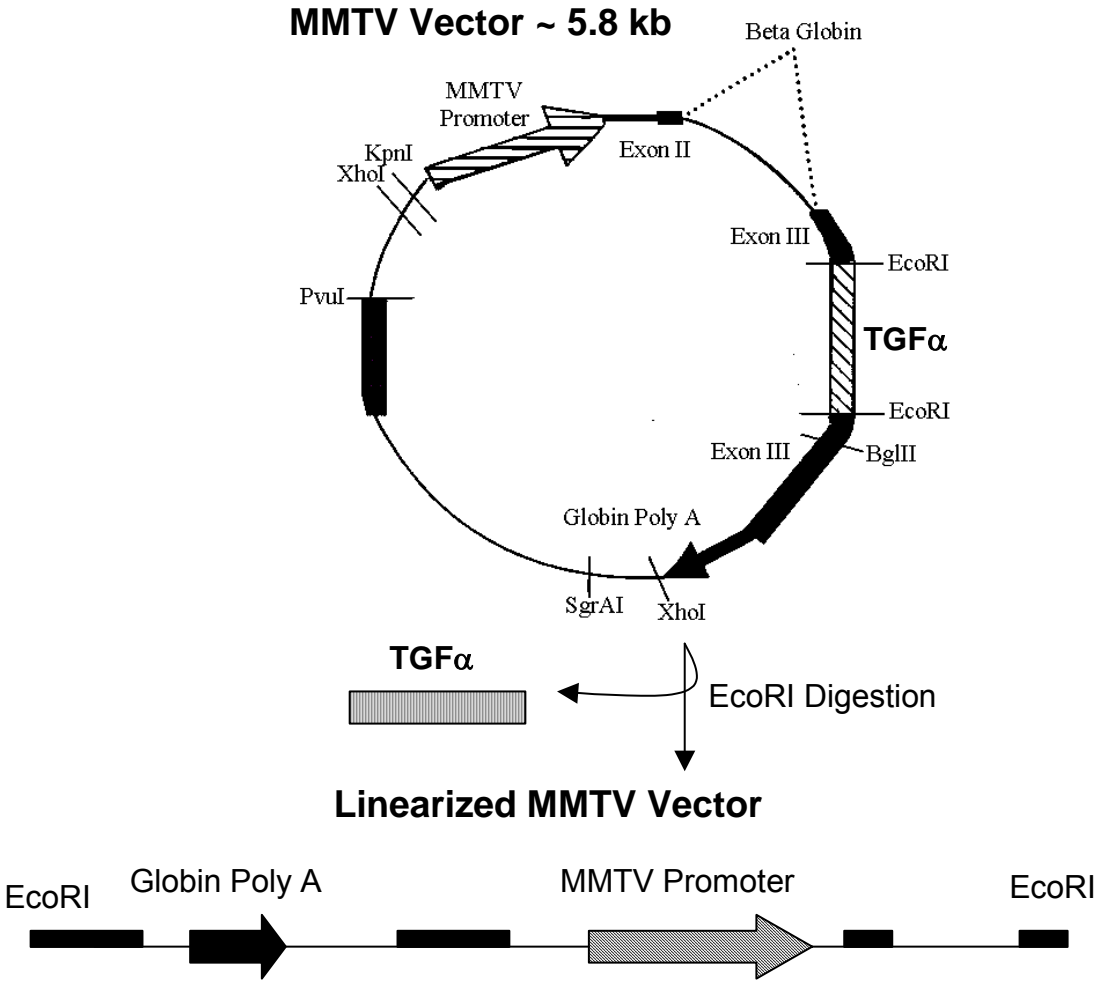


Figure 31. Mouse Mammary Tumor Virus vector map. The MMTV vector map shown here indicates the significant restriction endonuclease sites in the subcloning of human RhoA and RhoB into this vector as well as the linearized vector following EcoRI digestion.

The Rho inserts were then ligated to the linearized MMTV vector. To this end, a small volume (<1 μ l) of MMTV vector along with 16 times more RhoA insert, RhoB insert or no insert was combined with T4 DNA ligase in ligation specific buffer. These reactions were incubated at 16°C for a period of 16 hours. The products were once again purified with the gel extraction kit, as noted earlier, in order to remove any salt from the ligation buffer that could potentially interfere with the next step. DH10B bacteria cells were then transformed with 1 μ l MMTV-RhoA, MMTV-RhoB or MMTV control purified ligation product in electroporation cuvettes. The cuvettes were each placed in the electroporation machine that force current through the sample in order to induce transformation. This apparatus was set at 2.5 kV/resistance, 2.45 kV and 129 for resistance. The bacteria were then transferred into 500 μ l SOC media and placed in the 37° shaker until sufficient bacterial growth was apparent (approximately 1 hour). 100 μ l from each sample was plated onto LB agarose ampicillin plates, and incubated at 37°C overnight. DH10B competent cells and the pcDNA3 vector were purchased from Invitrogen (Carlsbad, CA) along with SOC media and LB broth base. Bacto-agar was obtained from Difco Laboratories (West Molesey Surrey, UK). Electroporation cuvettes plus were ordered from Fisher (Pittsburgh, PA). Maxi prep and mini prep kits were obtained from Qiagen (Valencia, CA). The following oligonucleotide primer sequences were designed based on the RhoB and RhoA cDNA and MMTV promoter sequences.

The following day the MMTV control plate had 12 clones, while RhoA had 25 clones and RhoB had 50. 10 clones each were picked from the RhoA and the

RhoB plates. These 20 clones were grown in LB overnight and the DNA was prepared using a mini prep kit, following the protocol provided in the kit. The purified DNA was then digested with EcoRI, as noted earlier, in order to identify clones containing the RhoB or RhoA insert. RhoB clones positive for an insert were then digested with NotI and BglII restriction enzymes, while the RhoA plasmids were digested with EcoRV and BglII to identify the clones that contained the RhoB or RhoA insert in the correct orientation. Correctly orientated MMTV-RhoB clones result in 6 kb and 463 base pair bands, while clones containing an incorrectly orientated RhoB insert results in 6 kb and 288 base pair bands when digested in this manner. Correctly orientated MMTV-RhoA clones would result in 6 kb and 527 base pair bands, while clones containing an incorrectly orientated RhoA insert would result in 6 kb and 215 base pair bands when digested in this manner. Three RhoA clones, clones 1, 2 and 8, and two RhoB clones, clones 2 and 3, were found to have correctly orientated inserts (Figure 31).

Figure 32. Isolation of MMTV, RhoB and RhoA DNA and confirmation of insertion in the correct orientation of RhoB and RhoA sequences in the MMTV vector

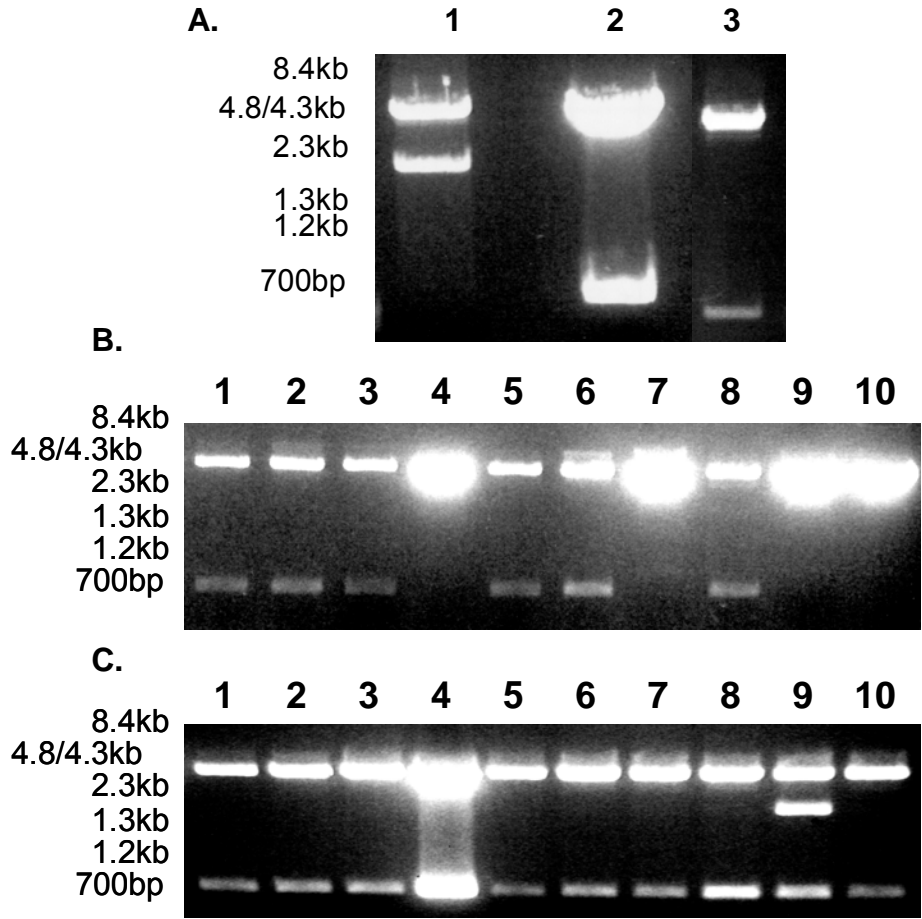


Figure 32. Isolation of MMTV vector, RhoA and RhoB inserts. MMTV vector, HA-RhoB insert, HA-RhoA insert isolation through 1.5% agarose gel electrophoresis following EcoRI digestion. 28 A. illustrates the isolation of the 5.4 kb MMTV vector (Lane 1) from the 2.3 kb insert. This figure also shows the isolation of the 622 bp HA-RhoB insert (Lane 2) from its original pcDNA3 vector. Figure 28 A. shows the isolation of the 611 bp HA-RhoA insert (Lane 3) from its original pcDNA3 vector. All three isolations were executed using EcoRI restriction enzyme. Figure 28 B. demonstrates ligation of MMTV vector and RhoA or RhoB insert mini prep. Figure 28 B. shows 10 clones from the MMTV-RhoA ligation plate from which plasmids have been isolated and digested with EcoRI in order to locate clones that had incorporated the RhoA insert. Clones 1,2,3,5,6 and 8 in this figure contain the RhoA insert. Figure 28 C. shows 10 clones picked from the MMTV-RhoB ligation plate from which plasmids have been isolated and digested with EcoRI in order to locate clones that had incorporated the RhoB insert. Clones 1,2,3,4,5,6,7,8 and 10 in this figure contain the RhoB insert. All digests were run on 1.5% agarose gel.

One RhoA and one RhoB clone were grown separately in large (500 ml) culture, producing the desired DNA plasmid. Qiagen Maxi Prep kits were used to isolate the MMTV-Ha-RhoA and MMTV-Ha-RhoB plasmid DNA by following the protocol provided with the kit. The MMTV-Ha-RhoA and MMTV-Ha-RhoB vectors were then sequenced at the Molecular Biology Core Facility at Moffitt Cancer Center using the following primers (GIBCO BRL Life Technologies, Carlsbad, CA):

#1 RhoB 5': ATG GCG GCC ATC CGC AAG AAG C

Used to sequence RhoB from beginning of insert downstream.

#2 RhoA 5': GCT GCC ATC CGG AAG AAA CT

Used to sequence RhoA from beginning of insert downstream.

#3 RhoB 3': CGC AGG CGG TCG TAG TCC TCC

Used to sequence RhoB from middle of insert upstream to Beta Globin portion of vector.

#4 RhoA 3': GCC TCA GGC GAT CAT AAT CTT CCT G

Used to sequence RhoA from middle of the insert upstream to Beta Globin portion of vector.

#5 MMTV 5': GGC GTA TCA CGA GGC CCT TTC G

Used with RhoA and RhoB to sequence MMTV promoter from beginning of the promoter downstream.

#6 MMTV 3': GGG TCC CCA AAC TCA CCC TGA AG

Used with RhoA and RhoB to sequence MMTV promoter from end of the promoter upstream.

These sequencing results verified that the RhoA and the RhoB genes were successfully inserted downstream of the MMTV promoter, without mutation.

MMTV-RhoB and MMTV-RhoA transgenes were then isolated from the remaining portions of the MMTV vectors via restriction enzyme digestion and agarose gel electrophoresis for the transgene constructs to be inserted into the genome of mouse models through oocyte injections. This step was originally intended to be accomplished using KpnI and SgrAI restriction endonucleases for the MMTV-RhoB transgene, while the MMTV-RhoA transgene could be isolated using XhoI. The result of this XhoI digest, however, was to cut the MMTV-RhoA plasmid exactly in half, resulting in two 3.3 kb bands that overlapped in agarose gels. This problem was solved by adding PvuI restriction endonuclease, which cuts the undesired portion of the vector into 2.6 kb and 700 base pair bands (Figure 33). After reaching this step in the transgene generation process, it was found that the SgrAI enzyme that had been chosen to digest and isolate the MMTV-Ha-RhoB transgene was not functioning correctly (Figure 33).

Figure 33. RhoA, but not RhoB DNA insertion is confirmed in MMTV vector after restriction enzyme digestion

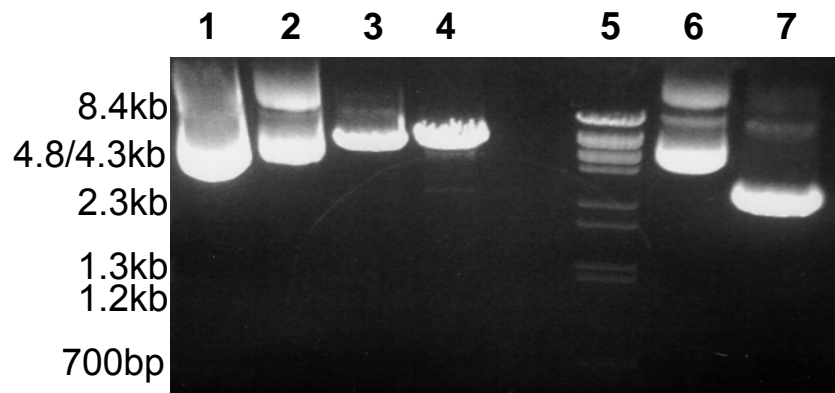


Figure 33. MMTV-RhoB and MMTV-RhoA transgene isolation. Restriction enzyme digestion to isolate the MMTV-RhoB transgene with KpnI and SgrAI enzymes was done to confirm insertion into the MMTV vector. Lane 1 shows MMTV-RhoB plasmid uncut. Lanes 2 and 3 show MMTV-RhoB plasmid digested with only SgrAI and KpnI respectively. Lane 4 shows the result of combining these two enzymes. Lane 5 shows the Lambda DNA digest ladder used as a standard. Likewise RhoA insertion was verified by restriction enzyme digestion. Lane 6 shows MMTV-RhoA plasmid uncut and lane 7 shows the MMTV-RhoA plasmid digested with XhoI alone.

Because there was no restriction enzyme that would cut the vector within 200 base pairs downstream of the poly-A sequence, it was necessary to again subclone the MMTV-Ha-RhoB transgene into a new vector in order to acquire a unique restriction enzyme site immediately downstream of the transgene. This was accomplished by digesting the MMTV-RhoB transgene with KpnI and XhoI in NEB buffer #2, which yielded two bands of interest, one 2.7 kb band and one 600 base pair band and a third undesired 3.2 kb band (Figure 34 B.). The new vector, pcDNA3 (Figure 34 A.) (approximately 5.4 kb), was digested and also linearized with these enzymes in NEB buffer #2 and the resulting sticky ends were dephosphorylated by incubation with CIP. These three bands were then isolated via agarose gel (1.5%) electrophoresis and purified as described above. The pcDNA3 vector was chosen for this model because it contains a KpnI restriction site upstream of the XhoI site with a unique XbaI site immediately downstream of the cloning site. The pcDNA3 vector and the 2.7 kb band, both containing KpnI and XhoI digested ends were then ligated using T4 ligase and the protocol mentioned earlier, along with a control lacking the 2.7 kb band.

Figure 34. pcDNA3 vector is linearized by KpnI and XhoI digestion and MMTV-RhoB is inserted into the plasmid

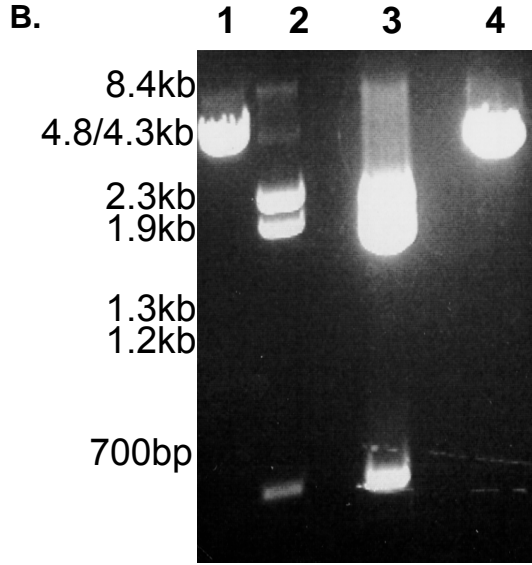
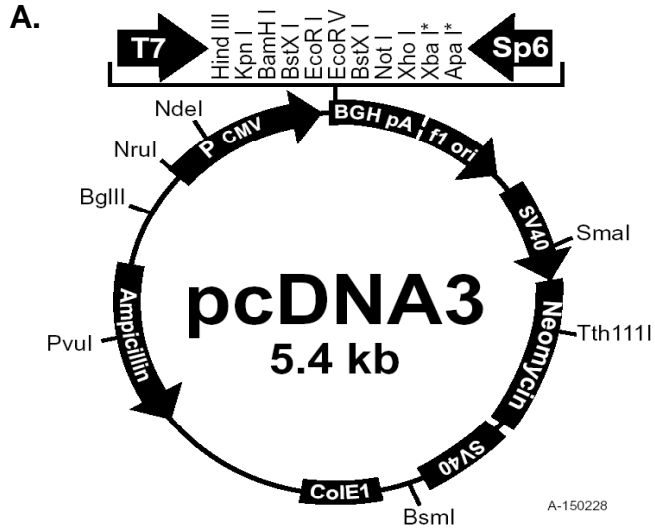


Figure 34. A. The pcDNA3 vector map and insertion of MMTV-RhoB. This map shows the restriction sites that were important in the selection of this vector for its use in creating the new MMTV-RhoB construct. B. Isolation of pcDNA3 vector and MMTV-RhoB transgene 2.7 and 600 bp bands by XhoI plus KpnI digestion. Lane 1 shows MMTV-RhoB plasmid digested with KpnI alone (6.5 kb). Lane 2 shows MMTV-RhoB plasmid digested with XhoI alone (3.3 kb, 2.7 kb and 600 bp bands). Lane 3 shows MMTV-RhoB plasmid digested with both KpnI and XhoI (3.3 kb, 2.7 kb and 600 bp bands). Lane 4 shows the pcDNA3 vector linearized through KpnI plus XhoI digestion.

DH10B competent bacteria cells were transformed using the ligation product and plated onto penicillin LB plate, following the protocol mentioned above. The control plate grew no colonies, while the ligation plate contained 12 colonies. Clones were then picked, cultured and mini-prepped using a Qiagen kit. The resulting plasmid DNA was digested with XhoI, incubated with CIP and run on agarose gel (1.0%) in order to locate clones that had the 2.7 kb band integrated (Figure 35). Clones containing this insert would result in an 8.1 kb band, such as the clones in lanes 4,6,10 and 11, while those lacking the insert would have a 5.4 kb band. The DNA from the pcDNA3 clones that had integrated the 2.7 kb insert of MMTV-HA-RhoB transgene were then isolated and used for ligation of the 600 base pairs band. Both the pcDNA3 plus 2.7 kb linearized plasmid and the 600 base pairs insert include two XhoI sticky ends.

Figure 35. MMTV-RhoB insertion into the pcDNA3 vector is verified by the presence of the 2.7 kb MMTV-RhoB ligation band

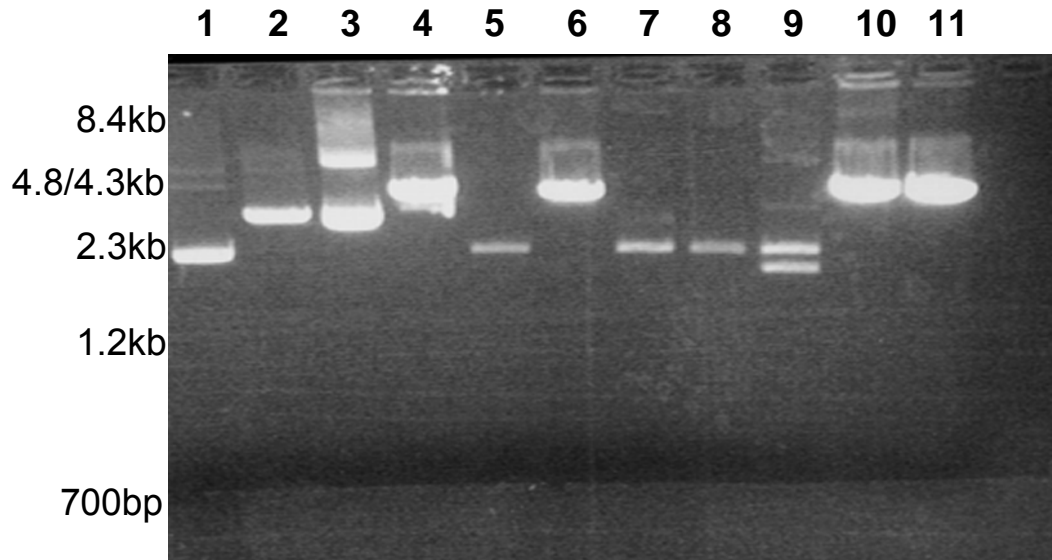


Figure 35. Verification of pcDNA3 plus MMTV-RhoB 2.7 kb band ligation. This gel demonstrates uncut pcDNA3 (Lane1), XhoI digested pcDNA3 (Lane 2) and uncut clone #5 in lane 3. Clones 5 through 12 all digested with XhoI are located respectively in lanes 4-11. This gel was run in 1.5% agarose and clones 5, 7, 11 and 12, which shift up with respect to lane 2, are positive for the 2.7 kb MMTV-RhoB insert.

DH10B cells were then transformed with this ligation product and plated. Following the over night incubation, 10 clones formed on the control plate while 39 grew on the ligation plate with the 600 base pair insert. 12 of the 39 clones that resulted on the ligation plate were picked, cultured and purified by mini-prep. The DNA was then digested with EcoRI restriction enzyme in order to locate clones that had incorporated this 600 base pairs band in the correct orientation. Correctly orientated clones resulted in 8 kb and 600 base pairs bands, while incorrectly orientated clones resulted in 7.5kb and 1.2 kb bands (Figure 36). The two positive plasmids that were found were then sequenced using the MMTV and RhoB primers listed above so that the desired orientation and lack of mutations could be verified. Sequencing results confirmed that the MMTV-Ha-RhoB transgene had been successfully subcloned into the pcDNA3 vector without mutation. The final step in this procedure was to digest 50 μ g pcDNA3-MMTV-Ha-RhoB plasmid with KpnI and XbaI along with digesting 50 μ g MMTV-Ha-RhoA plasmid with XhoI and PvuI, both in 400 μ l reactions to isolate the transgenes (Figure 37).

Figure 36. Verification of the integration of the 600 bp MMTV-RhoB insert

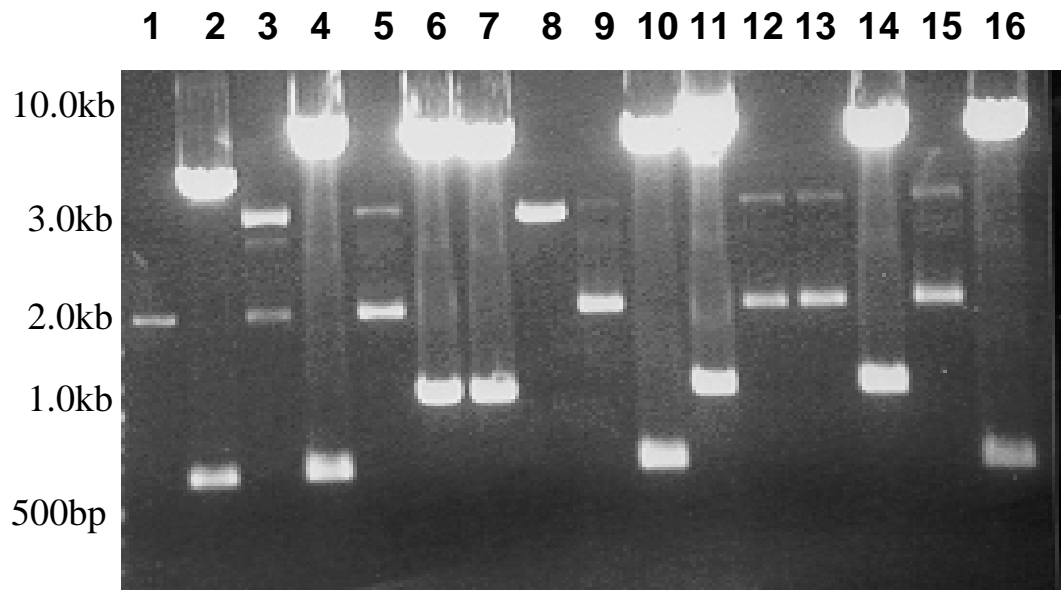


Figure 36. Verification of the integration of the 600 bp MMTV-RhoB insert. After the pcDNA3 plus 2.7 kb band was ligated with the 600 bp band of the MMTV-RhoB transgene, clones were picked and digested with EcoRI in order to verify integration and orientation of the insert. EcoRI digested pcDNA3 (Lane 1) and MMTV-RhoB plasmid (Lane 2) are shown as controls in this 1.5 % gel. The remaining lanes contain EcoRI digested clones 1-14, respectively. Clones resulting in a 600 bp band are oriented correctly , while those resulting in 1.2 kb band are not and those resulting in neither 500 bp band nor 1.2 kb band did not integrate the insert.

Figure 37. Final isolation of MMTV-RhoA and MMTV-RhoB transgenes

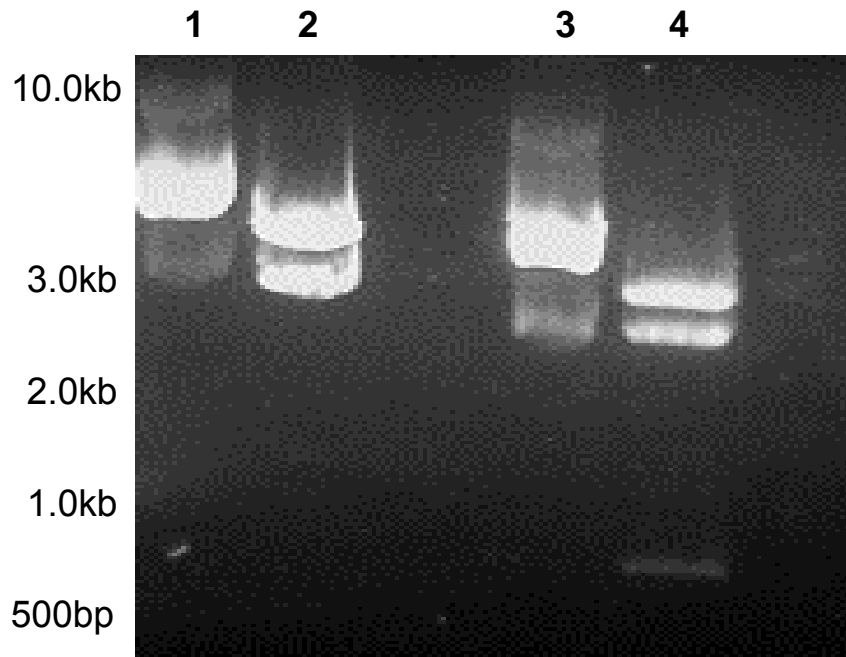


Figure 37. Final isolation of MMTV-RhoA and MMTV-RhoB transgenes. This 1.5% gel displays the final isolation of the two desired transgenes. Both MMTV-RhoA and MMTV-RhoB transgenes are 3.3 kb in length. The pcDNA3-MMTV-RhoB plasmid is shown uncut (Lane 1), then digested with KpnI and XbaI resulting in 5.4 kb and 3.3 kb bands (Lane 2). The MMTV-RhoA plasmid is shown uncut (Lane3), then digested with XhoI and PvuI resulting in 3.3 kb, 2.6 kb and 700 bp bands (Lane 4).

A small aliquot of these samples were then run on agarose gel. The transgene restriction endonuclease reactions were then submitted to the Moffitt Cancer Center Mouse Models Core Facility.

The first step in the transgenic mouse model generation is the isolation of the MMTV-Ha-RhoB and MMTV-Ha-RhoA transgenes via agarose gel electrophoresis. Once this was accomplished, FvB/N strain female mice were bred with FvB/N males. 12 hours following copulation, the female was euthanized, ovaries and fallopian tubes were harvested. Fertilized eggs (i.e. oocytes) were isolated from the reproductive organs. For each of the RhoA and RhoB transgenes about 180 eggs were harvested and microinjected with the DNA constructs. Only one of the two pre-nuclei of each oocyte was microinjected with about .003 μ l transgene DNA solution (9 femtograms DNA). The injected oocytes were then incubated for 24-48 hours at 39°C, the normal body temperature of mice. Once oocytes had divided into two or more cells, 20-30 of these microinjected eggs were implanted into the fallopian tube of each of 6 foster mothers. Of these 180 injected eggs, only about 20% were expected to survive. A projected 20% of these expected 36 survivors (approximately 7-8 mice) should have the transgene incorporated into the genome, assuming that the transgenes are not lethal.

Southern Blot and Genotyping

One RhoA founder and 5 RhoB founders were identified based on genotyping from tail DNA. The insertion of the transgene was confirmed by Southern blot, which confirmed the integration of the MMTV-HA-RhoB or MMTV-HA-RhoA in B1, B2, B5, B6, and B9 founders, as well as A5 founder (Figure 38). Founder mice were tail snipped and ~1 cm of the tail snip was used for each mouse for genomic DNA extraction with the DNA-easy kit (Qiagen) following the provided protocol. Southern blot analysis of founder mice was done by isolating approximately 5 ug tail DNA, and samples were digested overnight with EcoRI restriction enzyme prior to electrophoresis on 0.8 % agarose in TAE gels. Gels were then transferred to Zetaprobe GT (BioRad) membranes. Southern blots were hybridized overnight to ³²P-dCTP-labelled Rho A or Rho B cDNAs. Additionally, F2 generation mice were genotyped by slot blot hybridization of genomic DNA isolated from tail biopsies to ³²P-dCTP-labelled probes specific for non-murine transgene sequences; SV40 poly A signal for MMTV-ErbB2 mice and rabbit beta-globin intron for MMTV-Rho A and -Rho B mice. Slot blot genotyping analysis was performed by the Mouse Models Core facility at Moffitt Cancer Center as described previously(194).

Figure 38. Southern blot of DNA from transgenic founder mice confirms integration of RhoA or RhoB into the host genome

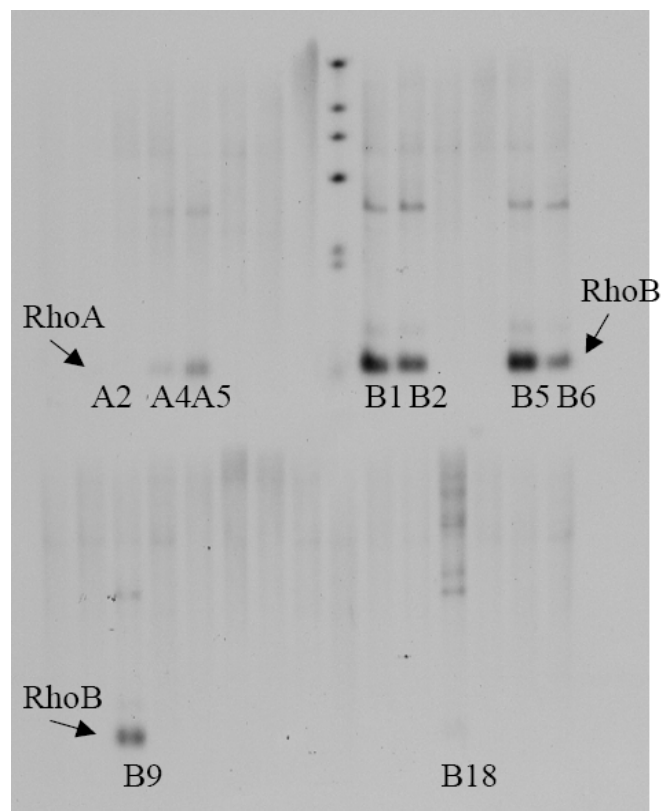


Figure 38. MMTV-HA-RhoA and MMTV-HA-RhoB constructs were given to the mouse models core facility at Moffitt Cancer Center to generate transgenic mice over expressing the HA-RhoA or HA-RhoB in the mammary fat pads. DNA from the tails of the founder mice were analyzed by southern blot to confirm integration into the host DNA.

DNA Preparation and PCR

The mice were tail snipped and ~1 cm of the tail snip was used for each mouse for genomic DNA extraction with the DNA-easy kit purchased from Qiagen following the provided protocol. The purified DNA samples were dissolved in 0.1 x TE and stored in 4 degree until PCR reaction was set up. The standard PCR cycles were utilized to examine the presence of transgenic RhoB or RhoA genes in the DNA samples. In brief, for each PCR reaction, 50 ng (0.5-1 μ l) of DNA was mixed with 1.5 μ l dNTPs mixture, 5.0 μ l of 10x buffer, 2 unit Taq enzyme, and 100 ng of 5' and 3' primer each, the final volume of the reaction was supplemented to 50 μ l with autoclaved DD water. The PCR reactions were started at 94 degree for 3 minutes, then 50 degree for annealing for 1min, then 72 degree for 2 min for elongation. The PCRs were cycled for 35 cycles and the PCR products were run in 1.3% agarose gels and the picture taken.

Protein Preparation and Analysis

Tissue from tumor resection dissection was homogenized in a lysis buffer containing 20 mM Tris-HCl (pH 7.5), 150 mM NaCl, 1% NP-40, 1 mM phenylmethylsulfonyl fluoride, 1.5 μ g each of aprotinin and leupeptin per ml, 10 mM NaF, and 10 mM NaPPi. The crude lysates were placed on ice for 25 min and vortexed every 5 min and finally spun at 13000 rpm for 15 min. The cleared

lysates were stored at -80 degree until Western Blotting analysis. 50 µg of the lysates was loaded into SDS-PAGE gel and analyzed for each sample. Antigen-bound antibody was detected by enhanced chemiluminescence Western blotting kit (Amersham Pharmacia Biotech, Piscataway, New Jersey). Anti-HA antibody (12AC5) was purchased from Roche. Monoclonal antibody to β-actin was obtained from Sigma.

Tumor Onset, Growth Rate, and Multiplicity Calculation

F1 generations of ErbB2, ErbB2/RhoA and ErbB2/RhoB mice were backcrossed to generate F2 litters. The F2 generation mice were used to study the tumor onset of each strain. Mice were physically checked for new tumors by palpitation of the mammary fat pads 3-4 days per week by vivarium technicians as well as laboratory staff. Once mice formed tumors the onset date was noted and tumor measurements were taken every other day to determine the growth rates. Tumors were measured by digital Vernier caliper, and volume was calculated using the formula $V = W^2 \times L$, where width is the largest diameter measurements and length is the smaller diameter measurement perpendicular to the width. Tumors were allowed to grow until the largest diameter reached the pre-determined size of 2 centimeters. At this time the mice were sacrificed and tumor tissue was harvested. Tumor growth rates were determined by subtracting the volume at time of sacrifice from the first measurable volume and dividing by the number of days between the measurements. Multiplicity was determined by

counting the number of distinct tumors at time of sacrifice. Graph Pad software was used for graphical representation and statistical analysis. Tumor onset data was analyzed using a log-ranked (Mantel-Cox) test comparing ErbB2 and ErbB2/RhoA or ErbB2 and ErbB2/RhoB mice. Student's t-test was used to determine statistical significance comparing growth rates and multiplicity for the three groups.

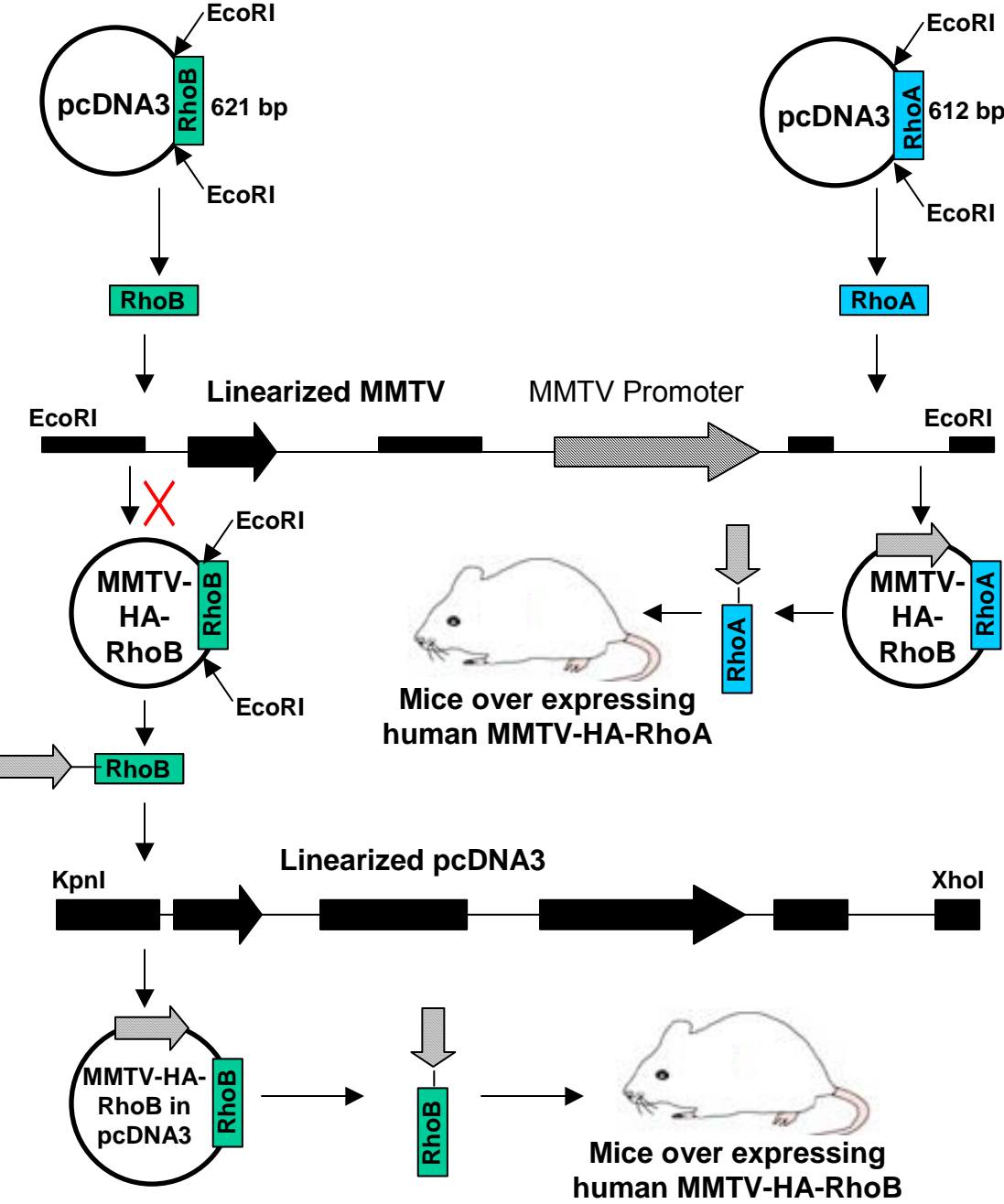
Results

Generation of DNA constructs for the creation of MMTV-HA-RhoB and MMTV-HA-RhoA transgenic mice

DNA sequences for the MMTV promoter, HA epitope tagged human RhoB and HA tagged RhoA were sourced from vectors containing MMTV-TGF α and pcDNA3 vectors containing HA-RhoB and HA-RhoA as described in detail in the Materials and Methods. Figure 39 demonstrates a schematic representation for generation of the constructs, where RhoA and RhoB inserts were removed from pcDNA vectors and subcloned into the linearized MMTV vector in which the TGF α gene was removed. The insertion of RhoA into the MMTV vector was verified by subsequent removal of the HA-RhoA insert and identification by agarose gel electrophoresis, as described in Materials and Methods. However, the insertion of RhoB could not be verified by this method. Ultimately, the HA-RhoB insert along with the MMTV promoter was removed from the MMTV vector and subcloned back into the pcDNA3 vector. The insertion of MMTV-RhoB was then confirmed by excision and identification by agarose gel electrophoresis. The MMTV-HA-RhoA and MMTV-HA-RhoB transgenes were removed from their plasmid vectors and submitted to the Mouse Models Core facility at Moffitt

Cancer Center for injection into FVB/N mouse 0.5 days post coitum zygotes, and implanted into the pseudopregnant CDI foster recipients for development.

Figure 39. Schematic for generation of MMTV-RhoB and MMTV-RhoA constructs for generation of transgenic mice that over express human HA-RhoB and HA-RhoA under the MMTV promoter



Microinjection of MMTV-HA-RhoB and MMTV-HA-RhoA inserts into mouse zygotes

Fertilized eggs (oocytes) were harvested from the reproductive organs of superovulated female FVB/N mice as described in Materials and Methods. The DNA inserts containing MMTV-HA-RhoB and MMTV-HA-RhoA were microinjected into approximately 180 zygotes each. Which were then incubated for 24-48 hours and, once cell division occurred, 20-30 eggs each were subsequently implanted into the oviducts of 6 pseudopregnant CDI mice per transgene (12 mice total). Females implanted with the RhoB-injected embryos gave birth to 20 pups, while the females implanted with the RhoA-injected embryos give birth to 8 pups.

PCR and Southern blot genotyping reveals 6 MMTV-HA-RhoB founders and 2 MMTV-HA-RhoA founders

PCR and Southern blots on DNA from tail snips were used to confirm the integration of the transgene into the host mouse genome. Six MMTV-HA-RhoB founders and 2 MMTV-HA-RhoA founders were confirmed, and the founders were then backcrossed with wild type mice to generate F1 colonies of RhoB and RhoA heterozygous mice. Littermates from the F1 generation were intercrossed to increase the portion of transgenic mice and potentially generate homozygous RhoB and RhoA transgenic F2 colonies. The genotyping of the pups from the F1

and F2 generations was done by PCR as well as slot blot analysis as detailed in Materials and Methods. Furthermore, RhoB and RhoA transgenic mice from the F2 generations were crossed with mice that over express the receptor tyrosine kinase ErbB2 under the MMTV promoter to study the affects of RhoB and RhoA overexpression in the mammary fat pads on ErbB2-mediated breast tumorigenesis.

Overexpression of RhoB, but not RhoA, delays ErbB2-mediated mammary tumor onset

ErbB2, the Human Epidermal Growth Factor Receptor-2, is the protein product of the ErbB2 gene. ErbB2 is found over expressed in 25-30% of breast and ovarian cancers, and confers poor prognosis clinically(195). Transgenic mouse models of breast cancer have been engineered using overexpression of both mutated and wild type ErbB2 genes in mammary epithelial cells driven by the mouse mammary tumor virus (MMTV) promoter(196, 197). The exact signaling events leading to transformation downstream of ErbB2 overexpression are still under investigation, however, signaling through Ras and PI3K are likely mediators(89). The protooncogenic transgenic model of breast tumor formation driven by overexpression of ErbB2 has been well characterized and studied since the early 1990's. With this model, female mice produce spontaneous breast tumors around the age of 250 days, which is far less aggressive than the mutated Neu transgenic model which develops multiple tumors around 80

days(196, 198, 199). In this Chapter of the thesis we describe work where we generated transgenic mice that over express HA-RhoA and HA-RhoB under the control of the mouse mammary tumor virus promoter, and crossed these mice with transgenic mice that over express the protooncogenic ErbB2 gene under MMTV promoter control. These bitransgenic mice were used to determine the tumor effects of the small GTPases *in-vivo* on ErbB2 breast oncogenesis.

Figure 40 shows the percent tumor free animals for the ErbB2 (EE) mono-transgenic, ErbB2/RhoB (EB) and ErbB2/RhoA (EA) bitransgenic mice. Likewise, Table 7 reports tumor onset, growth rates and multiplicity for EE, EA and EB mice with statistical analysis. In accordance with previously reported data from the literature, the EE females averaged 246.5 ± 4.6 days to tumor onset. Overexpression of RhoA along with ErbB2 neither significantly enhanced nor suppressed tumor onset, with EA females developing tumors at approximately 261 ± 9.1 days. Log-rank statistical analysis was used to determine significance of the entire curve of EE compared to EA mice, which gave a non-significant p value of 0.514. Hazard ratio analysis determined that EA mice were only 1.14 times more likely to have a delayed tumor onset event compared to EE mice. However, there was a statistically significant delay in tumor onset when RhoB was over expressed in concert with ErbB2. The average tumor onset for EB females was 306 ± 10.4 days compared to 246.5 ± 4.6 for the EE females. The Log-ranked statistical output gave a significant difference between the two groups with a p value of 0.0003. Hazard ratio analysis showed EB females to be over twice as likely to have a delayed tumor

onset over the EE females. The tumor growth rates for all 3 groups showed no statistically significant difference, with EE mice growing at 89 ± 10.7 cubic millimeters per day, and EA and EB mice growing at 75.1 ± 9.7 ($p = 0.16$) and 74.4 ± 7.7 ($p = 0.13$) cubic millimeters per day, respectively. Finally, tumor multiplicity was calculated to determine if overexpression of RhoA or RhoB affected the number of tumors that developed per mouse. Mice over expressing ErbB2 and ErbB2/RhoA developed 2.1 ± 0.22 and 2.1 ± 0.3 tumors per mouse, respectively, while mice over expressing ErbB2/RhoB developed a significantly lower 1.5 ± 0.15 tumors per mouse ($p = 0.018$). Student's T-test was used to determine significance between growth rates as well as multiplicity.

Figure 40. RhoB, but not RhoA over expression results in a statistically significant delay in ErbB2-mediated tumor onset

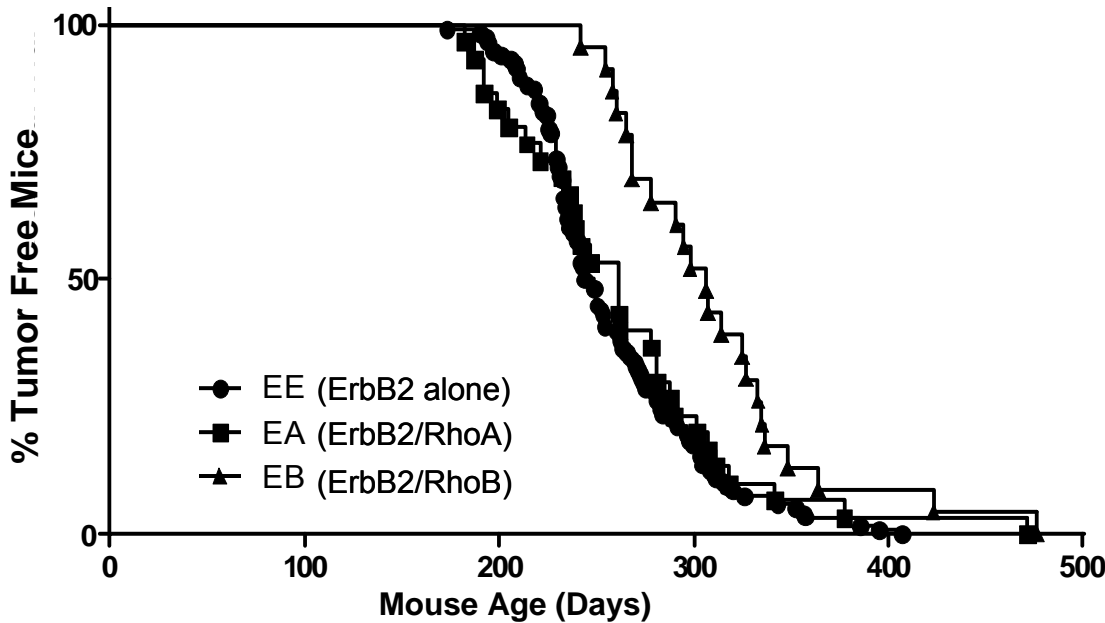


Figure 40. Tumor onset dates for bi-transgenic mice over expressing ErbB2/RhoB (EB) or ErbB2/RhoA (EA) were compared to tumor onsets for mono-transgenic ErbB2 mice as described in Materials and Methods.

Table 7. RhoB, but not RhoA over expression results in a significant delay in ErbB2-mediated tumor onset and multiplicity, but not tumor growth rate

Mouse Strain	Tumor Onset (Days)	P Value	Hazard Ratio	Tumor Growth Rate	P Value	Tumor Multiplicity	P Value
ErbB2 (n=127)	246.5 ± 4.6	-	-	89.0 ± 10.7	-	2.1 ± 0.22	-
ErbB2/ RhoB (n=17)	306.0 ± 10.4	0.000 3	2.022	75.1 ± 9.7	0.16	1.5 ± 0.15	0.018
ErbB2/ RhoA (n=28)	261.0 ± 9.1	0.514 1	1.14	74.4 ± 7.7	0.13	2.1 ± 0.30	0.45

Table 7. Tumor onset, growth rate and multiplicity for bi-transgenic mice over expressing ErbB2/RhoB (EB) or ErbB2/RhoA (EA) were compared to tumor onsets for mono-transgenic ErbB2 (EE) mice. Kaplan-Meyer survival curves were generated using graph pad software. Log-ranked and student T-tests were used for statistical analysis.

Taken together, these data demonstrate a tumor suppressive role for RhoB, in that RhoB overexpression resulted in a significant delay in tumor onset and decreased the overall tumor multiplicity. In contrast, RhoA had no significant effect on ErbB2 oncogenesis. However, it is not known to what extent RhoB is over expressed in the tumor tissue, or which signaling events RhoB affects to implement these tumor suppressive effects. Tumor tissue was harvested after development to validate the expression of RhoB and RhoA. Figure 41 shows the western blot analysis of lysates from EB, EA and EE tumors. Exogenous RhoA and RhoB are tagged with an HA epitope for identification, whereas the EE mice do not express the HA epitope tag. All tumors aside from the one from mouse, number EB24, demonstrated HA-RhoB expression to some degree. Figure 41 also shows that all tumors from HA-RhoA transgenic mice expressed HA-RhoA, and that the HA antibody was specific to exogenous RhoB and RhoA as none of the tumors from EE mice demonstrated HA expression.

Figure 41. Tumors from EB and EA transgenic mice express RhoB and RhoA as determined by detection of HA by western blot

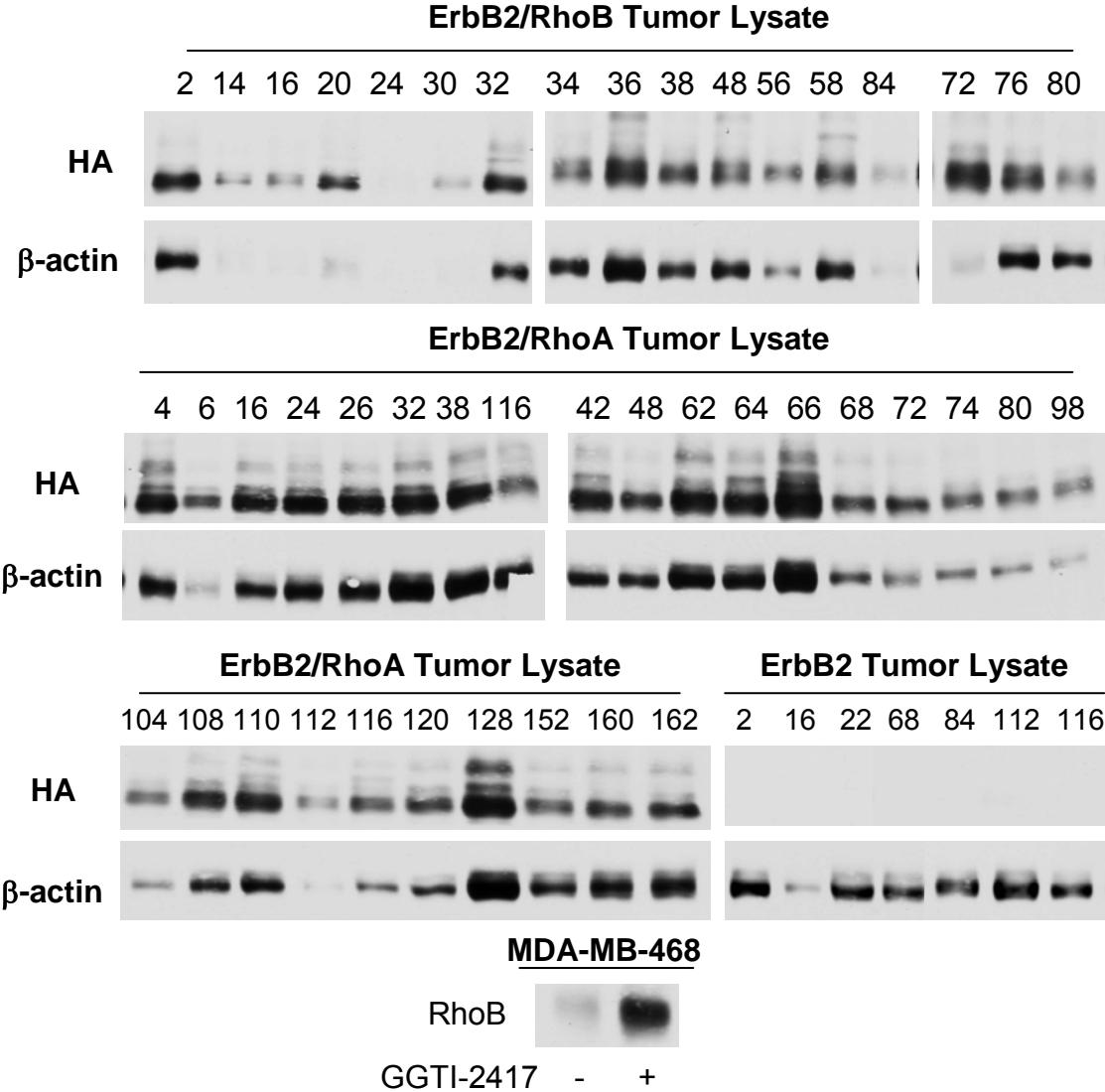


Figure 41. Tumors were resected from ErbB2/RhoB, ErbB2/RhoA and ErbB2 transgenic mice once the maximum tumor size was reached according to IACUC guidelines. Tissue was snap frozen upon collection, homogenized in lysis buffer and the protein was separated by 10 % PAGE, as described in Materials and Methods.

Discussion

Rho proteins in the RhoA-like family are highly identical and were once thought to be evolutionarily redundant because they share many cellular functions(155, 174). However, recently RhoA and RhoB have been shown to also have divergent roles in the context of oncogenesis(16, 21, 22, 168). The role of RhoA in cell cycle progression, malignant transformation and tumor invasiveness is well established(171, 174, 186). These traits demonstrate physiological necessities for cellular transformation. RhoA has also been associated with STAT3 and STAT5, which leads to increased tumor cell survival, cell proliferation, cell migration and epithelial to mesenchymal transition (EMT)(184, 185). RhoB, on the other hand, has recently been shown to suppress oncogenic events that lead to tumorigenesis. Supporting evidence comes from data that shows RhoB expression is decreased by upstream oncogenic signaling through EGFR, ErbB2 and Ras, which is mediated through the PI3K/Akt pathway(15, 16, 200). Furthermore, ectopic expression of RhoB has been shown to inhibit transformation induced by H-Ras and PI3K, overcome resistance to chemotherapeutic induced apoptosis and block cell migration and invasion(15, 175, 181). Likewise, ectopic expression of RhoB significantly inhibited metastasis in the B16/F10 mouse melanoma animal model, and

transgenic mice lacking RhoB showed a higher propensity for chemically induced skin carcinogenesis(16). On the contrary, RhoA did not have tumor suppressive activity in any of these events compared to RhoB. Correlations in the clinic have been made in head and neck as well as lung cancers that demonstrate loss of RhoB expression as the tumors became more aggressive, from carcinoma in-situ to highly infiltrating carcinoma(22, 23).

To further elucidate the anti-cancer properties of RhoB we set out to determine the effects of overexpression of both RhoA and RhoB on ErbB2 mediated breast neoplasia. By utilizing transgenic mouse models we bridge the gap of data between ectopic overexpression *in-vitro*, and the correlative evidence from the studies done in human cancer patients. This strategy allows for examination of overexpression of these Rho family members in a physiologically relevant setting for breast cancer by producing tissue-specific expression in the mammary fat pads. By crossing these mice with commercially available ErbB2 transgenic mice we determined that overexpression of RhoB, but not RhoA, led to a significant delay in the tumor onset mediated by ErbB2. RhoA, on the other hand, did not affect the onset of ErbB2 mediated mammary tumors. These results were not surprising, however, because RhoA is downstream of ErbB2, constitutively expressed and most likely is already activated by ErbB2 in these transgenic mice. Therefore, it is likely that the increased RhoA expression in this system is redundant to ErbB2 signaling and cannot add to transforming effects. RhoB on the other hand, is not constitutively expressed and its expression is downregulated by ErbB2 in cultured cells. Therefore, forced expression of RhoB

could antagonize ErbB2 oncogenesis in this model. This is consistent with our work in cell culture that showed that ectopic expression of RhoB blocked ErbB2 transformation. RhoB expression in the mammary fat pads also reduced the number of tumors that developed per mouse. This suggests that RhoB not only delayed the tumorigenic events, but also reduced the oncogenic potency of ErbB2 signaling creating a higher threshold for transformation leading to fewer tumor sites in the mammary fat pads. However, RhoB did not affect tumor growth, suggesting that once the ErbB2 oncogenic signaling overcame the tumor suppressive threshold of the over expressed RhoB the tumors grew at the same rate. Similarly, overexpression of RhoA did not add to the ability of ErbB2 to induce tumor growth in multiple sites, or increase the growth rates of the tumors once established. Once again, this is most likely due to redundancy in the signaling between ErbB2 and RhoA. The mechanism by which RhoB delays tumor onset and multiplicity is not known. We hypothesize that this is most likely due to RhoB antagonizing ErbB2 signaling such as those mediated by Ras, PI3K, Akt, Erk, and STAT3. These studies should be done in the mammary fat pads prior to tumor onset as well as early on while the tumors are fairly small. This would allow for the comparison of the effects of transgene expression on signaling in the fat pads just prior to, or during the transition from normal ductal epithelial cells to hyperplasia or neo-plasia. Furthermore, future work should investigate the role of RhoB and RhoA on normal breast morphogenesis. Future analysis may be done on the fat pads of RhoA and RhoB transgenic mice by comparing timed matings during the proliferative, differentiation, and involution

time points. Here, P-Akt, P-Erk1/2, and P-STAT3 signaling along with HA, RhoB and RhoA expression can be analyzed by both western blot and immunohistochemistry.

These data both support the recent findings of the divergent roles of RhoA and RhoB in cancer, as well as bring up additional questions regarding signaling events in which RhoB antagonizes, while RhoA potentiates tumorigenesis. Future work with this model and the tumors that arise should focus on signaling pathways that are responsible for the anti-neoplastic role of RhoB. Furthermore, the physiological consequences of RhoA and RhoB expression in the mammary fat pads should be analyzed during the natural progression of fat pads throughout pregnancy. To this end, timed matings should be done to analyze fat pads harvested from RhoA and RhoB mice during the proliferative period of early pregnancy. Likewise, fat pads should be harvested from mice at day 18 of pregnancy to determine if RhoA or RhoB expression alters the differentiation of the ductal epithelial cells that develop glandular structures for milk production. Finally, fat pads should be harvested from mice post pregnancy, after weaning of the pups, to determine the effects of RhoA and RhoB expression on involution-induced apoptosis of the ductal epithelial cells. Taken together, this data clearly demonstrate that RhoB suppresses ErbB2-mediated mammary oncogenesis by delaying the tumor onset and by decreasing tumor multiplicity. These studies further validate RhoB tumor suppressive activity and enhanced our understanding of RhoB's involvement in the regulation of tumorigenesis.

Conclusions and Future Directions

In an attempt to discover novel inhibitors of the Raf/Mek/Erk1/2 kinase cascade we identified pirbuterol, a known β 2 selective adrenergic receptor agonist(150), as an activator of a tumor suppressive pathway that was poorly characterized in cancer. In Chapter 1 of the thesis we demonstrated that in MDA-MB-231 (breast), ACHN (renal) and SF-539 (CNS) cancer cells, stimulation of the β 2 AR with ARA-211 (pirbuterol) led to the production of cAMP and activation of PKA, which resulted in inhibition of C-Raf, but not B-Raf, kinase activity. By blocking C-Raf, and subsequently Mek kinase activity, the activation of Erk1/2 proteins were inhibited, correlating with inhibition of anchorage-dependent and –independent cell growth, induction of apoptosis, and complete inhibition of the growth of MDA-MB-231 and ACHN xenografts in nude mice. Through the use of pharmacological inhibitors, and genetic manipulation, we found that the inhibition of C-Raf/Mek/Erk1/2 signaling was dependent on cAMP-mediated activation of PKA, but not cAMP activation of the guanine nucleotide exchange factors EPAC 1 and 2. Furthermore, we demonstrated that the inhibition of cell proliferation in MDA-MB-231 cells was dependent upon the ability of ARA-211 to bind β 2 AR and to inhibit Mek1/2 activity.

Prior to our studies there was evidence that cAMP can control the proliferation of normal cells through regulation of the Raf/Mek/Erk1/2 pathway. However, this regulation has been shown to be cell type specific, and can result in either activation or inhibition of Raf/Mek/Erk signaling(201). For example, in adipocytes, endothelial cells, NIH 3T3 cells, rat fibroblasts, smooth muscle cells, hepatocytes and pancreatic acinar cells the stimulation of cAMP results in inhibition of Erk1/2 activation and decreased cell proliferation(40, 48-56). However, in rat thyroid cells, bone cells, polycystic kidney epithelium, Sertoli cells, cardiac myocytes, granulosa cells, pre-adiposites, pituitary cells and PC12 cells the stimulation of cAMP results in the activation of Erk1/2 resulting in differentiation or stimulation of proliferation(39-46). As discussed previously, the physiological effects of cAMP stimulation have been well characterized in normal cells. The effects of cAMP stimulation has only been studied in a few cancer cells, and most importantly until this thesis work, there has never been a succinct report detailing the signaling mechanisms by which cAMP affects cancer cells. For instance, two reports demonstrated that in MDA-MB-231 (breast), HL-60 (leukemia) and SH-CY5Y (neuroblastoma) cancer cells stimulation of cAMP results in inhibition of DNA synthesis, but no mechanistic signaling studies were done(66, 67). Inconsistent with this, other reports demonstrate that activation of β AR results in stimulation of growth in cell lines derived from pancreatic ductal carcinoma, as well as pulmonary adenocarcinoma, through activation of arachidonic acid(202-204). Furthermore, the effects or β 2 AR stimulation of

cAMP production on anchorage-dependent and –independent growth, apoptosis and growth of human tumors in nude mice are not known.

In this thesis we demonstrated that stimulation of β 2 AR inhibits anchorage-dependent and –independent growth, induces apoptosis and induces regression of human tumors in nude mice. In normal cells, PKA-mediated inhibition of C-Raf kinase activity has been demonstrated, although the mechanism by which this occurs is still controversial in the literature for normal cells, and lacking for cancer cells. As mentioned earlier in the discussion of Chapter 1, we have demonstrated the dependency of the crosstalk between cAMP and Raf/Mek/Erk1/2 signaling on PKA-mediated inhibition of C-Raf kinase activity, but were unable to pinpoint the mechanism by which this occurs. It has been suggested in the literature that PKA can directly phosphorylate C-Raf on inhibitory serine residues 43 and 259, however, we were unable to detect any changes in phosphorylation of these residues by western blot analysis. Further studies are warranted to this end, and should include phosphopeptide mapping of C-Raf in the presence or absence of ARA-211 to determine the major amino acid residues phosphorylated by PKA. Likewise, the binding partners of C-Raf in the presence or absence of ARA-211 should be analyzed by a proteomic approach to determine if PKA is activating an inhibitory protein that binds C-Raf and sequesters it in an inactive form. These results would be important in the determination of the mechanism by which PKA inhibits C-Raf activity, and could lead to the design of better therapeutic approaches to inhibit C-Raf for cancer therapy.

The studies herein provide significant insight into the tumor suppressive activity of the β 2 AR in cancer cells, resulting in inhibition of anchorage-dependent and -independent growth, induction of apoptosis and complete inhibition of tumor xenograft growth. However, from this work we have not demonstrated how the cAMP/PKA-dependent suppression of P-Erk1/2 levels results in apoptosis. There are studies in the literature that show that inhibition of P-Erk1/2 can lead to apoptosis in cancer cells through modulation of mitochondrial-associated proapoptotic proteins such as Bim and Bad(136, 139). However, further studies are warranted to determine if the afore mentioned Erk1/2 effectors mediate the apoptosis induced via stimulation of cAMP, or if the apoptosis events are independent of Erk1/2 activity. To this end, constitutively activated Mek should be overexpressed followed by ARA-211 treatment to determine if apoptosis is rescued when Erk1/2 cannot be inhibited by ARA-211. Similarly, PKA could be inhibited by H89 or siRNA prior to ARA-211 treatment to determine if apoptosis induction is mediated by cAMP/PKA dependent signaling. Also, effectors downstream of Erk1/2 such as Bim and Bad should be knocked down, and ARA-211-mediated apoptosis should be examined to determine if the ablation results in a rescue from apoptosis.

In Chapter 2 of the thesis we demonstrate from analysis of both tumor tissue array and fresh human tumor biopsies that β 2 AR and P-Erk1/2 are expressed in approximately 25% of the tumors tested. This data, combined with the preclinical data in Chapter 1, led us to believe that ARA-211 treatment was a realistic goal for cancer therapy. Furthermore, the fact that pirbuterol was

previously tested clinically in patients with asthma and congestive heart failure will allow for an easier transition to anti-cancer clinical testing since the safe doses in humans is already known. However, since in normal cells cAMP has been shown to either stimulate or inhibit proliferation, we investigated the response of fresh tumor biopsies to ARA-211 treatment *ex-vivo*. This method of testing ARA-211 in fresh biopsies, unfortunately, yielded highly variable results, which in some cases was masked by necrosis. The detection of β 2 AR and P-Erk1/2 proteins proved to be problematic as well, as the cellular localization and staining percentages were not as expected. Much of the β 2 AR staining was found in the cytoplasm or nucleus, but was expected to be in the plasma membrane. Similarly, P-Erk1/2 staining was localized to the nucleus and cytoplasm, which was expected, but the % positive staining was lower than expected. After consultation with a molecular pathologist it was determined that the antibody concentrations for β 2 AR and P-Erk1/2 were not correctly optimized. The β 2 AR antibody concentration was most likely too high exhibiting non-specific staining, and the P-Erk1/2 antibody was most likely too dilute resulting in false negatives for tissues expected to express high levels of P-Erk1/2, such as late stage breast and pancreatic tumors. Aside from optimizing the IHC staining procedures, western blot analysis of protein levels could be used to determine expression of β 2 AR and P-Erk1/2. However, this method would not account for the tumor stroma that was captured with the tumor during the biopsy. This could result in β 2 AR and P-Erk1/2 expression detection from blood vessels or fibroblasts that are not actually indicative of the expression levels in the tumor.

Ultimately, the best method for the detection of the $\beta 2$ AR would be laser capture microdissection (LCM) of tumor tissue, followed by RT-PCR. Furthermore, microarray analysis of LCM from fresh human tumor biopsy treated *ex-vivo*, with and without ARA-211, could be done to distinguish the effects of the treatment on global gene expression. Another approach to determining the efficacy of ARA-211 on human tumors would be to implant small pieces of the fresh tumor tissues in athymic, nude mice, and treat the mice with ARA-211, as discussed earlier. This method would not be practical for all patient biopsies, but would serve as a good method to determine proof of concept for a human clinical trial. Ultimately, these studies would provide validation of the tumor suppressive effects of $\beta 2$ AR signaling in human cancer.

Chapter 3 of the thesis focuses on validating the tumor suppressive effects of the small GTPase RhoB. We set out to show that, *in-vivo*, RhoB can suppress the tumorigenic effects of upstream signaling through the ErbB2 receptor. As discussed earlier, the ErbB family of receptors is found overexpressed or mutated in many human cancers, such as lung, breast, head and neck, and bladder(205). *In-vitro* data from the Sebti lab and others demonstrated the ability of RhoB to abrogate transformation induced by H-Ras and PI3K. Studies also demonstrate that RhoB expression is decreased by oncogenic signaling through EGFR, ErbB2 and H-Ras. Likewise, IHC studies in paraffin-embedded tumor specimens from patients with lung and head and neck cancer shows that RhoB expression is lost as cancers progress from hyperplastic to deeply invasive carcinoma. However, data supporting the tumor suppressive

effects of RhoB *in-vivo* is lacking. Therefore, we used a physiologically relevant transgenic animal model to test the tumor suppressive effects of RhoB compared to its close family member RhoA. Mice were generated that express RhoB or RhoA in the mammary fat pads under the control of the MMTV promoter. These mice were then crossed with mice that overexpress the ErbB2 receptor under the same promoter control to create Erb2/RhoB and ErbB2/RhoA bitransgenic mice. ErbB2 overexpressing mice are known to develop spontaneous breast tumors at approximately 250 days(199). By introducing human RhoB in the mammary fat pads, the tumor onset mediated by ErbB2 was delayed by approximately 60 days. This data was statistically significant with a p value of 0.0003 as measured by a log-ranked statistical test. We hypothesized that this delay was due to the ability of RhoB to antagonize ErbB2 signaling through Ras, PI3K, Akt, Erk, and other well-known downstream ErbB2 signals. However, gathering data to support this hypothesis was difficult as the tumors were allowed to grow to maximum capacity to determine the effects of RhoB on tumor growth rate. It is possible that once the tumors were harvested they had already overcome the suppressed signaling from RhoB. To test this hypothesis, fat pads would need to be tested in a time course study to determine if RhoB expression resulted in inhibition of P-Akt, P-Erk1/2 or P-STAT3 during the transition from normal to transformed tissue. Although the tumor onset was delayed breast tumors eventually developed, and the tumor growth rate was not significantly different. This suggests that RhoB acts as a gatekeeper for transformation early on. However, as the tumors accumulate more oncogenic alterations the RhoB tumor

suppressive effects can be overcome. This may occur through further genetic alterations that surpass the regulation of RhoB, or signaling events that could eventually lead to expression of negative regulators of RhoB that result in faster degradation, or protein turnover. Time course studies are needed for RhoB expression in normal, hyperplastic and transformed cells isolated from the fat pads of ErbB2/RhoB bitransgenic mice. These studies could determine if RhoB is suppressed at the transcriptional level by methylation or acetylation during the transformation of the mammary ductal epithelial cells, although silencing at the promoter level is not likely since RhoB is under the control of the MMTV promoter in this case. However, a proteomic approach could allow for the identification of novel proteins that bind and inactivate RhoB. Here, RhoB would be immunoprecipitated from fat pad lysate at different time points and isolated by native gel electrophoresis. Once separated, RhoB binding partners could be identified, cloned and tested in tissue culture for their ability to reverse the tumor suppressive effects of RhoB. Although RhoB overexpression did not change the growth rate of the tumors once formed, the multiplicity, or tumor number per mouse, was significantly decreased by 25% (p value = 0.018) by RhoB, but not RhoA. Once again, the means by which RhoB inhibited tumor multiplicity in this setting was not determined, but it suggests that overall the oncogenic potency of ErbB2 signaling was diminished to the point that transformation was blocked in some of the mammary fat pad tissue. To gain insight to the mechanism by which RhoB decreases the oncogenic potential of ErbB2, microarray studies could be done comparing ErbB2 to ErbB2/RhoB and ErbB2/RhoA fat pads. In contrast to

RhoB, RhoA, which has been shown to promote tumorigenesis by inducing proliferation and contributing to invasion and metastasis, was found to have no effects on the tumor onset, growth rate or multiplicity of ErbB2-mediated oncogenesis in our transgenic mouse model. It is likely that the increase in RhoA expression is redundant to ErbB2 overexpression and could not add to the transforming effects of ErbB2. For example, ErbB2 is known to activate Ras, which in turn, can activate RhoA. Therefore, overexpression of RhoA in this setting would not be expected to add to the transforming activity of ErbB2.

While the generation of RhoA and RhoB transgenic mice allowed for the investigation of the effects of these small G-proteins in ErbB2 breast oncogenesis, they will also be instrumental in determining their role in normal mammary morphogenesis. As described previously, future work will be done with RhoA and RhoB monotransgenic mice for timed mating experiments to analyze their effects on ductal lobular formation, normal cell proliferation at day 7 pregnancy, differentiation at day 18 pregnancy and apoptosis at day 4 weaning. This would allow for the precise timed measuring of the effect of RhoA and RhoB on signaling events linked to the induction of apoptosis or inhibition of proliferation.

In conclusion, this work adds significant value to our understanding of the tumor suppressive roles of the β 2 AR and small GTPase RhoB. We now know that in cancer cells, PKA can mediate crosstalk between the β 2 AR and C-Raf/Mek/Erk1/2 kinase cascade resulting in inhibition of anchorage-dependent and -independent tumor cell growth, induction of apoptosis and complete

inhibition of human tumor growth in nude mice. Here we have shown that the inhibition of proliferation is dependent on stimulating cAMP production and inhibiting Mek/Erk1/2 signaling. However, translating this work to the clinic proved to be problematic. We determined that approximately 25% of tumors tested for β 2 AR and P-Erk1/2 actually co-express these markers from IHC examining a tissue array and fresh human tumor biopsies from Moffitt Cancer Center, but the expression patterns alone do not predict response to ARA-211 therapy on tissue *ex-vivo*. Further testing of *ex-vivo* tumor treatment techniques is necessary in order to more accurately predict a patient's tumor response to ARA-211. Finally, we provide data that supports the tumor suppressive effects of the small GTPase RhoB, but not RhoA, in a transgenic mouse model highly relevant to human breast cancer where ErbB2 drives oncogenesis. Future work should include studies designed to interrogate the signaling mechanisms by which RhoB delays tumor onset and reduces tumor multiplicity.

List of References

1. Stern, D. F. Tyrosine kinase signalling in breast cancer: ErbB family receptor tyrosine kinases. *Breast Cancer Res*, 2: 176-183, 2000.
2. Yarden, Y. Biology of HER2 and its importance in breast cancer. *Oncology*, 61 *Suppl* 2: 1-13, 2001.
3. Yarden, Y. and Sliwkowski, M. X. Untangling the ErbB signalling network. *Nat Rev Mol Cell Biol*, 2: 127-137, 2001.
4. Graus-Porta, D., Beerli, R. R., Daly, J. M., and Hynes, N. E. ErbB-2, the preferred heterodimerization partner of all ErbB receptors, is a mediator of lateral signaling. *Embo J*, 16: 1647-1655, 1997.
5. Tzahar, E., Waterman, H., Chen, X., Levkowitz, G., Karunagaran, D., Lavi, S., Ratzkin, B. J., and Yarden, Y. A hierarchical network of interreceptor interactions determines signal transduction by Neu differentiation factor/neuregulin and epidermal growth factor. *Mol Cell Biol*, 16: 5276-5287, 1996.
6. Li, Q. and Loeb, J. A. Neuregulin-heparan-sulfate proteoglycan interactions produce sustained erbB receptor activation required for the induction of acetylcholine receptors in muscle. *J Biol Chem*, 276: 38068-38075, 2001.
7. Brennan, P. J., Kumagai, T., Berezov, A., Murali, R., and Greene, M. I. HER2/neu: mechanisms of dimerization/oligomerization. *Oncogene*, 19: 6093-6101, 2000.
8. Ross, J. S., Fletcher, J. A., Bloom, K. J., Linette, G. P., Stec, J., Clark, E., Ayers, M., Symmans, W. F., Pusztai, L., and Hortobagyi, G. N. HER-2/neu testing in breast cancer. *Am J Clin Pathol*, 120 *Suppl*: S53-71, 2003.
9. Bos, J. L. ras oncogenes in human cancer: a review. *Cancer Res*, 49: 4682-4689, 1989.
10. Varghese, H. J., Davidson, M. T., MacDonald, I. C., Wilson, S. M., Nadkarni, K. V., Groom, A. C., and Chambers, A. F. Activated ras regulates the proliferation/apoptosis balance and early survival of developing micrometastases. *Cancer Res*, 62: 887-891, 2002.
11. Sahai, E., Olson, M. F., and Marshall, C. J. Cross-talk between Ras and Rho signalling pathways in transformation favours proliferation and increased motility. *Embo J*, 20: 755-766, 2001.
12. Zondag, G. C., Evers, E. E., ten Klooster, J. P., Janssen, L., van der Kammen, R. A., and Collard, J. G. Oncogenic Ras downregulates Rac activity, which leads to increased Rho activity and epithelial-mesenchymal transition. *J Cell Biol*, 149: 775-782, 2000.

13. Vial, E., Sahai, E., and Marshall, C. J. ERK-MAPK signaling coordinately regulates activity of Rac1 and RhoA for tumor cell motility. *Cancer Cell*, 4: 67-79, 2003.
14. Berenjeno, I. M., Nunez, F., and Bustelo, X. R. Transcriptomal profiling of the cellular transformation induced by Rho subfamily GTPases. *Oncogene*, 26: 4295-4305, 2007.
15. Jiang, K., Delarue, F. L., and Sebti, S. M. EGFR, ErbB2 and Ras but not Src suppress RhoB expression while ectopic expression of RhoB antagonizes oncogene-mediated transformation. *Oncogene*, 23: 1136-1145, 2004.
16. Jiang, K., Sun, J., Cheng, J., Djeu, J. Y., Wei, S., and Sebti, S. Akt mediates Ras downregulation of RhoB, a suppressor of transformation, invasion, and metastasis. *Mol Cell Biol*, 24: 5565-5576, 2004.
17. Huang, M., Kamasani, U., and Prendergast, G. C. RhoB facilitates c-Myc turnover by supporting efficient nuclear accumulation of GSK-3. *Oncogene*, 25: 1281-1289, 2006.
18. Huang, M. and Prendergast, G. C. RhoB in cancer suppression. *Histol Histopathol*, 21: 213-218, 2006.
19. Kamasani, U., Liu, A. X., and Prendergast, G. C. Genetic response to farnesyltransferase inhibitors: proapoptotic targets of RhoB. *Cancer Biol Ther*, 2: 273-280, 2003.
20. Liu, A. X., Rane, N., Liu, J. P., and Prendergast, G. C. RhoB is dispensable for mouse development, but it modifies susceptibility to tumor formation as well as cell adhesion and growth factor signaling in transformed cells. *Mol Cell Biol*, 21: 6906-6912, 2001.
21. Liu, A., Cerniglia, G. J., Bernhard, E. J., and Prendergast, G. C. RhoB is required to mediate apoptosis in neoplastically transformed cells after DNA damage. *Proc Natl Acad Sci U S A*, 98: 6192-6197, 2001.
22. Adnane, J., Muro-Cacho, C., Mathews, L., Sebti, S. M., and Munoz-Antonia, T. Suppression of rho B expression in invasive carcinoma from head and neck cancer patients. *Clin Cancer Res*, 8: 2225-2232, 2002.
23. Mazieres, J., Antonia, T., Daste, G., Muro-Cacho, C., Berchery, D., Tillement, V., Pradines, A., Sebti, S., and Favre, G. Loss of RhoB expression in human lung cancer progression. *Clin Cancer Res*, 10: 2742-2750, 2004.
24. Revillion, F., Bonnetterre, J., and Peyrat, J. P. ERBB2 oncogene in human breast cancer and its clinical significance. *Eur J Cancer*, 34: 791-808, 1998.
25. Benovic, J. L., Shorr, R. G., Caron, M. G., and Lefkowitz, R. J. The mammalian beta 2-adrenergic receptor: purification and characterization. *Biochemistry*, 23: 4510-4518, 1984.
26. Bilezikian, J. P., Dornfeld, A. M., and Gammon, D. E. Structure-binding-activity analysis of beta-adrenergic amines--II. Binding to the beta receptor and inhibition of adenylate cyclase. *Biochem Pharmacol*, 27: 1455-1461, 1978.

27. Bilezikian, J. P., Dornfeld, A. M., and Gammon, D. E. Structure-binding-activity analysis of beta-adrenergic amines--I. Binding to the beta receptor and activation of adenylate cyclase. *Biochem Pharmacol*, 27: 1445-1454, 1978.
28. Lefkowitz, R. J. and Hamp, M. Comparison of specificity of agonist and antagonist radioligand binding to beta adrenergic receptors. *Nature*, 268: 453-454, 1977.
29. Lefkowitz, R. J. and Williams, L. T. Catecholamine binding to the beta-adrenergic receptor. *Proc Natl Acad Sci U S A*, 74: 515-519, 1977.
30. Harden, T. K., Wolfe, B. B., and Molinoff, P. B. Binding of iodinated beta adrenergic antagonists to proteins derived from rat heart. *Mol Pharmacol*, 12: 1-15, 1976.
31. Leichtling, B. H., Su, Y. F., Wimalasena, J., Harden, T. K., Wolfe, B. B., and Wicks, W. D. Studies of cAMP metabolism in cultured hepatoma cells: presence of functional adenylate cyclase despite low cAMP content and lack of hormonal responsiveness. *J Cell Physiol*, 96: 215-223, 1978.
32. Cho, Y. J., Kim, J. Y., Jeong, S. W., Lee, S. B., and Kim, O. N. Cyclic AMP induces activation of extracellular signal-regulated kinases in HL-60 cells: role in cAMP-induced differentiation. *Leuk Res*, 27: 51-56, 2003.
33. Vossler, M. R., Yao, H., York, R. D., Pan, M. G., Rim, C. S., and Stork, P. J. cAMP activates MAP kinase and Elk-1 through a B-Raf- and Rap1-dependent pathway. *Cell*, 89: 73-82, 1997.
34. Stork, P. J. and Schmitt, J. M. Crosstalk between cAMP and MAP kinase signaling in the regulation of cell proliferation. *Trends Cell Biol*, 12: 258-266, 2002.
35. Maudsley, S., Pierce, K. L., Zamah, A. M., Miller, W. E., Ahn, S., Daaka, Y., Lefkowitz, R. J., and Luttrell, L. M. The beta(2)-adrenergic receptor mediates extracellular signal-regulated kinase activation via assembly of a multi-receptor complex with the epidermal growth factor receptor. *J Biol Chem*, 275: 9572-9580, 2000.
36. Enserink, J. M., Christensen, A. E., de Rooij, J., van Triest, M., Schwede, F., Genieser, H. G., Doskeland, S. O., Blank, J. L., and Bos, J. L. A novel Epac-specific cAMP analogue demonstrates independent regulation of Rap1 and ERK. *Nat Cell Biol*, 4: 901-906, 2002.
37. Rangarajan, S., Enserink, J. M., Kuiperij, H. B., de Rooij, J., Price, L. S., Schwede, F., and Bos, J. L. Cyclic AMP induces integrin-mediated cell adhesion through Epac and Rap1 upon stimulation of the beta 2-adrenergic receptor. *J Cell Biol*, 160: 487-493, 2003.
38. Christensen, A. E., Selheim, F., de Rooij, J., Dremier, S., Schwede, F., Dao, K. K., Martinez, A., Maenhaut, C., Bos, J. L., Genieser, H. G., and Doskeland, S. O. cAMP analog mapping of Epac1 and cAMP kinase. Discriminating analogs demonstrate that Epac and cAMP kinase act synergistically to promote PC-12 cell neurite extension. *J Biol Chem*, 278: 35394-35402, 2003.

39. Iacovelli, L., Capobianco, L., Salvatore, L., Sallese, M., D'Ancona, G. M., and De Blasi, A. Thyrotropin activates mitogen-activated protein kinase pathway in FRTL-5 by a cAMP-dependent protein kinase A-independent mechanism. *Mol Pharmacol*, 60: 924-933, 2001.
40. Fujita, T., Meguro, T., Fukuyama, R., Nakamuta, H., and Koida, M. New signaling pathway for parathyroid hormone and cyclic AMP action on extracellular-regulated kinase and cell proliferation in bone cells. Checkpoint of modulation by cyclic AMP. *J Biol Chem*, 277: 22191-22200, 2002.
41. Yamaguchi, T., Pelling, J. C., Ramaswamy, N. T., Eppler, J. W., Wallace, D. P., Nagao, S., Rome, L. A., Sullivan, L. P., and Grantham, J. J. cAMP stimulates the in vitro proliferation of renal cyst epithelial cells by activating the extracellular signal-regulated kinase pathway. *Kidney Int*, 57: 1460-1471, 2000.
42. Deeble, P. D., Murphy, D. J., Parsons, S. J., and Cox, M. E. Interleukin-6- and cyclic AMP-mediated signaling potentiates neuroendocrine differentiation of LNCaP prostate tumor cells. *Mol Cell Biol*, 21: 8471-8482, 2001.
43. Crepieux, P., Marion, S., Martinat, N., Fafeur, V., Vern, Y. L., Kerboeuf, D., Guillou, F., and Reiter, E. The ERK-dependent signalling is stage-specifically modulated by FSH, during primary Sertoli cell maturation. *Oncogene*, 20: 4696-4709, 2001.
44. Zou, Y., Komuro, I., Yamazaki, T., Kudoh, S., Uozumi, H., Kadowaki, T., and Yazaki, Y. Both Gs and Gi proteins are critically involved in isoproterenol-induced cardiomyocyte hypertrophy. *J Biol Chem*, 274: 9760-9770, 1999.
45. Seger, R., Hanoch, T., Rosenberg, R., Dantes, A., Merz, W. E., Strauss, J. F., 3rd, and Amsterdam, A. The ERK signaling cascade inhibits gonadotropin-stimulated steroidogenesis. *J Biol Chem*, 276: 13957-13964, 2001.
46. Greenberg, A. S., Shen, W. J., Muliro, K., Patel, S., Souza, S. C., Roth, R. A., and Kraemer, F. B. Stimulation of lipolysis and hormone-sensitive lipase via the extracellular signal-regulated kinase pathway. *J Biol Chem*, 276: 45456-45461, 2001.
47. Hattori, M. and Minato, N. Rap1 GTPase: functions, regulation, and malignancy. *J Biochem*, 134: 479-484, 2003.
48. Sevetson, B. R., Kong, X., and Lawrence, J. C., Jr. Increasing cAMP attenuates activation of mitogen-activated protein kinase. *Proc Natl Acad Sci U S A*, 90: 10305-10309, 1993.
49. D'Angelo, G., Lee, H., and Weiner, R. I. cAMP-dependent protein kinase inhibits the mitogenic action of vascular endothelial growth factor and fibroblast growth factor in capillary endothelial cells by blocking Raf activation. *J Cell Biochem*, 67: 353-366, 1997.

50. Schmitt, J. M. and Stork, P. J. Cyclic AMP-mediated inhibition of cell growth requires the small G protein Rap1. *Mol Cell Biol*, 21: 3671-3683, 2001.
51. Chen, J. and Iyengar, R. Suppression of Ras-induced transformation of NIH 3T3 cells by activated G alpha s. *Science*, 263: 1278-1281, 1994.
52. Cook, S. J. and McCormick, F. Inhibition by cAMP of Ras-dependent activation of Raf. *Science*, 262: 1069-1072, 1993.
53. Wu, J., Dent, P., Jelinek, T., Wolfman, A., Weber, M. J., and Sturgill, T. W. Inhibition of the EGF-activated MAP kinase signaling pathway by adenosine 3',5'-monophosphate. *Science*, 262: 1065-1069, 1993.
54. Scott, P. H., Belham, C. M., al-Hafidh, J., Chilvers, E. R., Peacock, A. J., Gould, G. W., and Plevin, R. A regulatory role for cAMP in phosphatidylinositol 3-kinase/p70 ribosomal S6 kinase-mediated DNA synthesis in platelet-derived-growth-factor-stimulated bovine airway smooth-muscle cells. *Biochem J*, 318 (Pt 3): 965-971, 1996.
55. Osinski, M. T. and Schror, K. Inhibition of platelet-derived growth factor-induced mitogenesis by phosphodiesterase 3 inhibitors: role of protein kinase A in vascular smooth muscle cell mitogenesis. *Biochem Pharmacol*, 60: 381-387, 2000.
56. Thoresen, G. H., Johansen, E. J., and Christoffersen, T. Effects of cAMP on ERK mitogen-activated protein kinase activity in hepatocytes do not parallel the bidirectional regulation of DNA synthesis. *Cell Biol Int*, 23: 13-20, 1999.
57. Tortora, G. and Ciardiello, F. Protein kinase A as target for novel integrated strategies of cancer therapy. *Ann N Y Acad Sci*, 968: 139-147, 2002.
58. Cho-Chung, Y. S., Nesterova, M., Becker, K. G., Srivastava, R., Park, Y. G., Lee, Y. N., Cho, Y. S., Kim, M. K., Neary, C., and Cheadle, C. Dissecting the circuitry of protein kinase A and cAMP signaling in cancer genesis: antisense, microarray, gene overexpression, and transcription factor decoy. *Ann N Y Acad Sci*, 968: 22-36, 2002.
59. Schmitt, J. M. and Stork, P. J. PKA phosphorylation of Src mediates cAMP's inhibition of cell growth via Rap1. *Mol Cell*, 9: 85-94, 2002.
60. Hafner, S., Adler, H. S., Mischak, H., Janosch, P., Heidecker, G., Wolfman, A., Pippig, S., Lohse, M., Ueffing, M., and Kolch, W. Mechanism of inhibition of Raf-1 by protein kinase A. *Mol Cell Biol*, 14: 6696-6703, 1994.
61. Graves, L. M., Bornfeldt, K. E., Raines, E. W., Potts, B. C., Macdonald, S. G., Ross, R., and Krebs, E. G. Protein kinase A antagonizes platelet-derived growth factor-induced signaling by mitogen-activated protein kinase in human arterial smooth muscle cells. *Proc Natl Acad Sci U S A*, 90: 10300-10304, 1993.

62. Dumaz, N. and Marais, R. Integrating signals between cAMP and the RAS/RAF/MEK/ERK signalling pathways. Based on the anniversary prize of the Gesellschaft für Biochemie und Molekularbiologie Lecture delivered on 5 July 2003 at the Special FEBS Meeting in Brussels. *Febs J*, 272: 3491-3504, 2005.
63. English, J. M. and Cobb, M. H. Pharmacological inhibitors of MAPK pathways. *Trends Pharmacol Sci*, 23: 40-45, 2002.
64. Khosravi-Far, R., White, M. A., Westwick, J. K., Solski, P. A., Chrzanowska-Wodnicka, M., Van Aelst, L., Wigler, M. H., and Der, C. J. Oncogenic Ras activation of Raf/mitogen-activated protein kinase-independent pathways is sufficient to cause tumorigenic transformation. *Mol Cell Biol*, 16: 3923-3933, 1996.
65. Weinstein-Oppenheimer, C. R., Blalock, W. L., Steelman, L. S., Chang, F., and McCubrey, J. A. The Raf signal transduction cascade as a target for chemotherapeutic intervention in growth factor-responsive tumors. *Pharmacol Ther*, 88: 229-279, 2000.
66. Kim, S. N., Ahn, Y. H., Kim, S. G., Park, S. D., Cho-Chung, Y. S., and Hong, S. H. 8-Cl-cAMP induces cell cycle-specific apoptosis in human cancer cells. *Int J Cancer*, 93: 33-41, 2001.
67. Slotkin, T. A., Zhang, J., Dancel, R., Garcia, S. J., Willis, C., and Seidler, F. J. Beta-adrenoceptor signaling and its control of cell replication in MDA-MB-231 human breast cancer cells. *Breast Cancer Res Treat*, 60: 153-166, 2000.
68. Hanahan, D. and Weinberg, R. A. The hallmarks of cancer. *Cell*, 100: 57-70, 2000.
69. Borg, A., Tandon, A. K., Sigurdsson, H., Clark, G. M., Ferno, M., Fuqua, S. A., Killander, D., and McGuire, W. L. HER-2/neu amplification predicts poor survival in node-positive breast cancer. *Cancer Res*, 50: 4332-4337, 1990.
70. Slamon, D. J., Clark, G. M., Wong, S. G., Levin, W. J., Ullrich, A., and McGuire, W. L. Human breast cancer: correlation of relapse and survival with amplification of the HER-2/neu oncogene. *Science*, 235: 177-182, 1987.
71. Johnson, G. L. and Lapadat, R. Mitogen-activated protein kinase pathways mediated by ERK, JNK, and p38 protein kinases. *Science*, 298: 1911-1912, 2002.
72. Ballif, B. A. and Blenis, J. Molecular mechanisms mediating mammalian mitogen-activated protein kinase (MAPK) kinase (MEK)-MAPK cell survival signals. *Cell Growth Differ*, 12: 397-408, 2001.
73. Hagemann, C. and Blank, J. L. The ups and downs of MEK kinase interactions. *Cell Signal*, 13: 863-875, 2001.
74. Fresno Vara, J. A., Casado, E., de Castro, J., Cejas, P., Belda-Iniesta, C., and Gonzalez-Baron, M. PI3K/Akt signalling pathway and cancer. *Cancer Treat Rev*, 30: 193-204, 2004.

75. Alvarez, J. V. and Frank, D. A. Genome-wide analysis of STAT target genes: elucidating the mechanism of STAT-mediated oncogenesis. *Cancer Biol Ther*, 3: 1045-1050, 2004.
76. Sebolt-Leopold, J. S. Development of anticancer drugs targeting the MAP kinase pathway. *Oncogene*, 19: 6594-6599, 2000.
77. Sebolt-Leopold, J. S., Dudley, D. T., Herrera, R., Van Becelaere, K., Wiland, A., Gowan, R. C., Teclé, H., Barrett, S. D., Bridges, A., Przybranowski, S., Leopold, W. R., and Saltiel, A. R. Blockade of the MAP kinase pathway suppresses growth of colon tumors in vivo. *Nat Med*, 5: 810-816, 1999.
78. Blaskovich, M. A., Sun, J., Cantor, A., Turkson, J., Jove, R., and Sebt, S. M. Discovery of JSI-124 (cucurbitacin I), a selective Janus kinase/signal transducer and activator of transcription 3 signaling pathway inhibitor with potent antitumor activity against human and murine cancer cells in mice. *Cancer Res*, 63: 1270-1279, 2003.
79. Redell, M. S. and Tweardy, D. J. Targeting transcription factors for cancer therapy. *Curr Pharm Des*, 11: 2873-2887, 2005.
80. Hao, D. and Rowinsky, E. K. Inhibiting signal transduction: recent advances in the development of receptor tyrosine kinase and Ras inhibitors. *Cancer Invest*, 20: 387-404, 2002.
81. Johnson, J. R., Cohen, M., Sridhara, R., Chen, Y. F., Williams, G. M., Duan, J., Gobburu, J., Booth, B., Benson, K., Leighton, J., Hsieh, L. S., Chidambaram, N., Zimmerman, P., and Pazdur, R. Approval summary for erlotinib for treatment of patients with locally advanced or metastatic non-small cell lung cancer after failure of at least one prior chemotherapy regimen. *Clin Cancer Res*, 11: 6414-6421, 2005.
82. Sebt, S. M. and Hamilton, A. D. Inhibition of Ras prenylation: a novel approach to cancer chemotherapy. *Pharmacol Ther*, 74: 103-114, 1997.
83. Shields, J. M., Pruitt, K., McFall, A., Shaub, A., and Der, C. J. Understanding Ras: 'it ain't over 'til it's over'. *Trends Cell Biol*, 10: 147-154, 2000.
84. Lehman, T. A., Reddel, R., Peifer, A. M., Spillare, E., Kaighn, M. E., Weston, A., Gerwin, B. I., and Harris, C. C. Oncogenes and tumor-suppressor genes. *Environ Health Perspect*, 93: 133-134, 1991.
85. Lerner, E. C., Zhang, T. T., Knowles, D. B., Qian, Y., Hamilton, A. D., and Sebt, S. M. Inhibition of the prenylation of K-Ras, but not H- or N-Ras, is highly resistant to CAAX peptidomimetics and requires both a farnesyltransferase and a geranylgeranyltransferase I inhibitor in human tumor cell lines. *Oncogene*, 15: 1283-1288, 1997.
86. Barbacid, M. ras genes. *Annu Rev Biochem*, 56: 779-827, 1987.
87. Khosravi-Far, R. and Der, C. J. The Ras signal transduction pathway. *Cancer Metastasis Rev*, 13: 67-89, 1994.

88. Shukla, S., Maclennan, G. T., Marengo, S. R., Resnick, M. I., and Gupta, S. Constitutive activation of PI3K-Akt and NF-kappaB during prostate cancer progression in autochthonous transgenic mouse model. *Prostate*, 2005.
89. Lackey, K. E. Lessons from the drug discovery of lapatinib, a dual ErbB1/2 tyrosine kinase inhibitor. *Curr Top Med Chem*, 6: 435-460, 2006.
90. Barber, M. A. and Welch, H. C. PI3K and RAC signalling in leukocyte and cancer cell migration. *Bull Cancer*, 93: E44-52, 2006.
91. Kallergi, G., Agelaki, S., Markomanolaki, H., Georgoulas, V., and Stournaras, C. Activation of FAK/PI3K/Rac1 signaling controls actin reorganization and inhibits cell motility in human cancer cells. *Cell Physiol Biochem*, 20: 977-986, 2007.
92. Kolsch, V., Charest, P. G., and Firtel, R. A. The regulation of cell motility and chemotaxis by phospholipid signaling. *J Cell Sci*, 121: 551-559, 2008.
93. Qian, Y., Corum, L., Meng, Q., Blenis, J., Zheng, J. Z., Shi, X., Flynn, D. C., and Jiang, B. H. PI3K induced actin filament remodeling through Akt and p70S6K1: implication of essential role in cell migration. *Am J Physiol Cell Physiol*, 286: C153-163, 2004.
94. Falsetti, S. C., Wang, D. A., Peng, H., Carrico, D., Cox, A. D., Der, C. J., Hamilton, A. D., and Sebt, S. M. Geranylgeranyltransferase I inhibitors target RalB to inhibit anchorage-dependent growth and induce apoptosis and RalA to inhibit anchorage-independent growth. *Mol Cell Biol*, 27: 8003-8014, 2007.
95. Hamad, N. M., Elconin, J. H., Karnoub, A. E., Bai, W., Rich, J. N., Abraham, R. T., Der, C. J., and Counter, C. M. Distinct requirements for Ras oncogenesis in human versus mouse cells. *Genes Dev*, 16: 2045-2057, 2002.
96. Lim, K. H., Baines, A. T., Fiordalisi, J. J., Shipitsin, M., Feig, L. A., Cox, A. D., Der, C. J., and Counter, C. M. Activation of RalA is critical for Ras-induced tumorigenesis of human cells. *Cancer Cell*, 7: 533-545, 2005.
97. Lim, K. H., O'Hayer, K., Adam, S. J., Kendall, S. D., Campbell, P. M., Der, C. J., and Counter, C. M. Divergent roles for RalA and RalB in malignant growth of human pancreatic carcinoma cells. *Curr Biol*, 16: 2385-2394, 2006.
98. Peterson, S. N., Trabalzini, L., Brtva, T. R., Fischer, T., Altschuler, D. L., Martelli, P., Lapetina, E. G., Der, C. J., and White, G. C., 2nd Identification of a novel RalGDS-related protein as a candidate effector for Ras and Rap1. *J Biol Chem*, 271: 29903-29908, 1996.
99. Gonzalez-Garcia, A., Pritchard, C. A., Paterson, H. F., Mavria, G., Stamp, G., and Marshall, C. J. RalGDS is required for tumor formation in a model of skin carcinogenesis. *Cancer Cell*, 7: 219-226, 2005.
100. Roberts, P. J. and Der, C. J. Targeting the Raf-MEK-ERK mitogen-activated protein kinase cascade for the treatment of cancer. *Oncogene*, 26: 3291-3310, 2007.

101. Wellbrock, C., Karasarides, M., and Marais, R. The RAF proteins take centre stage. *Nat Rev Mol Cell Biol*, 5: 875-885, 2004.
102. Weston, C. R., Lambricht, D. G., and Davis, R. J. Signal transduction. MAP kinase signaling specificity. *Science*, 296: 2345-2347, 2002.
103. Yoon, S. and Seger, R. The extracellular signal-regulated kinase: multiple substrates regulate diverse cellular functions. *Growth Factors*, 24: 21-44, 2006.
104. Zuber, J., Tchernitsa, O. I., Hinzmann, B., Schmitz, A. C., Grips, M., Hellriegel, M., Sers, C., Rosenthal, A., and Schafer, R. A genome-wide survey of RAS transformation targets. *Nat Genet*, 24: 144-152, 2000.
105. Brose, M. S., Volpe, P., Feldman, M., Kumar, M., Rishi, I., Gerrero, R., Einhorn, E., Herlyn, M., Minna, J., Nicholson, A., Roth, J. A., Albelda, S. M., Davies, H., Cox, C., Brignell, G., Stephens, P., Futreal, P. A., Wooster, R., Stratton, M. R., and Weber, B. L. BRAF and RAS mutations in human lung cancer and melanoma. *Cancer Res*, 62: 6997-7000, 2002.
106. Davies, H., Bignell, G. R., Cox, C., Stephens, P., Edkins, S., Clegg, S., Teague, J., Woffendin, H., Garnett, M. J., Bottomley, W., Davis, N., Dicks, E., Ewing, R., Floyd, Y., Gray, K., Hall, S., Hawes, R., Hughes, J., Kosmidou, V., Menzies, A., Mould, C., Parker, A., Stevens, C., Watt, S., Hooper, S., Wilson, R., Jayatilake, H., Gusterson, B. A., Cooper, C., Shipley, J., Hargrave, D., Pritchard-Jones, K., Maitland, N., Chenevix-Trench, G., Riggins, G. J., Bigner, D. D., Palmieri, G., Cossu, A., Flanagan, A., Nicholson, A., Ho, J. W., Leung, S. Y., Yuen, S. T., Weber, B. L., Seigler, H. F., Darrow, T. L., Paterson, H., Marais, R., Marshall, C. J., Wooster, R., Stratton, M. R., and Futreal, P. A. Mutations of the BRAF gene in human cancer. *Nature*, 417: 949-954, 2002.
107. Yuen, S. T., Davies, H., Chan, T. L., Ho, J. W., Bignell, G. R., Cox, C., Stephens, P., Edkins, S., Tsui, W. W., Chan, A. S., Futreal, P. A., Stratton, M. R., Wooster, R., and Leung, S. Y. Similarity of the phenotypic patterns associated with BRAF and KRAS mutations in colorectal neoplasia. *Cancer Res*, 62: 6451-6455, 2002.
108. Li, N., Batt, D., and Warmuth, M. B-Raf kinase inhibitors for cancer treatment. *Curr Opin Investig Drugs*, 8: 452-456, 2007.
109. Tsai, J., Lee, J. T., Wang, W., Zhang, J., Cho, H., Mamo, S., Bremer, R., Gillette, S., Kong, J., Haass, N. K., Sproesser, K., Li, L., Smalley, K. S., Fong, D., Zhu, Y. L., Marimuthu, A., Nguyen, H., Lam, B., Liu, J., Cheung, I., Rice, J., Suzuki, Y., Luu, C., Settachatgul, C., Shellooe, R., Cantwell, J., Kim, S. H., Schlessinger, J., Zhang, K. Y., West, B. L., Powell, B., Habets, G., Zhang, C., Ibrahim, P. N., Hirth, P., Artis, D. R., Herlyn, M., and Bollag, G. Discovery of a selective inhibitor of oncogenic B-Raf kinase with potent antimelanoma activity. *Proc Natl Acad Sci U S A*, 105: 3041-3046, 2008.
110. McClean, M. N., Mody, A., Broach, J. R., and Ramanathan, S. Cross-talk and decision making in MAP kinase pathways. *Nat Genet*, 39: 409-414, 2007.

111. Raman, M., Chen, W., and Cobb, M. H. Differential regulation and properties of MAPKs. *Oncogene*, 26: 3100-3112, 2007.
112. Dhillon, A. S. and Kolch, W. Untying the regulation of the Raf-1 kinase. *Arch Biochem Biophys*, 404: 3-9, 2002.
113. Dritschilo, A., Huang, C. H., Rudin, C. M., Marshall, J., Collins, B., Dul, J. L., Zhang, C., Kumar, D., Gokhale, P. C., Ahmad, A., Ahmad, I., Sherman, J. W., and Kasid, U. N. Phase I study of liposome-encapsulated c-raf antisense oligodeoxyribonucleotide infusion in combination with radiation therapy in patients with advanced malignancies. *Clin Cancer Res*, 12: 1251-1259, 2006.
114. Wilhelm, S. M., Carter, C., Tang, L., Wilkie, D., McNabola, A., Rong, H., Chen, C., Zhang, X., Vincent, P., McHugh, M., Cao, Y., Shujath, J., Gawlak, S., Eveleigh, D., Rowley, B., Liu, L., Adnane, L., Lynch, M., Auclair, D., Taylor, I., Gedrich, R., Voznesensky, A., Riedl, B., Post, L. E., Bollag, G., and Trail, P. A. BAY 43-9006 exhibits broad spectrum oral antitumor activity and targets the RAF/MEK/ERK pathway and receptor tyrosine kinases involved in tumor progression and angiogenesis. *Cancer Res*, 64: 7099-7109, 2004.
115. Hahn, O. and Stadler, W. Sorafenib. *Curr Opin Oncol*, 18: 615-621, 2006.
116. Zheng, C. F. and Guan, K. L. Cloning and characterization of two distinct human extracellular signal-regulated kinase activator kinases, MEK1 and MEK2. *J Biol Chem*, 268: 11435-11439, 1993.
117. Catling, A. D., Schaeffer, H. J., Reuter, C. W., Reddy, G. R., and Weber, M. J. A proline-rich sequence unique to MEK1 and MEK2 is required for raf binding and regulates MEK function. *Mol Cell Biol*, 15: 5214-5225, 1995.
118. Chen, Z., Gibson, T. B., Robinson, F., Silvestro, L., Pearson, G., Xu, B., Wright, A., Vanderbilt, C., and Cobb, M. H. MAP kinases. *Chem Rev*, 101: 2449-2476, 2001.
119. Lewis, T. S., Shapiro, P. S., and Ahn, N. G. Signal transduction through MAP kinase cascades. *Adv Cancer Res*, 74: 49-139, 1998.
120. Crews, C. M., Alessandrini, A., and Erikson, R. L. The primary structure of MEK, a protein kinase that phosphorylates the ERK gene product. *Science*, 258: 478-480, 1992.
121. Haycock, J. W., Ahn, N. G., Cobb, M. H., and Krebs, E. G. ERK1 and ERK2, two microtubule-associated protein 2 kinases, mediate the phosphorylation of tyrosine hydroxylase at serine-31 in situ. *Proc Natl Acad Sci U S A*, 89: 2365-2369, 1992.
122. Seger, R. and Krebs, E. G. The MAPK signaling cascade. *Faseb J*, 9: 726-735, 1995.
123. Duff, J. L., Monia, B. P., and Berk, B. C. Mitogen-activated protein (MAP) kinase is regulated by the MAP kinase phosphatase (MKP-1) in vascular smooth muscle cells. Effect of actinomycin D and antisense oligonucleotides. *J Biol Chem*, 270: 7161-7166, 1995.

124. Loda, M., Capodieci, P., Mishra, R., Yao, H., Corless, C., Grigioni, W., Wang, Y., Magi-Galluzzi, C., and Stork, P. J. Expression of mitogen-activated protein kinase phosphatase-1 in the early phases of human epithelial carcinogenesis. *Am J Pathol*, 149: 1553-1564, 1996.
125. Magi-Galluzzi, C. and Loda, M. Molecular events in the early phases of prostate carcinogenesis. *Eur Urol*, 30: 167-176, 1996.
126. Cox, M. E., Deeble, P. D., Bissonette, E. A., and Parsons, S. J. Activated 3',5'-cyclic AMP-dependent protein kinase is sufficient to induce neuroendocrine-like differentiation of the LNCaP prostate tumor cell line. *J Biol Chem*, 275: 13812-13818, 2000.
127. Carman, C. V. and Benovic, J. L. G-protein-coupled receptors: turn-ons and turn-offs. *Curr Opin Neurobiol*, 8: 335-344, 1998.
128. Troadec, J. D., Marien, M., Mourlevat, S., Debeir, T., Ruberg, M., Colpaert, F., and Michel, P. P. Activation of the mitogen-activated protein kinase (ERK(1/2)) signaling pathway by cyclic AMP potentiates the neuroprotective effect of the neurotransmitter noradrenaline on dopaminergic neurons. *Mol Pharmacol*, 62: 1043-1052, 2002.
129. Steinberg, S. F. The cellular actions of beta-adrenergic receptor agonists: looking beyond cAMP. *Circ Res*, 87: 1079-1082, 2000.
130. Sun, J., Wang, D. A., Jain, R. K., Carie, A., Paquette, S., Ennis, E., Blaskovich, M. A., Baldini, L., Coppola, D., Hamilton, A. D., and Sebti, S. M. Inhibiting angiogenesis and tumorigenesis by a synthetic molecule that blocks binding of both VEGF and PDGF to their receptors. *Oncogene*, 24: 4701-4709, 2005.
131. Sun, J., Ohkanda, J., Coppola, D., Yin, H., Kothare, M., Busciglio, B., Hamilton, A. D., and Sebti, S. M. Geranylgeranyltransferase I inhibitor GGTI-2154 induces breast carcinoma apoptosis and tumor regression in H-Ras transgenic mice. *Cancer Res*, 63: 8922-8929, 2003.
132. Jiang, Z., Wu, C. L., Woda, B. A., Iczkowski, K. A., Chu, P. G., Tretiakova, M. S., Young, R. H., Weiss, L. M., Blute, R. D., Jr., Brendler, C. B., Krausz, T., Xu, J. C., Rock, K. L., Amin, M. B., and Yang, X. J. Alpha-methylacyl-CoA racemase: a multi-institutional study of a new prostate cancer marker. *Histopathology*, 45: 218-225, 2004.
133. Sidovar, M. F., Kozlowski, P., Lee, J. W., Collins, M. A., He, Y., and Graves, L. M. Phosphorylation of serine 43 is not required for inhibition of c-Raf kinase by the cAMP-dependent protein kinase. *J Biol Chem*, 275: 28688-28694, 2000.
134. Veber, N., Prevost, G., Planchon, P., and Starzec, A. Evidence for a growth effect of epidermal growth factor on MDA-MB-231 breast cancer cells. *Eur J Cancer*, 30A: 1352-1359, 1994.
135. Yan, L., Herrmann, V., Hofer, J. K., and Insel, P. A. beta-adrenergic receptor/cAMP-mediated signaling and apoptosis of S49 lymphoma cells. *Am J Physiol Cell Physiol*, 279: C1665-1674, 2000.

136. Eisenmann, K. M., VanBrocklin, M. W., Staffend, N. A., Kitchen, S. M., and Koo, H. M. Mitogen-activated protein kinase pathway-dependent tumor-specific survival signaling in melanoma cells through inactivation of the proapoptotic protein bad. *Cancer Res*, 63: 8330-8337, 2003.
137. Zha, J., Harada, H., Yang, E., Jockel, J., and Korsmeyer, S. J. Serine phosphorylation of death agonist BAD in response to survival factor results in binding to 14-3-3 not BCL-X(L). *Cell*, 87: 619-628, 1996.
138. Harada, H. and Grant, S. Apoptosis regulators. *Rev Clin Exp Hematol*, 7: 117-138, 2003.
139. Harada, H., Quearry, B., Ruiz-Vela, A., and Korsmeyer, S. J. Survival factor-induced extracellular signal-regulated kinase phosphorylates BIM, inhibiting its association with BAX and proapoptotic activity. *Proc Natl Acad Sci U S A*, 101: 15313-15317, 2004.
140. O'Neill, E. and Kolch, W. Taming the Hippo: Raf-1 controls apoptosis by suppressing MST2/Hippo. *Cell Cycle*, 4: 365-367, 2005.
141. Di Marco, E., Pierce, J. H., Fleming, T. P., Kraus, M. H., Molloy, C. J., Aaronson, S. A., and Di Fiore, P. P. Autocrine interaction between TGF alpha and the EGF-receptor: quantitative requirements for induction of the malignant phenotype. *Oncogene*, 4: 831-838, 1989.
142. Fleming, T. P., Matsui, T., and Aaronson, S. A. Platelet-derived growth factor (PDGF) receptor activation in cell transformation and human malignancy. *Exp Gerontol*, 27: 523-532, 1992.
143. Watanabe, M., Nobuta, A., Tanaka, J., and Asaka, M. An effect of K-ras gene mutation on epidermal growth factor receptor signal transduction in PANC-1 pancreatic carcinoma cells. *Int J Cancer*, 67: 264-268, 1996.
144. Graells, J., Vinyals, A., Figueras, A., Llorens, A., Moreno, A., Marcoval, J., Gonzalez, F. J., and Fabra, A. Overproduction of VEGF concomitantly expressed with its receptors promotes growth and survival of melanoma cells through MAPK and PI3K signaling. *J Invest Dermatol*, 123: 1151-1161, 2004.
145. Weldon, C. B., Scandurro, A. B., Rolfe, K. W., Clayton, J. L., Elliott, S., Butler, N. N., Melnik, L. I., Alam, J., McLachlan, J. A., Jaffe, B. M., Beckman, B. S., and Burow, M. E. Identification of mitogen-activated protein kinase kinase as a chemoresistant pathway in MCF-7 cells by using gene expression microarray. *Surgery*, 132: 293-301, 2002.
146. Jin, W., Wu, L., Liang, K., Liu, B., Lu, Y., and Fan, Z. Roles of the PI-3K and MEK pathways in Ras-mediated chemoresistance in breast cancer cells. *Br J Cancer*, 89: 185-191, 2003.
147. Strobl, J. S., Wonderlin, W. F., and Flynn, D. C. Mitogenic signal transduction in human breast cancer cells. *Gen Pharmacol*, 26: 1643-1649, 1995.
148. Erhardt, P., Troppmair, J., Rapp, U. R., and Cooper, G. M. Differential regulation of Raf-1 and B-Raf and Ras-dependent activation of mitogen-activated protein kinase by cyclic AMP in PC12 cells. *Mol Cell Biol*, 15: 5524-5530, 1995.

149. Grassi, V., Daniotti, S., Schiassi, M., Dottorini, M., and Tantucci, C. Oral beta 2-selective adrenergic bronchodilators. *Int J Clin Pharmacol Res*, 6: 93-103, 1986.
150. Moore, P. F., Constantine, J. W., and Barth, W. E. Pirbuterol, a selective beta2 adrenergic bronchodilator. *J Pharmacol Exp Ther*, 207: 410-418, 1978.
151. Steen, S. N., Ziment, I., and Thomas, J. S. Pirbuterol: a new bronchodilator. Phase I-single dose study. *Curr Ther Res Clin Exp*, 16: 1077-1081, 1974.
152. Boucher, M. J., Duchesne, C., Laine, J., Morisset, J., and Rivard, N. cAMP protection of pancreatic cancer cells against apoptosis induced by ERK inhibition. *Biochem Biophys Res Commun*, 285: 207-216, 2001.
153. Budillon, A., Di Gennaro, E., Caraglia, M., Barbarulo, D., Abbruzzese, A., and Tagliaferri, P. 8-Cl-cAMP antagonizes mitogen-activated protein kinase activation and cell growth stimulation induced by epidermal growth factor. *Br J Cancer*, 81: 1134-1141, 1999.
154. Marangoni, E., Vincent-Salomon, A., Auger, N., Degeorges, A., Assayag, F., de Cremoux, P., de Plater, L., Guyader, C., De Pinieux, G., Judde, J. G., Rebucci, M., Tran-Perennou, C., Sastre-Garau, X., Sigal-Zafrani, B., Delattre, O., Dieras, V., and Poupon, M. F. A new model of patient tumor-derived breast cancer xenografts for preclinical assays. *Clin Cancer Res*, 13: 3989-3998, 2007.
155. Bishop, A. L. and Hall, A. Rho GTPases and their effector proteins. *Biochem J*, 348 Pt 2: 241-255, 2000.
156. Van Aelst, L. and D'Souza-Schorey, C. Rho GTPases and signaling networks. *Genes Dev*, 11: 2295-2322, 1997.
157. Bourne, H. R., Sanders, D. A., and McCormick, F. The GTPase superfamily: conserved structure and molecular mechanism. *Nature*, 349: 117-127, 1991.
158. Kjoller, L. and Hall, A. Signaling to Rho GTPases. *Exp Cell Res*, 253: 166-179, 1999.
159. Gosser, Y. Q., Nomanbhoy, T. K., Aghazadeh, B., Manor, D., Combs, C., Cerione, R. A., and Rosen, M. K. C-terminal binding domain of Rho GDP-dissociation inhibitor directs N-terminal inhibitory peptide to GTPases. *Nature*, 387: 814-819, 1997.
160. Hoffman, G. R., Nassar, N., and Cerione, R. A. Structure of the Rho family GTP-binding protein Cdc42 in complex with the multifunctional regulator RhoGDI. *Cell*, 100: 345-356, 2000.
161. Jaffe, A. B. and Hall, A. Rho GTPases in transformation and metastasis. *Adv Cancer Res*, 84: 57-80, 2002.
162. Olofsson, B. Rho guanine dissociation inhibitors: pivotal molecules in cellular signalling. *Cell Signal*, 11: 545-554, 1999.
163. Adamson, P., Marshall, C. J., Hall, A., and Tilbrook, P. A. Post-translational modifications of p21rho proteins. *J Biol Chem*, 267: 20033-20038, 1992.

164. Fritz, G. and Kaina, B. Rho GTPases: promising cellular targets for novel anticancer drugs. *Curr Cancer Drug Targets*, 6: 1-14, 2006.
165. Michaelson, D., Silletti, J., Murphy, G., D'Eustachio, P., Rush, M., and Philips, M. R. Differential localization of Rho GTPases in live cells: regulation by hypervariable regions and RhoGDI binding. *J Cell Biol*, 152: 111-126, 2001.
166. Lebowitz, P. F., Sakamuro, D., and Prendergast, G. C. Farnesyl transferase inhibitors induce apoptosis of Ras-transformed cells denied substratum attachment. *Cancer Res*, 57: 708-713, 1997.
167. Wherlock, M., Gampel, A., Futter, C., and Mellor, H. Farnesyltransferase inhibitors disrupt EGF receptor traffic through modulation of the RhoB GTPase. *J Cell Sci*, 117: 3221-3231, 2004.
168. Chen, Z., Sun, J., Pradines, A., Favre, G., Adnane, J., and Sebti, S. M. Both farnesylated and geranylgeranylated RhoB inhibit malignant transformation and suppress human tumor growth in nude mice. *J Biol Chem*, 275: 17974-17978, 2000.
169. Hall, A. Rho GTPases and the actin cytoskeleton. *Science*, 279: 509-514, 1998.
170. Pruitt, K. and Der, C. J. Ras and Rho regulation of the cell cycle and oncogenesis. *Cancer Lett*, 171: 1-10, 2001.
171. Khosravi-Far, R., Solski, P. A., Clark, G. J., Kinch, M. S., and Der, C. J. Activation of Rac1, RhoA, and mitogen-activated protein kinases is required for Ras transformation. *Mol Cell Biol*, 15: 6443-6453, 1995.
172. Kobune, M., Chiba, H., Kato, J., Kato, K., Nakamura, K., Kawano, Y., Takada, K., Takimoto, R., Takayama, T., Hamada, H., and Niitsu, Y. Wnt3/RhoA/ROCK signaling pathway is involved in adhesion-mediated drug resistance of multiple myeloma in an autocrine mechanism. *Mol Cancer Ther*, 6: 1774-1784, 2007.
173. Adamson, P., Paterson, H. F., and Hall, A. Intracellular localization of the P21rho proteins. *J Cell Biol*, 119: 617-627, 1992.
174. Wheeler, A. P. and Ridley, A. J. Why three Rho proteins? RhoA, RhoB, RhoC, and cell motility. *Exp Cell Res*, 301: 43-49, 2004.
175. Zalcman, G., Closson, V., Linares-Cruz, G., Lerebours, F., Honore, N., Tavitian, A., and Olofsson, B. Regulation of Ras-related RhoB protein expression during the cell cycle. *Oncogene*, 10: 1935-1945, 1995.
176. Allal, C., Pradines, A., Hamilton, A. D., Sebti, S. M., and Favre, G. Farnesylated RhoB prevents cell cycle arrest and actin cytoskeleton disruption caused by the geranylgeranyltransferase I inhibitor GGTI-298. *Cell Cycle*, 1: 430-437, 2002.
177. Du, W., Lebowitz, P. F., and Prendergast, G. C. Cell growth inhibition by farnesyltransferase inhibitors is mediated by gain of geranylgeranylated RhoB. *Mol Cell Biol*, 19: 1831-1840, 1999.
178. Du, W. and Prendergast, G. C. Geranylgeranylated RhoB mediates suppression of human tumor cell growth by farnesyltransferase inhibitors. *Cancer Res*, 59: 5492-5496, 1999.

179. Fritz, G. and Kaina, B. Ras-related GTPase RhoB represses NF-kappaB signaling. *J Biol Chem*, 276: 3115-3122, 2001.
180. Clark, E. A., Golub, T. R., Lander, E. S., and Hynes, R. O. Genomic analysis of metastasis reveals an essential role for RhoC. *Nature*, 406: 532-535, 2000.
181. Yoshioka, K., Matsumura, F., Akedo, H., and Itoh, K. Small GTP-binding protein Rho stimulates the actomyosin system, leading to invasion of tumor cells. *J Biol Chem*, 273: 5146-5154, 1998.
182. Ridley, A. J. Rho proteins and cancer. *Breast Cancer Res Treat*, 84: 13-19, 2004.
183. Wu, M., Wu, Z. F., Kumar-Sinha, C., Chinnaiyan, A., and Merajver, S. D. RhoC induces differential expression of genes involved in invasion and metastasis in MCF10A breast cells. *Breast Cancer Res Treat*, 84: 3-12, 2004.
184. Benitah, S. A., Valeron, P. F., Rui, H., and Lacal, J. C. STAT5a activation mediates the epithelial to mesenchymal transition induced by oncogenic RhoA. *Mol Biol Cell*, 14: 40-53, 2003.
185. Debidda, M., Wang, L., Zang, H., Poli, V., and Zheng, Y. A role of STAT3 in Rho GTPase-regulated cell migration and proliferation. *J Biol Chem*, 280: 17275-17285, 2005.
186. Sun, H. W., Tong, S. L., He, J., Wang, Q., Zou, L., Ma, S. J., Tan, H. Y., Luo, J. F., and Wu, H. X. RhoA and RhoC -siRNA inhibit the proliferation and invasiveness activity of human gastric carcinoma by Rho/PI3K/Akt pathway. *World J Gastroenterol*, 13: 3517-3522, 2007.
187. Teramoto, H., Malek, R. L., Behbahani, B., Castellone, M. D., Lee, N. H., and Gutkind, J. S. Identification of H-Ras, RhoA, Rac1 and Cdc42 responsive genes. *Oncogene*, 22: 2689-2697, 2003.
188. Richert, M. M., Schwertfeger, K. L., Ryder, J. W., and Anderson, S. M. An atlas of mouse mammary gland development. *J Mammary Gland Biol Neoplasia*, 5: 227-241, 2000.
189. Nandi, S. Endocrine control of mammary gland development and function in the C3H/ He Crgl mouse. *J Natl Cancer Inst*, 21: 1039-1063, 1958.
190. Howlett, A. R. and Bissell, M. J. The influence of tissue microenvironment (stroma and extracellular matrix) on the development and function of mammary epithelium. *Epithelial Cell Biol*, 2: 79-89, 1993.
191. Quarrie, L. H., Addey, C. V., and Wilde, C. J. Programmed cell death during mammary tissue involution induced by weaning, litter removal, and milk stasis. *J Cell Physiol*, 168: 559-569, 1996.
192. Furth, P. A. Introduction: mammary gland involution and apoptosis of mammary epithelial cells. *J Mammary Gland Biol Neoplasia*, 4: 123-127, 1999.
193. Strange, R., Li, F., Saurer, S., Burkhardt, A., and Friis, R. R. Apoptotic cell death and tissue remodelling during mouse mammary gland involution. *Development*, 115: 49-58, 1992.

194. Sheikh, S. N. and Lazarus, P. Re-usable DNA template for the polymerase chain reaction. *Nucleic Acids Res*, 25: 3537-3542, 1997.
195. Slamon, D. J., Godolphin, W., Jones, L. A., Holt, J. A., Wong, S. G., Keith, D. E., Levin, W. J., Stuart, S. G., Udove, J., Ullrich, A., and et al. Studies of the HER-2/neu proto-oncogene in human breast and ovarian cancer. *Science*, 244: 707-712, 1989.
196. Siegel, P. M., Dankort, D. L., Hardy, W. R., and Muller, W. J. Novel activating mutations in the neu proto-oncogene involved in induction of mammary tumors. *Mol Cell Biol*, 14: 7068-7077, 1994.
197. Muller, W. J., Sinn, E., Pattengale, P. K., Wallace, R., and Leder, P. Single-step induction of mammary adenocarcinoma in transgenic mice bearing the activated c-neu oncogene. *Cell*, 54: 105-115, 1988.
198. Guy, C. T., Webster, M. A., Schaller, M., Parsons, T. J., Cardiff, R. D., and Muller, W. J. Expression of the neu protooncogene in the mammary epithelium of transgenic mice induces metastatic disease. *Proc Natl Acad Sci U S A*, 89: 10578-10582, 1992.
199. Muller, W. J., Arteaga, C. L., Muthuswamy, S. K., Siegel, P. M., Webster, M. A., Cardiff, R. D., Meise, K. S., Li, F., Halter, S. A., and Coffey, R. J. Synergistic interaction of the Neu proto-oncogene product and transforming growth factor alpha in the mammary epithelium of transgenic mice. *Mol Cell Biol*, 16: 5726-5736, 1996.
200. Adnane, J., Seijo, E., Chen, Z., Bizouarn, F., Leal, M., Sebti, S. M., and Munoz-Antonia, T. RhoB, not RhoA, represses the transcription of the transforming growth factor beta type II receptor by a mechanism involving activator protein 1. *J Biol Chem*, 277: 8500-8507, 2002.
201. Houslay, M. D. and Kolch, W. Cell-type specific integration of cross-talk between extracellular signal-regulated kinase and cAMP signaling. *Mol Pharmacol*, 58: 659-668, 2000.
202. Weddle, D. L., Tithoff, P., Williams, M., and Schuller, H. M. Beta-adrenergic growth regulation of human cancer cell lines derived from pancreatic ductal carcinomas. *Carcinogenesis*, 22: 473-479, 2001.
203. Schuller, H. M., Tithof, P. K., Williams, M., and Plummer, H., 3rd The tobacco-specific carcinogen 4-(methylnitrosamino)-1-(3-pyridyl)-1-butanone is a beta-adrenergic agonist and stimulates DNA synthesis in lung adenocarcinoma via beta-adrenergic receptor-mediated release of arachidonic acid. *Cancer Res*, 59: 4510-4515, 1999.
204. Schuller, H. M., Porter, B., and Riechert, A. Beta-adrenergic modulation of NNK-induced lung carcinogenesis in hamsters. *J Cancer Res Clin Oncol*, 126: 624-630, 2000.
205. Mendelsohn, J. and Baselga, J. Status of epidermal growth factor receptor antagonists in the biology and treatment of cancer. *J Clin Oncol*, 21: 2787-2799, 2003.

About the Author

Adam Carie received his bachelor's degree from the University of South Florida in the fall of 2002, and received the Biochemistry Student of the Year award. He joined the Sebti lab during his senior year for undergraduate research credit. After graduation he joined the Cancer Biology Ph.D. program, a joint collaboration between Moffitt Cancer Center and USF. He stayed in the Sebti lab for the remainder of his graduate work, where he published a first author paper in the journal *Oncogene*, and co-authored several other papers from inter- and intra-laboratory collaborations. Adam also presented his work in poster form at American Association of Cancer Research international meetings in 2006 and 2007. Likewise, Adam presented posters at a Gordon Research Conference in 2005, Moffitt Research Days in 2006 and 2007 and USF Health Science Research Days in 2006 and 2007. Adam was also invited to talk at the St. Jude National Graduate Student Symposia in 2007 and the CTEP Early Drug Discovery Meeting in 2007.